NAVAL POSTGRADUATE SCHOOL

MONTEREY, CALIFORNIA

THESIS

OSCILLATIONS OF A MULTI-STRING PENDULUM

by

Alexandros Dendis

June 2007

Thesis Advisor:	Fotis Papoulias
Second Reader:	Joshua Gordis

Approved for public release; distribution is unlimited

THIS PAGE INTENTIONALLY LEFT BLANK

REPORT DOCUMENTATION PAGE		Form Approved OMB No. 0704-0188

1. AGENCY USE ONLY *(Leave blank)*	2. REPORT DATE	3. REPORT TYPE AND DATES COVERED
	June 2007	Master's Thesis

4. TITLE AND SUBTITLE Oscillations of a Multi-String Pendulum	5. FUNDING NUMBERS
6. AUTHOR(S) Alexandros Dendis	
7. PERFORMING ORGANIZATION NAME(S) AND ADDRESS(ES) Naval Postgraduate School Monterey, CA 93943-5000	8. PERFORMING ORGANIZATION REPORT NUMBER
9. SPONSORING /MONITORING AGENCY NAME(S) AND ADDRESS(ES) N/A	10. SPONSORING/MONITORING AGENCY REPORT NUMBER

11. SUPPLEMENTARY NOTES The views expressed in this thesis are those of the author and do not reflect the official policy or position of the Department of Defense or the U.S. Government.

12a. DISTRIBUTION / AVAILABILITY STATEMENT	12b. DISTRIBUTION CODE
Approved for public release; distribution is unlimited	

13. ABSTRACT (maximum 200 words)

The mathematical pendulum is one of the most widely studied problems in engineering physics. This is, however, primarily limited to the classical pendulum with a single bar and mass configuration. Extensions to this include multi-degree of freedom systems, but many of the classical assumptions, such as a single bar per mass, are preserved. Several designs used in practice utilize multiple or trapezoidal configurations in order to enhance stability. Such designs have not been studied in great detail and there is a need for additional work in order to fully analyze their response characteristics. The two-string pendulum design characteristics are initially investigated, both in terms of oscillation characteristics and string tension. Analytical and numerical methodologies are applied in order to predict the response of the two-string pendulum in free and forced oscillations. Validation of the results is performed by comparisons to simulations conducted with a standard commercial software package. A preliminary optimization study is conducted for a driven two-string pendulum. Finally, it is shown how to apply the results of the analysis and optimization studies developed in this work in a typical design case.

14. SUBJECT TERMS	15. NUMBER OF PAGES
Mathematical Pendulum, Multi String Pendulum, Oscillations, String Tension, Optimization	155
	16. PRICE CODE

17. SECURITY CLASSIFICATION OF REPORT	18. SECURITY CLASSIFICATION OF THIS PAGE	19. SECURITY CLASSIFICATION OF ABSTRACT	20. LIMITATION OF ABSTRACT
Unclassified	Unclassified	Unclassified	UL

NSN 7540-01-280-5500

Standard Form 298 (Rev. 2-89)
Prescribed by ANSI Std. 239-18

THIS PAGE INTENTIONALLY LEFT BLANK

Approved for public release; distribution is unlimited

OSCILLATIONS OF A MULTI-STRING PENDULUM

Alexandros Dendis
Lieutenant Junior Grade, Hellenic Navy
B.S., Hellenic Naval Academy, 2000

Submitted in partial fulfillment of the
requirements for the degree of

MASTER OF SCIENCE IN MECHANICAL ENGINEERING

from the

NAVAL POSTGRADUATE SCHOOL
June 2007

Author: Lt. J. G. Alexandros Dendis, H.N.

Approved by: Fotis Papoulias
Thesis Advisor

Joshua Gordis
Second Reader

Anthony J. Healey
Chairman, Department of Mechanical and Astronautical Engineering

THIS PAGE INTENTIONALLY LEFT BLANK

ABSTRACT

The mathematical pendulum is one of the most widely studied problems in engineering physics. However, this is primarily limited to the classical pendulum with a single massless bar and mass configuration. Extensions to this include multi-degree of freedom systems, but many of the classical assumptions, such as a single bar per mass, are preserved. Several designs used in practice utilize multiple bars or trapezoidal configurations to enhance stability. Such designs have not been studied in detail. Also, there is a need for additional work to fully analyze their response characteristics. The two-string pendulum design characteristics are initially investigated, both in terms of oscillation and string tension. Analytical and numerical methodologies are applied to predict the response of the two-string pendulum in free and forced oscillations. Results are validated utilizing comparisons generated by simulations conducted with a standard commercial software package. A preliminary optimization study is conducted for a driven two-string pendulum. Finally, in a typical design case, it is shown how to apply the results of the analysis and optimization studies developed in this work.

THIS PAGE INTENTIONALLY LEFT BLANK

TABLE OF CONTENTS

LIST OF FIGURES

THIS PAGE INTENTIONALLY LEFT BLANK

LIST OF TABLES

THIS PAGE INTENTIONALLY LEFT BLANK

LIST OF ACRONYMS AND ABBREVIATIONS

2-pendulum	Two-string pendulum
4-pendulum	Four-string pendulum
SCPA	Slowly Changing Phase and Amplitude
VN 4-D	Visual Nastran 4-D
AUV	Autonomous Underwater Vehicle

THIS PAGE INTENTIONALLY LEFT BLANK

ACKNOWLEDGMENTS

To Alexandra.

THIS PAGE INTENTIONALLY LEFT BLANK

I. INTRODUCTION

A. BACKGROUND

The pendulum is one of the most commonly studied mechanical structures. Galileo himself made the first observation of the pendulum's performance. He set the roots of the pendulum's physics by realizing that the frequency of oscillation for a given pendulum is independent of its displacement's amplitude for small amplitude oscillations, which enables the linearization of the equations of motion. [1].

Following this initial observation, numerous studies were performed on the pendulum's physics. These studies were not limited to the simple or standard pendulum, but were extended to more complex pendulum structures. Some examples are the bifilar pendulum, the torsion pendulum, the double pendulum, and the Foucault pendulum.

To describe analytically the oscillatory behavior of the numerous types of pendula, several techniques were developed. These techniques attempted to predict the solution of the pendulum's dynamics, either by treating its attitude as a linear approximation, which produced acceptable and fairly accurate results for a limited number of cases (linearized pendulum, , etc.), or by facing its nonlinear character recruiting and applying complex methods (perturbation methods or the Lagrange method, which produces the exact nonlinear equation of motion).

From a mathematical analysis viewpoint, the more composite the structure of the pendulum, the more complex the solution approach method. Some types of pendula present a linear character when the oscillation is constrained in small displacement amplitudes (standard and double pendulum). Large amplitude oscillations are nonlinear and sometimes show chaotic behavior (double pendulum). If the problem is approached from an energy perspective, in linear or linearized undriven oscillations, energy is conserved. Nevertheless, there are examples where energy is not conserved. Such cases may be simple to analyze,

such as an oscillation with a constant damping coefficient. Others, such as oscillations, including jumps or variable accelerating support motion, are not simple to analyze.

B. MOTIVATION - OBJECTIVE

Several mechanical structures have dynamic behavior similar to that of a pendulum. Some examples are different types of cranes and crane-like mechanisms used for marine vehicles, such as AUVs, rescue boats, and naval vessels for launching and recovery. Their multi-rope suspension mechanism is not designed to oscillate; rather, it is designed to prevent swinging and to promote stability. Another example of a pendulum system designed to prevent swinging is the Blackburn pendulum. [1].

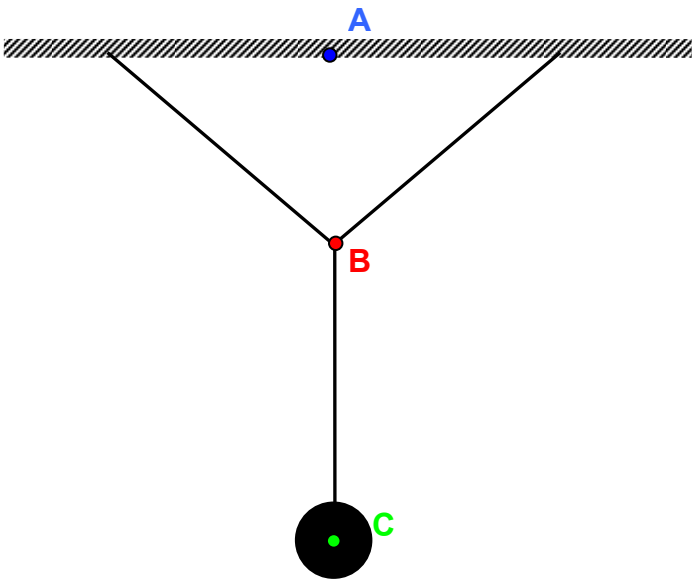

Figure 1. The Blackburn pendulum

The Blackburn pendulum's suspension system is comprised of two strings forming a ''Y'' shape. The purpose of this design is to provide two distinct and effective pendulum string lengths. Therefore, for an oscillatory motion within a

plane defined by the Y shape, the length of the pendulum is the distance from point B to point C. In contrast, for a motion within a plane perpendicular to the Y shape, the effective length is the distance from point A to point C. Therefore, two distinct frequencies of oscillation define the motion of the Blackburn pendulum in the two perpendicular planes. Thus, its modes of oscillation are described by superposition of the two basic frequencies.

Nevertheless, all the previously mentioned characteristics of the Blackburn pendulum depend on the assumption that point B will not be able to oscillate with respect to one of the two strings that starts from B and ends at the support points, i.e., the distance of B from the two support points will always be constant. However, this assumption is valid under restrictions. A violent motion of the support would theoretically be able to disturb the partial equilibrium of the ‘’Y’’ pendulum.

The motivation for this thesis was to obtain analytical expressions, as well as numerical solutions, to describe the behavior of oscillating pendula with designs similar to the one of the ‘’Y’’ pendulum. The basic model design that will be initially analyzed is the one of a Blackburn pendulum in which point A coincides with B, and is allowed to oscillate only within the plane defined by this “V’’ shape (more detailed description will be provided in the following sections). Moreover, since such a ‘’V’’ design is the basic element component of more complex suspension designs, its capability of preventing or damping oscillations will be investigated.

THIS PAGE INTENTIONALLY LEFT BLANK

II. THE TWO-STRING PENDULUM

A. MATHEMATICAL DESCRIPTION OF THE TWO-STRING PENDULUM

1. Introduction

The purpose of this section is to analyze the motion equations of the two-string pendulum. For brevity within this thesis, this will be referred to as the 2-pendulum. Several techniques will be used to analyze the motion of the 2-pendulum with the aim to present an accurate solution to the nonlinear equations of motion that describes its motion. The main purpose is to compare main features of the dynamic response of the 2-pendulum with those of the standard single-mass, single-string pendulum. These comparisons will be in terms of the amplitude of the resulting motion, the resulting natural frequency of the oscillator, as well as the string tension. Different values of initial velocity and initial angular displacement will be used to investigate the system's response to both an initial excitation and an initial displacement from its equilibrium position.

2. The Standard Pendulum

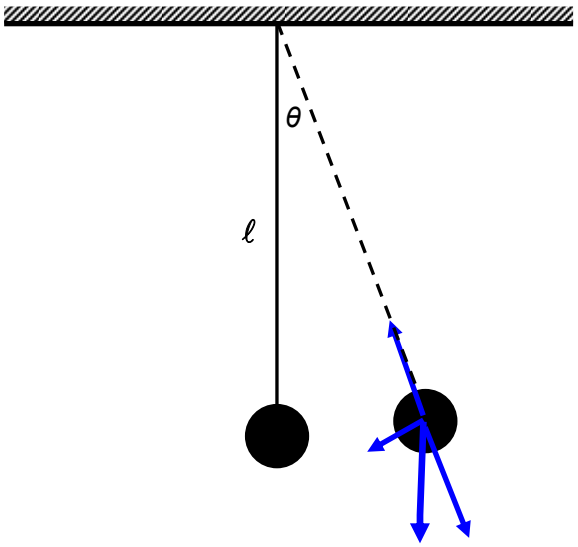

Figure 2. Small angle oscillation of the standard pendulum

First, we will investigate the motion of the simple gravity pendulum undergoing free undamped vibration. The model that we will use is shown in Figure 1 -- a sphere of mass *m* which is suspended with a massless string of length = ℓ from its center of gravity.

To derive the equations of motion, we will use the moment method. According to Newton's Law, the inertial moment of the mass *m* must be equal to the sum of moments applied on the mass.

$$m\ell^2\ddot{\theta} = -mg\ell\sin\theta \tag{2.1}$$

$$ml^2\ddot{\theta} + mgl\sin\theta = 0 \tag{2.2}$$

Equation (2) above is nonlinear since it contains the term $\sin\theta$. We can substitute the trigonometric nonlinearity with its Taylor series expansion

$$\sin\theta = \theta - \frac{\theta^3}{3!} + \frac{\theta^5}{5!}... \tag{2.3}$$

To simplify our calculations, we will initially assume only small amplitude oscillations. In this case, we can assume without compromising accuracy that

$$\sin\theta \approx \theta \tag{2.4}$$

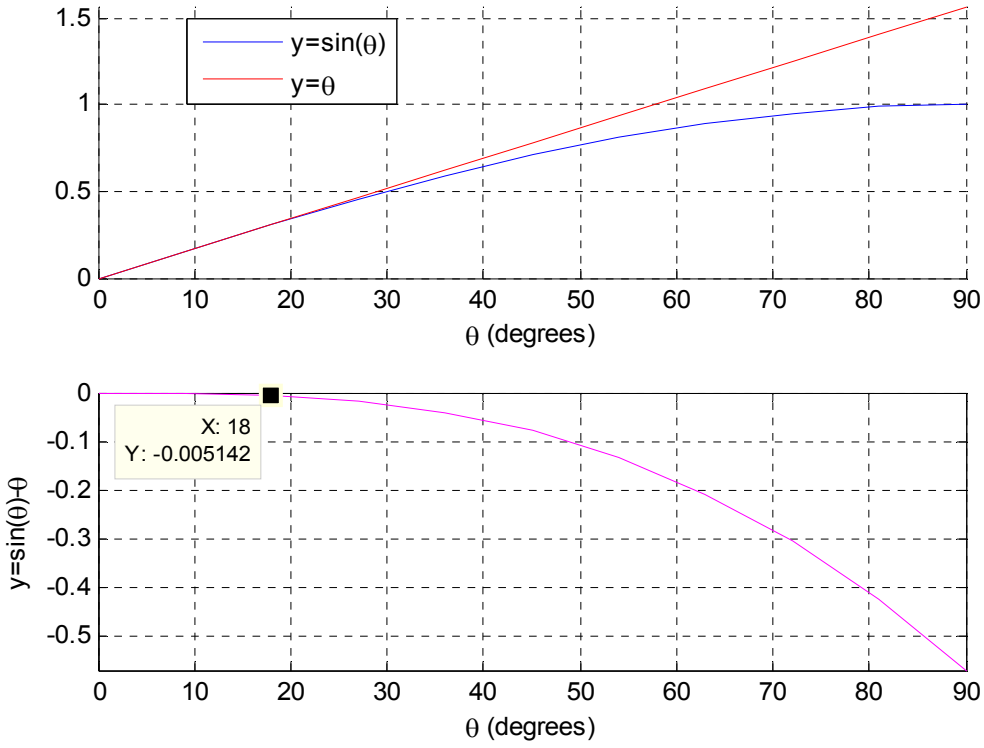

Figure 3. Linear-nonlinear discrepancy

As demonstrated by Figure 3, there is a range of θ where equation (4) is valid and provides a good approximation. As depicted in the same figure, the difference between the linearized and the nonlinear expression is negligible for values of $\theta < \frac{\pi}{10}$.

For such small amplitude oscillations, the equation of motion can be linearized

$$m\ell^2\ddot{\theta} + mg\ell\theta = 0 \tag{2.5}$$

or

$$\ddot{\theta} + \frac{g}{\ell}\theta = 0 \tag{2.6}$$

The solution to the above differential equation for initial displacement and velocity of

$$\theta(0) = \theta_0$$
$$\dot{\theta}(0) = \dot{\theta}_0 \tag{2.7}$$

becomes

$$\theta = \frac{\dot{\theta}(0)}{\omega_n}\sin\omega_n t + \theta(0)\cos\omega_n t \tag{2.8}$$

where

$$\omega_n = \sqrt{\frac{g}{\ell}} \tag{2.9}$$

is the natural frequency of the linear pendulum.

From Figure 2, the restoring moment is

$$F_r = mg\sin\theta \tag{2.10}$$

or, for small oscillations,

$$F_r = mg\theta \tag{2.11}$$

Another feature of the pendulum worth mentioning is the pendulum jump [5]. Pendulum jumps occur when the mass leaves the circular path defined by the string and follows other trajectories. Such response is only observed if the string tension becomes zero. This is dependent on the position of the pendulum and the initial conditions. From Figure 2, we can visualize that the centripetal force, which obliges the mass to follow a circular path, is

$$Fc = \frac{mu^2}{\ell} = T - mg\cos\theta \Leftrightarrow T = \frac{mu^2}{\ell} + mg\cos\theta \tag{2.12}$$

where *u* is the linear velocity of the mass. The magnitude of *u* depends only on the initial conditions, since only conservative forces govern the pendulum's motion. Assuming the initial conditions (2.7), which are equivalent to $z_0 = \ell(1-\cos\theta_0)$ and $u_0 = l\dot{\theta}_0$, the initial energy of the mass is $E_0 = T_0 + V_0 = \frac{1}{2}mu_0^2 + mgz_0$. During oscillation, the energy of the mass for an

arbitrary angle θ would be $E = T + V = \frac{1}{2}mu^2 + mgz$, where $z = \ell(1 - \cos\theta)$. Since the total energy is conserved throughout the oscillation (absence of damping or other non-conservative forces) $E = E_0$, the magnitude of the linear velocity would be

$$u = 2\sqrt{\frac{E_0}{m} - gz} \tag{2.13}$$

Finally, the tension of the string throughout the oscillation, from (2.12) and (2.13), will be equal to

$$T = \frac{2(E_0 - mgz)}{\ell} + mg\cos\theta \tag{2.14}$$

where a positive sign denotes orientation towards the center of oscillation. This promotes the circular path motion of the mass. The only term of the latest equation that may take negative values and, thus, lead to zeroing the string tension, is $mg\cos\theta$. It may only happen for angular displacements greater than $\frac{\pi}{2}$.

The possibility of jumps is present only if the initial conditions allow the oscillator to climb to $\theta > \frac{\pi}{2}$. After that point, the path of the mass would be governed by the regular equations which define a projectile with a given initial linear velocity magnitude and orientation; that is, until the position of the mass will again reach a distance equal to the natural length of the pendulum's string.

3. The 2-Pendulum

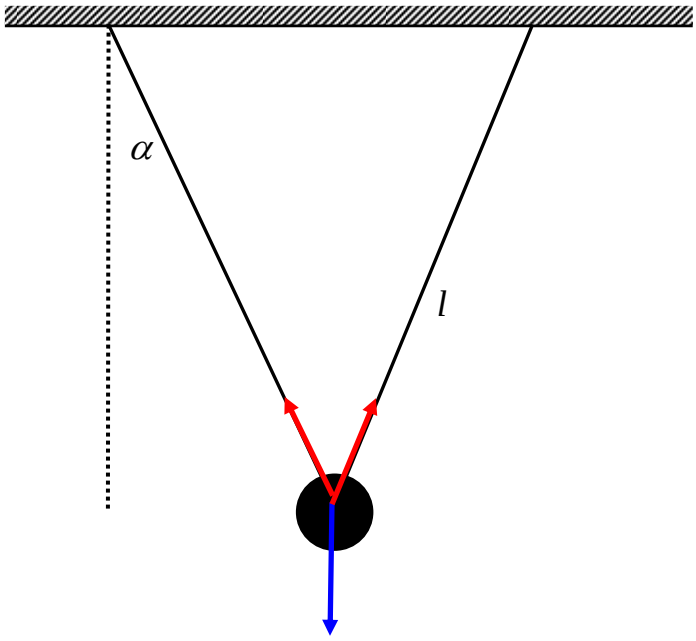

Figure 4. The 2-pendulum

The geometry of the 2-pendulum is pictured in Figure 4. The main distinguishable characteristic of the 2-pendulum, compared to the simple pendulum, is that the mass *m* is now suspended by two strings. To be consistent with the previous model, the strings' perpendicular distance from the plane of suspension will be l. Consequently, $l = \frac{\ell}{\cos\alpha}$. The point of application of the strings on the mass is again at its center of gravity while each string forms an angle *α* with respect to the perpendicular. Our aim is to evaluate the effect of this angle on the motion of the mass m**.**

For the purposes of this preliminary analysis, we will assume that the governing force during the pendulum oscillation is the weight. That means that

we will not, for now examine the forces applied on the mass to the point where it reaches the lower point of its trajectory and switches the string about which it swings.

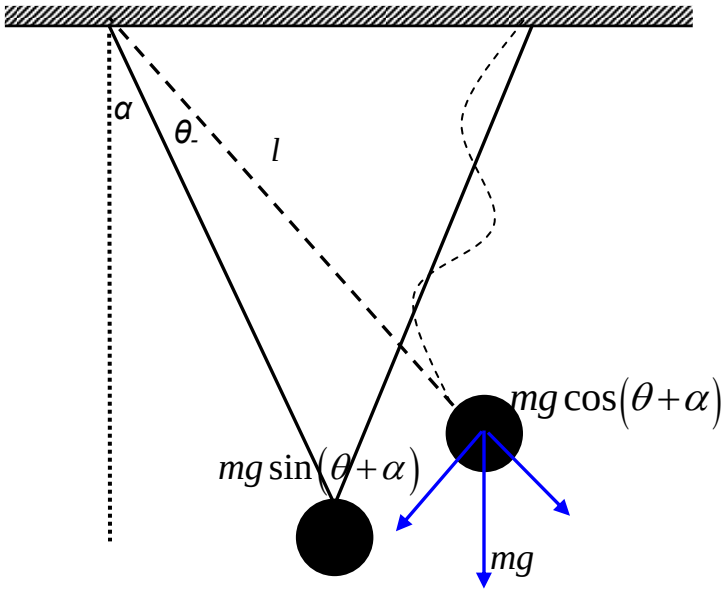

Figure 5. Small angle oscillation of the 2-pendulum, $\theta<0$

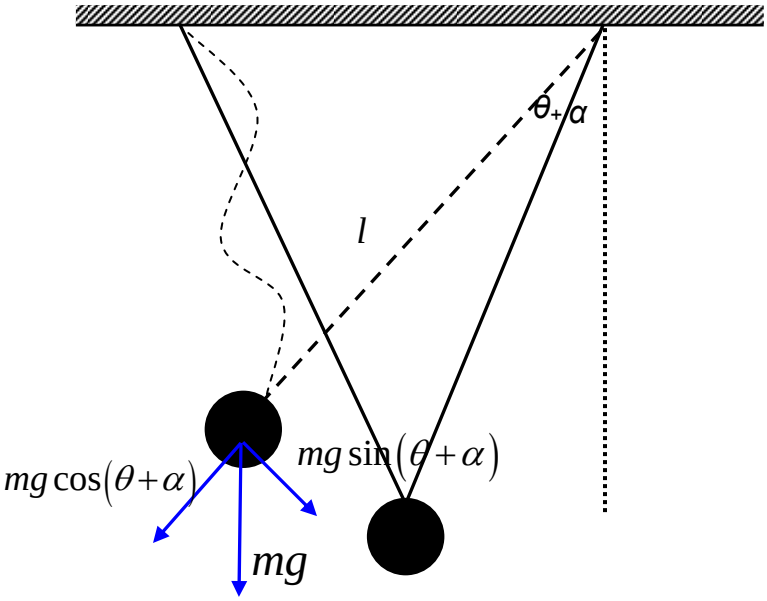

Figure 6. Small angle oscillation of the 2-pendulum, θ>0

Assuming an angle θ (counterclockwise for positive values), as in Figure 6, and equating inertia and non-inertia forces applied on the mass as before, the resulting equation of motion is

$$ml^2\ddot{\theta} + mgl\sin(\theta+\alpha) = 0 \tag{2.15}$$

or

$$\ddot{\theta} + \frac{g}{l}\sin(\theta+\alpha) = 0 \tag{2.16}$$

To further develop equation (2.16), we should take into account that the term $\sin(\theta+\alpha)$ takes positive values for the case of θ>0 (Figure 6), and negative values for the case of θ<0 (Figure 5). However, since the restoring force should always oppose further increase in the magnitude of the angle θ, it takes the same magnitude for the same $\|\alpha+\theta\|$. Furthermore, using the trigonometric identity $\sin(\alpha+b) = \sin\alpha\cos b + \cos\alpha\sin b$, equation (2.16) becomes

$$\ddot{\theta} + \frac{g}{l}(\sin\theta\cos\alpha + \cos\theta\sin\alpha) = 0 \tag{2.17}$$

Examining equation (2.17), we can see that the consistency of the restoring force orientation is preserved in the term $\sin\theta\cos\alpha$ (because of $\sin\theta$), but not in $\sin\alpha\cos\theta$ (since $\cos\theta$ does not change sign when θ changes sign). Consequently, to preserve the restoring force consistency for all values of θ, we should rewrite equation (2.17) as follows

$$\ddot{\theta}+\frac{g}{l}\sin\theta\cos\alpha\pm\frac{g}{l}\cos\theta\sin\alpha=0$$

This is equivalent to

$$\ddot{\theta}+\frac{g}{l}\sin\theta\cos\alpha+\frac{g}{l}\cos\theta\sin\alpha\,\mathrm{sign}\,\theta=0 \tag{2.18}$$

The sign nonlinearity assumes the value (+1) for positive and (-1) for negative arguments. In addition to the above, if we assume small angles of θ, we can rewrite (2.18) as follows

$$\ddot{\theta}+\frac{g}{l}\theta\cos\alpha+\frac{g}{l}\sin\alpha\,\mathrm{sign}\,\theta=0 \tag{2.19}$$

The restoring force from equation (2.15) is

$$F_r=mg\sin(\theta+\alpha) \tag{2.20}$$

For small oscillations, equation (2.20) becomes

$$F_r=mg\theta\cos\alpha+mg\sin\alpha\,\mathrm{sign}\,\theta \tag{2.21}$$

Our goal is to solve analytically and numerically differential equations (2.18).

Finally, based on the previous analysis performed on the jumps for the standard pendulum, we realize that the 2-pendulum may exhibit the same behavior, only now the required angular displacement is $\theta+\alpha>\frac{\pi}{2}\Leftrightarrow\theta>\frac{\pi}{2}-\alpha$.

4. Comments

Despite its similarity with the standard pendulum, equation (2.18) exhibits some major characteristic differences. The most significant difference between the standard pendulum and the 2-pendulum is that the latter possesses a

discontinuity in its stiffness around the equilibrium position. As can be seen from (2.19), there is an instantaneous jump in the value of the restoring moment around zero. This is depicted in Figure 7 where the normalized spring constant of the 2-pendulum is shown for different values of α, along with the linear spring constant of the standard pendulum. This discontinuity at zero prevents us from a classical linearization of the 2-pendulum and requires different techniques for the analysis. Such techniques, based on the perturbation theory, are the subject of the analysis that follows.

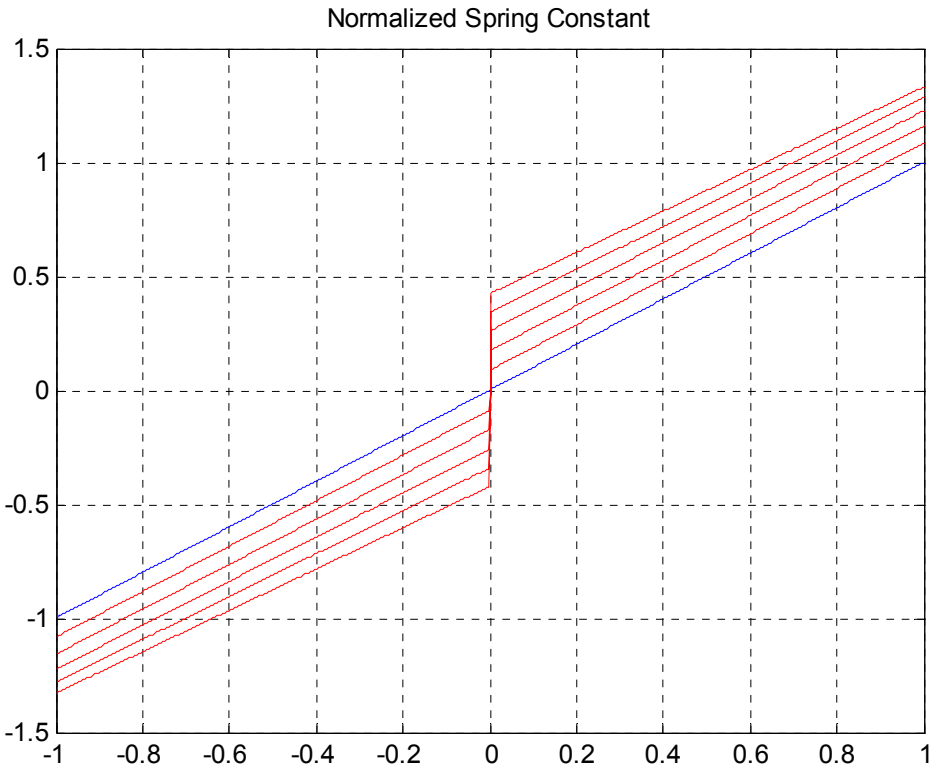

Figure 7. Normalized spring constant of the 2-pendulum

5. Velocity and Force Vector Analysis

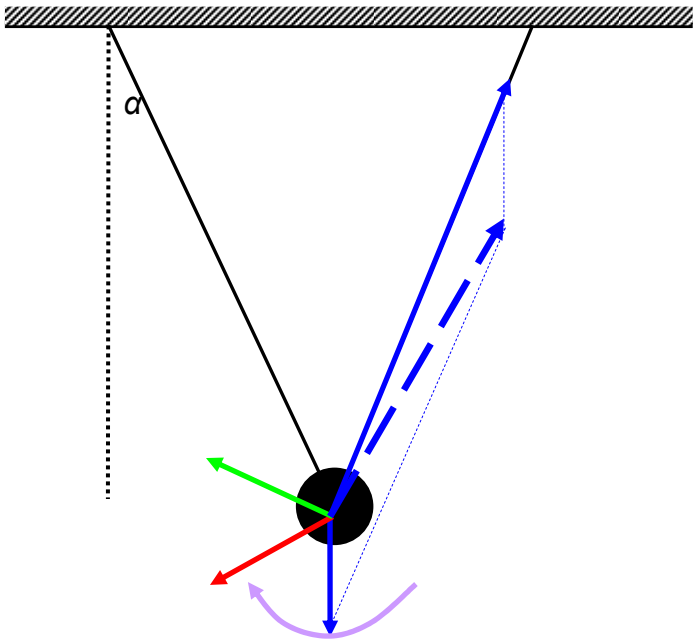

Figure 8. General force and velocity diagram at the switch point

Before advancing with the solution of equations (2.18) and (2.19), we should take into account the dynamics of the mass *m* at the point when it switches strings about which it swings. In Figure 8, we can visualize the forces, weight *B,* instantaneous string tension T_{inst} (blue with continuous line vectors), and their resultant *R* (blue dashed line vector). During the change, it acts on the mass and actually contributes to not only the switch at the center of rotation, but to the velocities just before $\vec{V}b$ (red vector), and just after, $\vec{V}a$ (green vector) -- the switch. Nevertheless, since the weight of the mass is a conservative force and does not undergo changes in magnitude during this switch, we can safely assume that its contribution in the velocity direction switch is negligible.

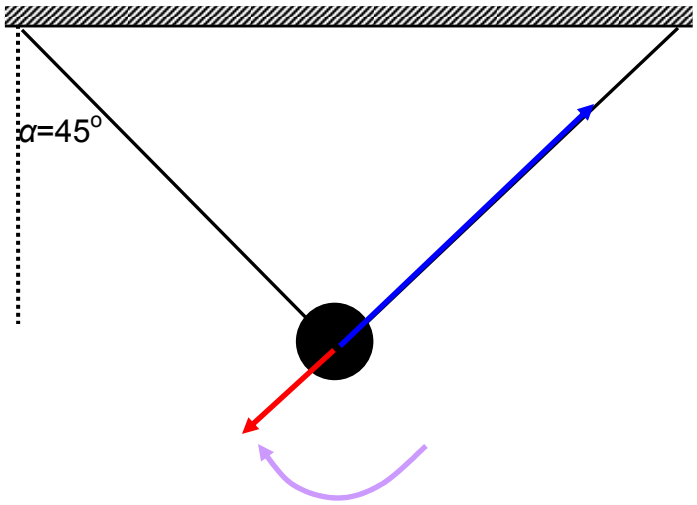

Figure 9. Force and velocity diagram at the switch point for α=45°

According to the vector diagram in Figure 9, there is a limiting value of angle α, which, if exceeded, the string switch is impossible. In the instance that T_{inst} lies in the same direction, but in opposite orientation to the $\vec{V}b$, this force is unable to change the direction of the velocity from $\vec{V}b$ to $\vec{V}a$, irrespective of its magnitude. This limiting value is shown to be α=45°. In this case, this exact value of the mass will either stop or bounce in the same direction. However, the orientation of T_{inst}, will have a velocity magnitude less than or equal to $\vec{V}b$ (depending on the energy absorption of the string). As a result, the following preliminary analysis, Chapter II, Section A, numbers 6, 7, and 8, will be valid only for α<45°. Furthermore, we will not consider the exact forces that affect dynamics and energy equivalence at the switch point. Rather, we will only take into account that their effect is the jump of the velocity from $\vec{V}b$ to $\vec{V}a$, where $\left\|\vec{V}a\right\| = \left\|\vec{V}b\right\|$.

6. Numerical Integration Solution

The numerical solution is performed using the Matlab function `ode45`. This `ode45` Matlab function solves numerically the equation of motion and is able

to take into account nonlinearities, such as trigonometric functions and sign changes. Thus, ode45 will provide the exact solution, provided that an appropriate, fine enough, time step is selected. The Program_1.m Matlab-file was used to plot the angular displacement θ versus time for different values of angle α, assuming initial conditions $\theta(0)=\theta_0$ and $\dot{\theta}(0)=0$. In parallel, we plotted the angular displacement θ versus time for a simple pendulum of string length ℓ. In addition, the Program_2.m provided the same kind of plots, where the initial conditions were $\theta(0)=0$ and $\dot{\theta}(0)=\dot{\theta}_0$.

7. Analytical Solution

Three different methods will be used to attempt to derive the exact or approximate solution to equation (14) or its equivalent (16).

a. Exact Solution for a Time Increment

One method we could use to obtain the solution of equation (2.18) is to solve it for the time period where the term $\frac{g}{l}\sin\alpha\,\mathrm{sign}\,\theta$ has a constant sign [2]. Thus, assuming an initial angular displacement $\theta(0)=A$, the equation of motion for $0<\theta<A$ is

$$\theta=-\frac{\frac{g}{l}\sin\alpha}{\frac{g}{l}\cos\alpha}+\left(A+\frac{\frac{g}{l}\sin\alpha}{\frac{g}{l}\cos\alpha}\right)\cos\left(\sqrt{\frac{g}{l}\cos\alpha}\right)t \tag{2.22}$$

or

$$\theta=-\tan\alpha+(A+\tan\alpha)\cos\left(\sqrt{\frac{g}{l}\cos\alpha}\right)t \tag{2.23}$$

Let us name the square of the pseudo-natural frequency of oscillation and of the equivalent pseudo-forcing amplitude as bellow

$$\begin{aligned}\omega_0^2&=\frac{g}{l}\cos\alpha\\ P&=\frac{g}{l}\sin\alpha\end{aligned} \tag{2.24}$$

At the time $t_1 = \frac{1}{\omega_0}\arccos\left(\frac{1}{1+\frac{A\omega_0^2}{P}}\right)$ when θ=0, the velocity is

$$u(t_1) = -\omega_0\left(A+\frac{P}{\omega_0^2}\right)\sin\omega_0 t$$

and then the equation of motion becomes

$$\ddot{\theta} + \omega_0^2\theta = P \tag{2.25}$$

with initial conditions $u(t_1) = -\omega_0\left(A+\frac{P}{\omega_0^2}\right)\sin\omega_0 t$ and $\theta(t_1) = 0$, and so on. The value t_1 is equivalent to one quarter of the period of oscillation.

Finally the period of oscillation is

$$T_{exact} = \frac{4}{\omega_0}\arccos\left(\frac{1}{1+\frac{A\omega_0^2}{P}}\right) \tag{2.26}$$

or

$$T_{exact} = \frac{4}{\sqrt{\frac{g}{l}\cos\alpha}}\arccos\left(\frac{1}{1+\frac{A}{\tan\alpha}}\right) \tag{2.27}$$

so the frequency of oscillation is

$$\omega_{exact} = \frac{2\pi}{T_{exact}} \tag{2.28}$$

b. Method of Slowly Changing Phase and Amplitude

A second method for obtaining the analytic solution only for the linearized equation (2.19) or , considering (2.24)

$$\ddot{\theta} + \omega_0^2\theta + P\,\mathrm{sign}\,\theta = 0\,, \tag{2.29}$$

is using the method of Slowly Changing Phase and Amplitude [2]. This method states that the equations of the slowly changing phase ψ and amplitude a are

$$\dot{\psi} = \frac{1}{2\pi \mathrm{a}(\omega_0)} \int_0^{2\pi} \left[-P\left\{ \mathrm{a}\sin(\theta+\psi) \right\} \right] \sin(\mathrm{a}+\psi)\, d\theta \tag{2.30}$$

$$\dot{\mathrm{a}} = \frac{1}{2\pi \mathrm{a}(\omega_0)} \int_0^{2\pi} \left[-P sign\left\{ \mathrm{a}\sin(\theta+\psi) \right\} \right] \sin(\mathrm{a}+\psi)\, d\mathrm{a} \tag{2.31}$$

Evaluating the above integrals,

$$\dot{\mathrm{a}} = 0 \quad \text{and} \quad \dot{\psi} = \frac{4P}{2\pi \mathrm{a}\omega_0}$$

$$\mathrm{a} = A \quad \text{and} \quad \psi = \frac{2P}{\pi A \omega_0} + \psi_0$$

Finally, if we choose the initial conditions, such as $\psi_0 = \frac{\pi}{2}$, the approximate solution is

$$\theta = \mathrm{A}\cos\left(\omega_0 + \frac{2P}{\pi A \omega_0} \right) t \tag{2.32}$$

and the approximate period is

$$T_{app} = \frac{2\pi}{\omega_0 \left(1 + \frac{2P}{\pi \omega_0^2 A} \right)} \tag{2.33}$$

while the approximate angular frequency is

$$\omega_{app} = \omega_0 \left(1 + \frac{2P}{\pi \omega_0^2 A} \right) \tag{2.34}$$

considering (2.24)

$$\omega_{app} = \sqrt{\frac{g}{l}\cos\alpha} \left(1 + \frac{2\tan\alpha}{\pi A} \right) \tag{2.35}$$

c. Energy Method

The application of this method suggests that we could approximate the equation of motion of the enhanced pendulum with one of a simple pendulum. However, the restoring force would be increased by a factor so that

the total work produced by this force along a time period would be the same as the forces that govern the motion of the enhanced pendulum.

From equation (2.20), the work produced by the restoring force of the enhanced pendulum for a motion $0<\theta<\theta_0$ is equal to

$$\int_0^{\theta_0} mg\sin(\alpha+\theta)d\theta \tag{2.36}$$

while the one of the simple pendulum is

$$\int_0^{\theta_0} mg\sin\theta d\theta \tag{2.37}$$

Dividing (2.36) by (2.37), we obtain a factor of

$$F=\int_0^{\theta_0} mg\sin(\alpha+\theta)d\theta \Big/ \int_0^{\theta_0} mg\sin\theta d\theta \tag{2.38}$$

which provides us with an order of increased magnitude of forces applied during the oscillation of the enhanced pendulum compared to the ones applied on the simple pendulum.

Thus, we will multiply the term $mg\sin\theta$ by F and solve the approximate equation of motion

$$\ddot{\theta}+F\frac{g}{l}\sin\theta=0 \tag{2.39}$$

or in linear form,

$$\ddot{\theta}+F\frac{g}{l}\theta=0 \tag{2.40}$$

Thus, the approximate angular frequency of oscillation is

$$\omega_{app}=\sqrt{\frac{g}{l}F} \tag{2.41}$$

8. Evaluation of Results

To evaluate both numerical and analytical approximations, we will first plot the three angular displacement solutions (ode45 numerical integration – Slowly Changing Phase and Amplitude method – Energy method). This will be compared to the solution of the standard pendulum in terms of gain and frequency of oscillation. This will best show that the 2-pendulum offers significant

gains in terms of increased restoring moment and frequency of oscillation. It, also, measures how close it comes to the exact solution (represented by the ode45 solution). The predicted response will be presented for two distinct initial conditions -- initial angular displacement and initial angular velocity. In addition to the above, we will plot the phase trajectories for the same initial conditions, as well as the comparison of the predicted angular frequencies of oscillation. This will help to better visualize the discrepancy of the prediction methods.

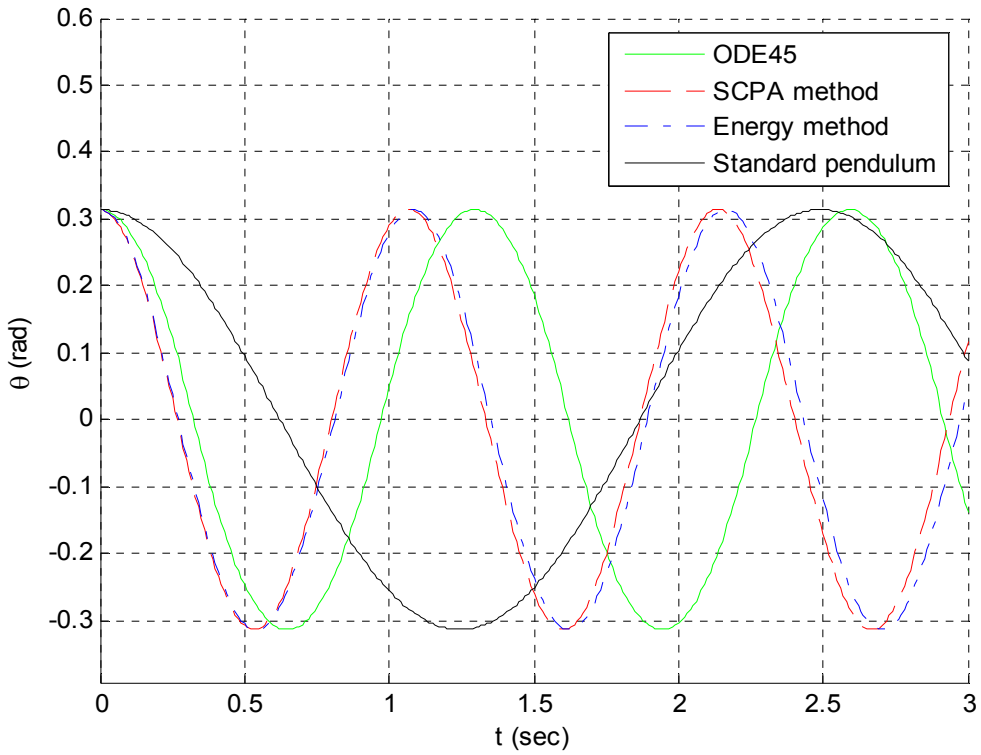

Figure 10. $\alpha=\pi/6$

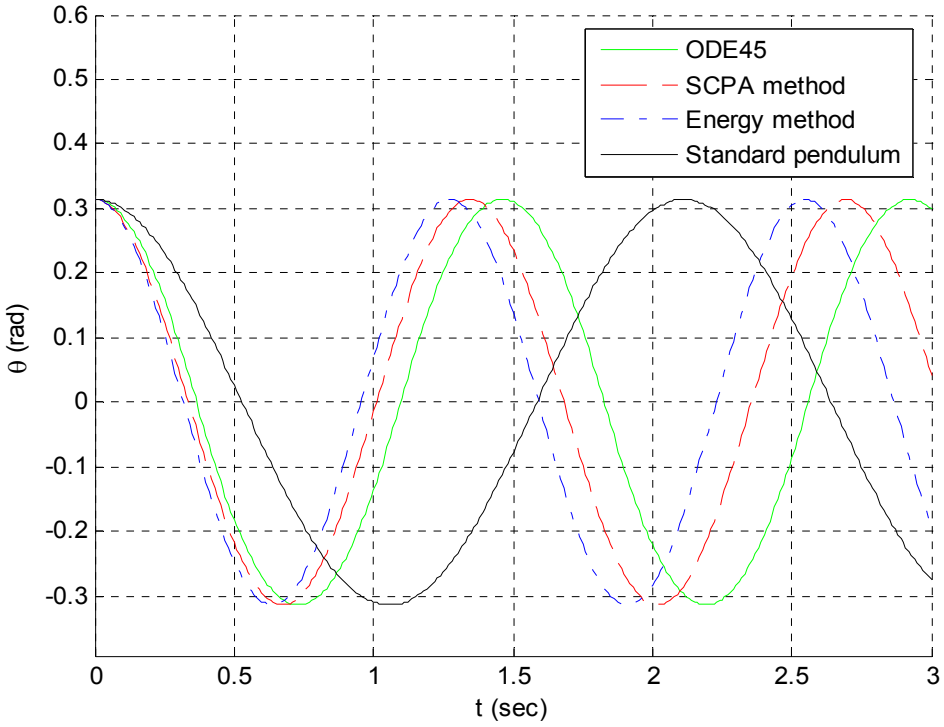

Figure 11. $\alpha=\pi/12$

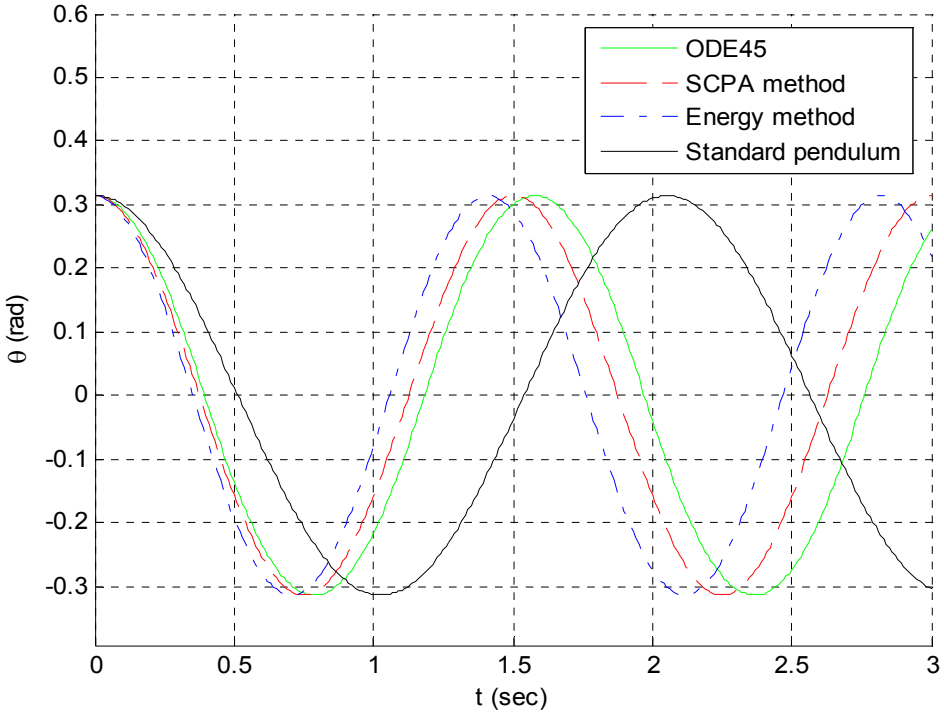

Figure 12. $\alpha=\pi/18$

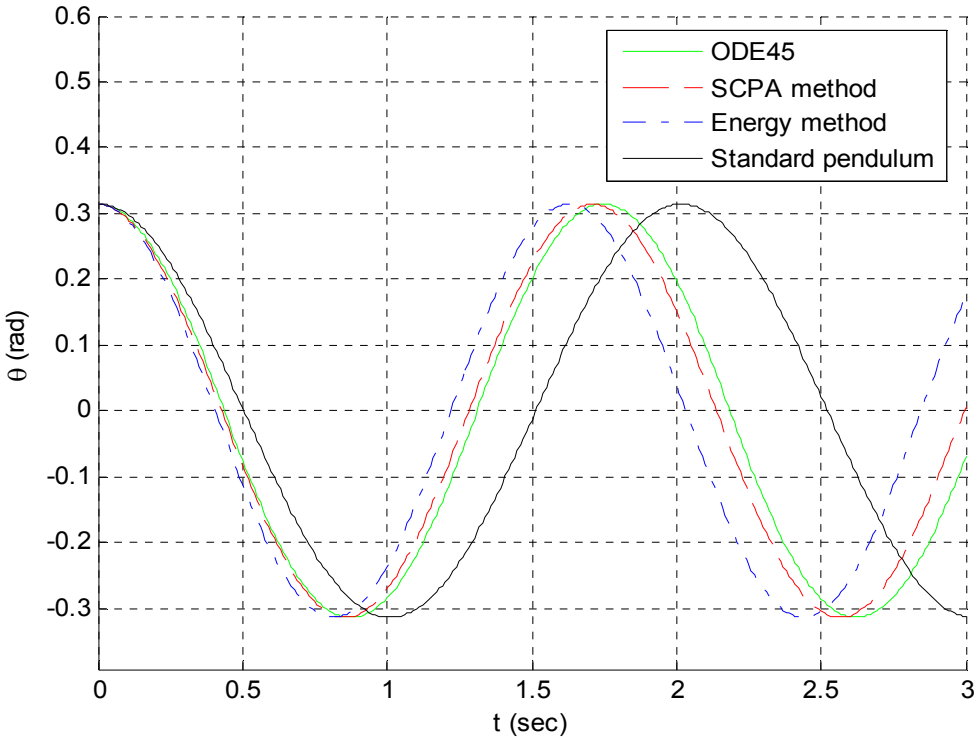

Figure 13. $\alpha=\pi/36$

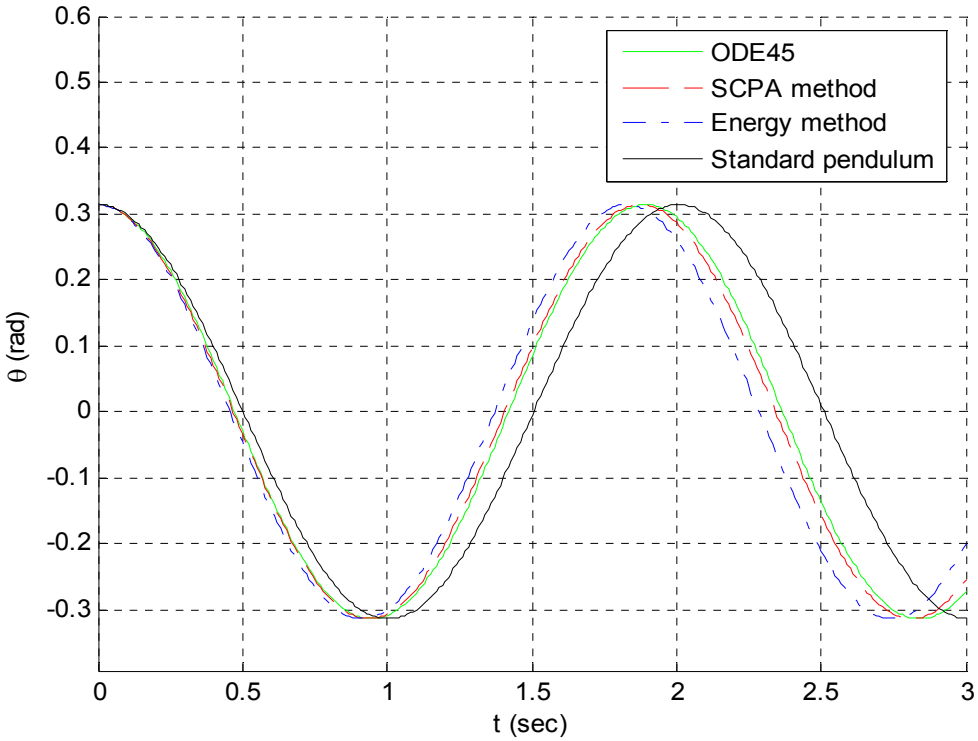

Figure 14. $\alpha=\pi/90$

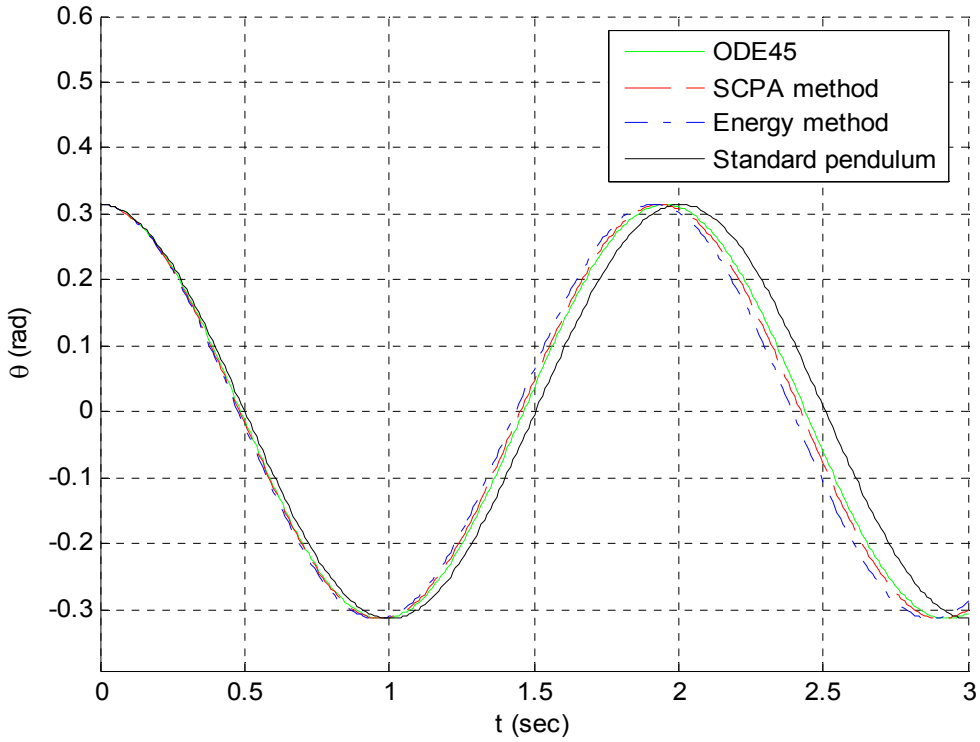

Figure 15. $\alpha=\pi/180$

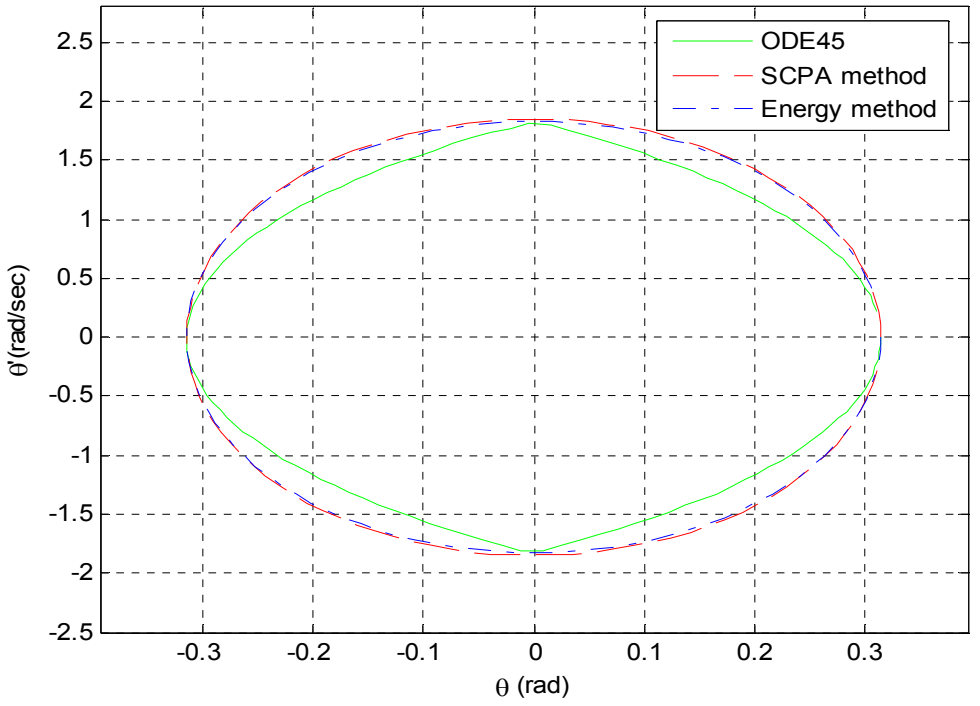

Figure 16. Phase diagram $\alpha=\pi/6$

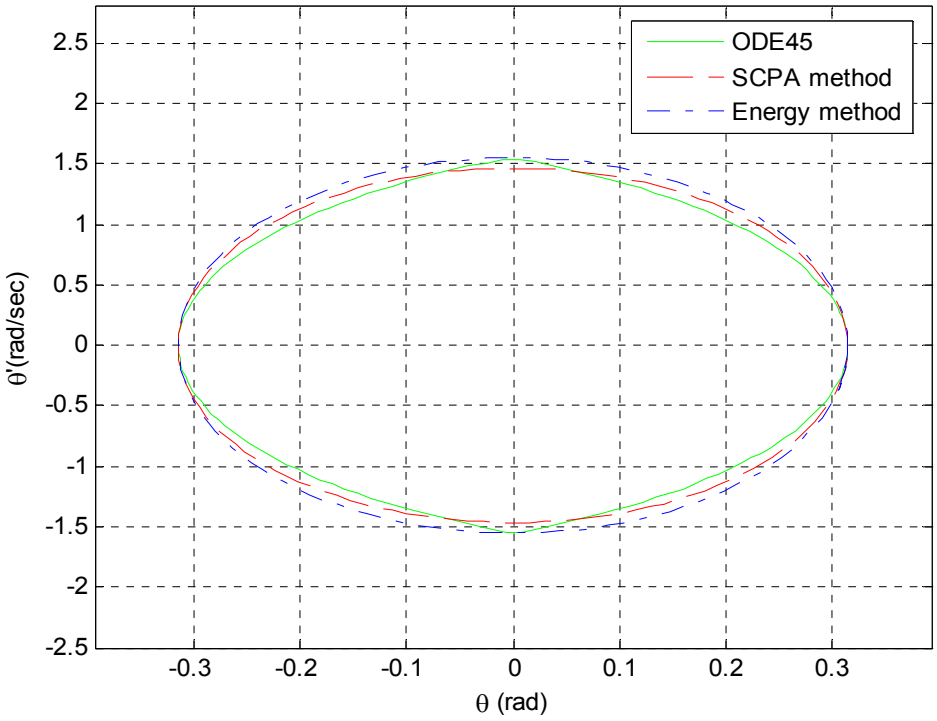

Figure 17. Phase diagram $\alpha=\pi/12$

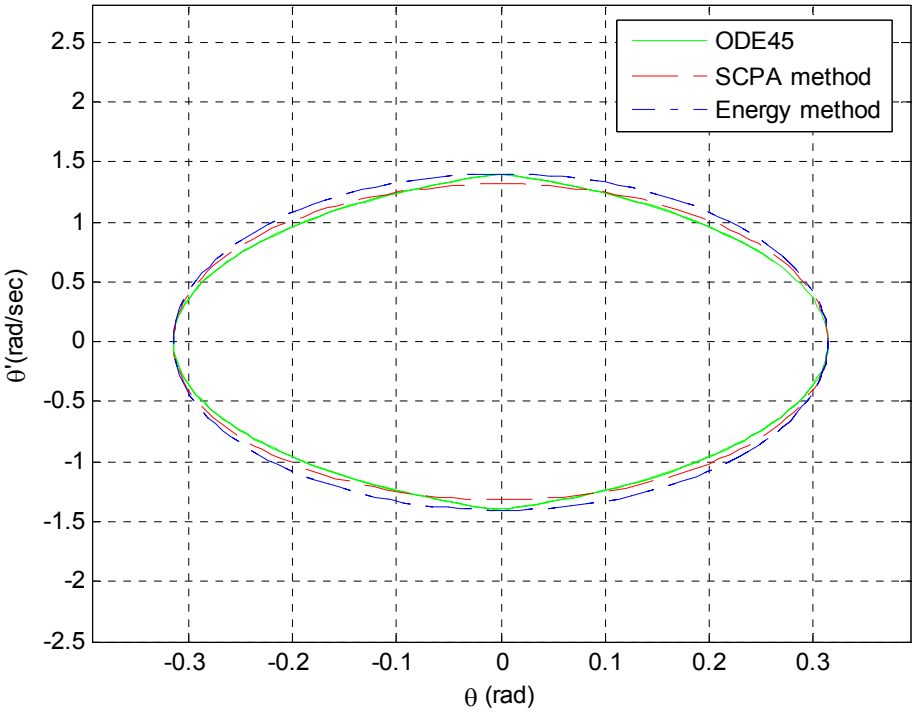

Figure 18. Phase diagram $\alpha=\pi/18$

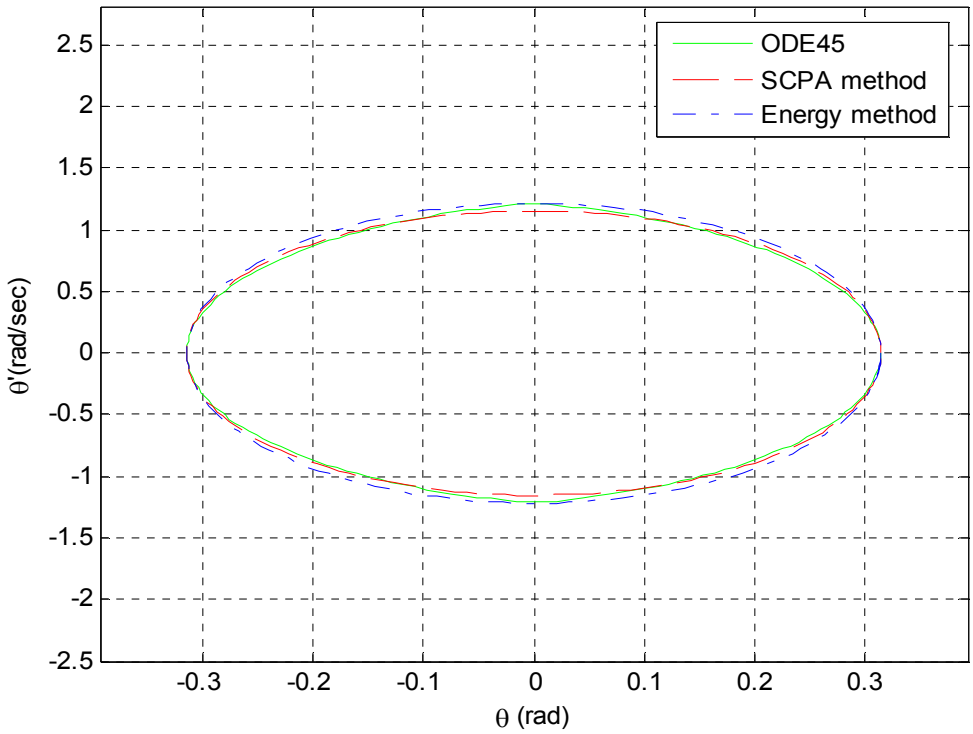

Figure 19. Phase diagram $\alpha=\pi/36$

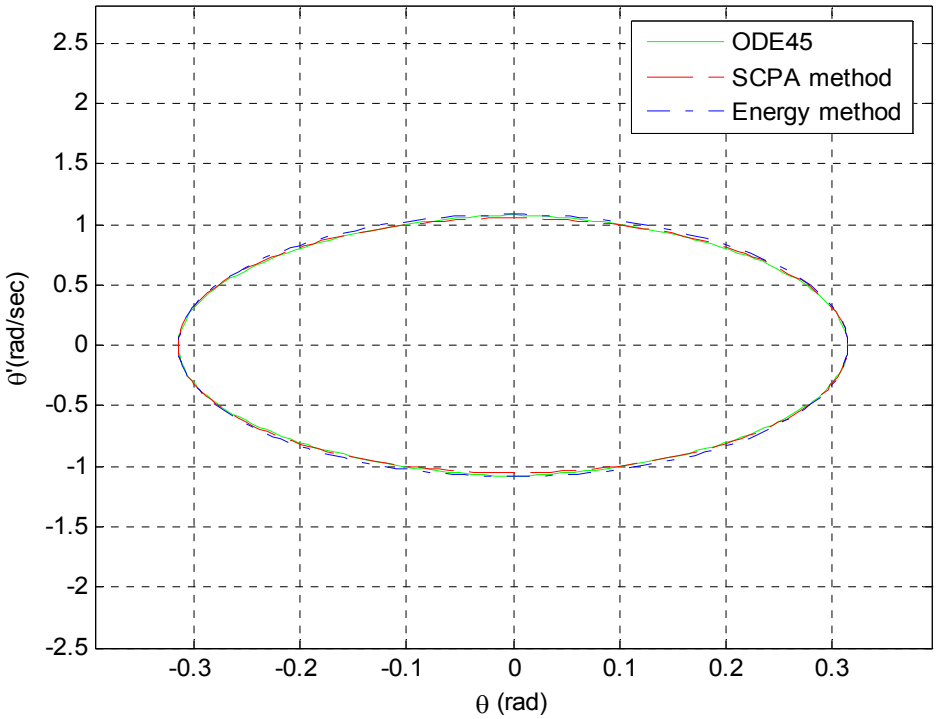

Figure 20. Phase diagram $\alpha=\pi/90$

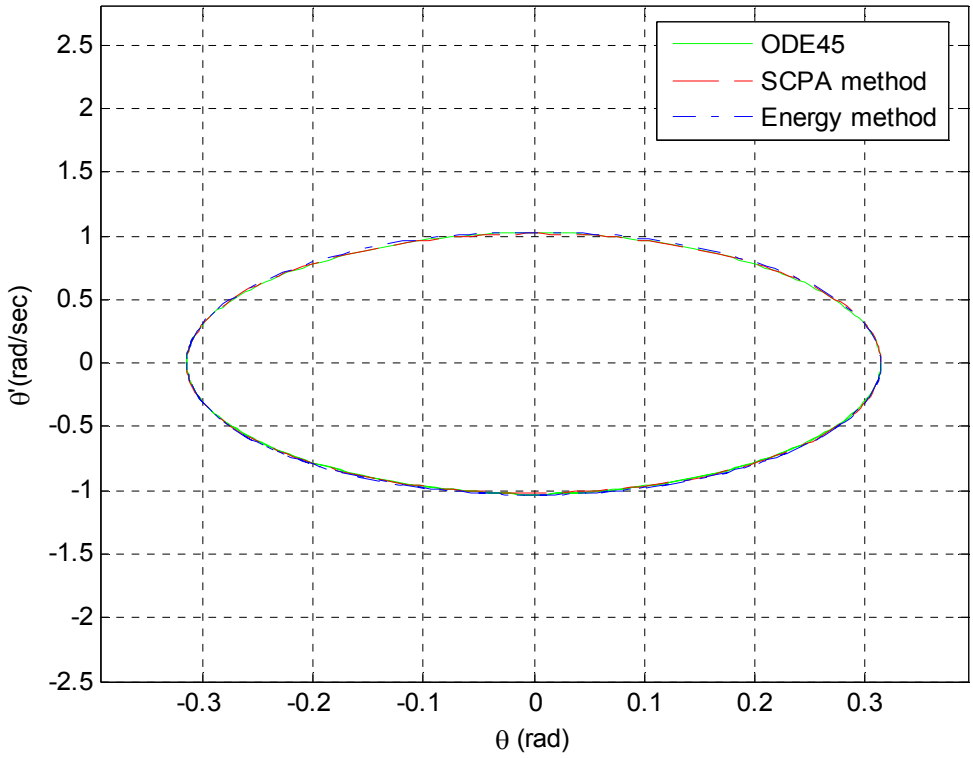

Figure 21. Phase diagram $\alpha=\pi/180$

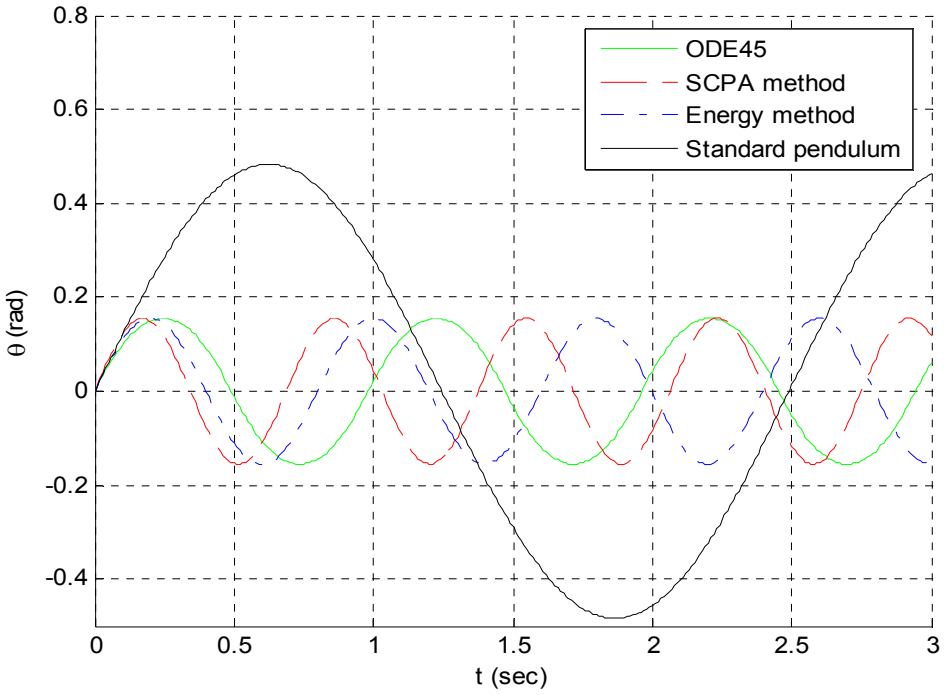

Figure 22. $\alpha=\pi/6$ with initial velocity

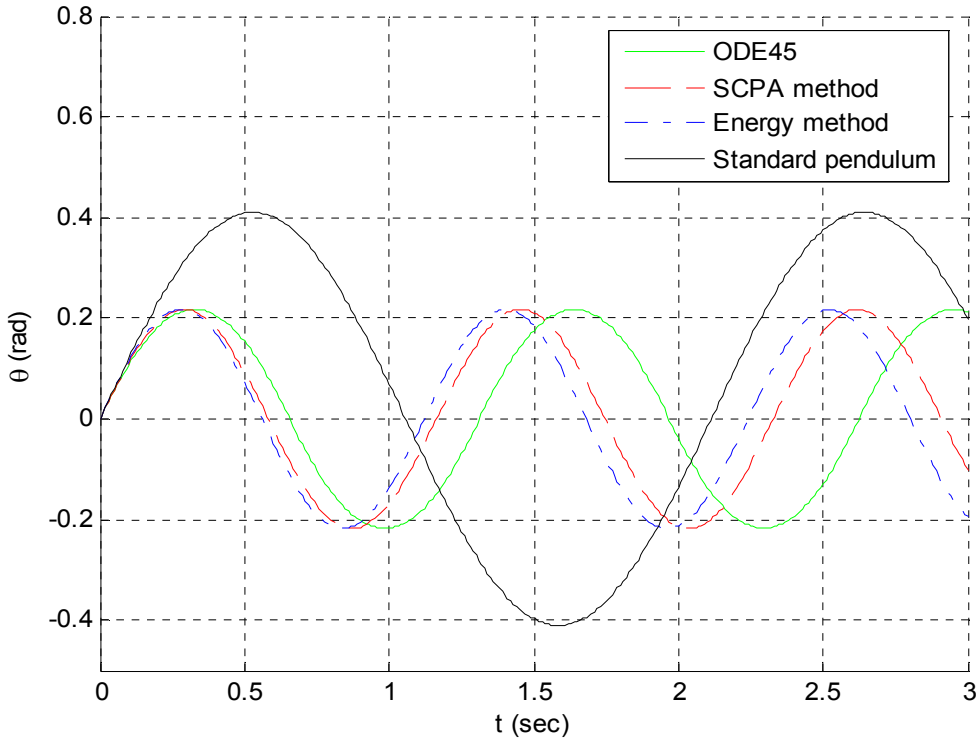

Figure 23. $\alpha=\pi/12$ with initial velocity

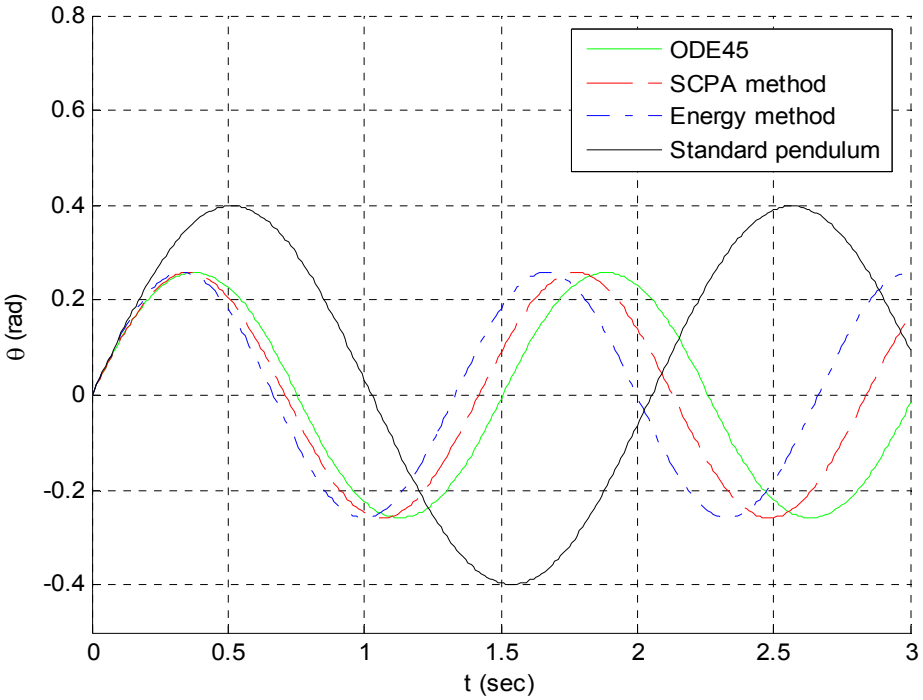

Figure 24. $\alpha=\pi/18$ with initial velocity

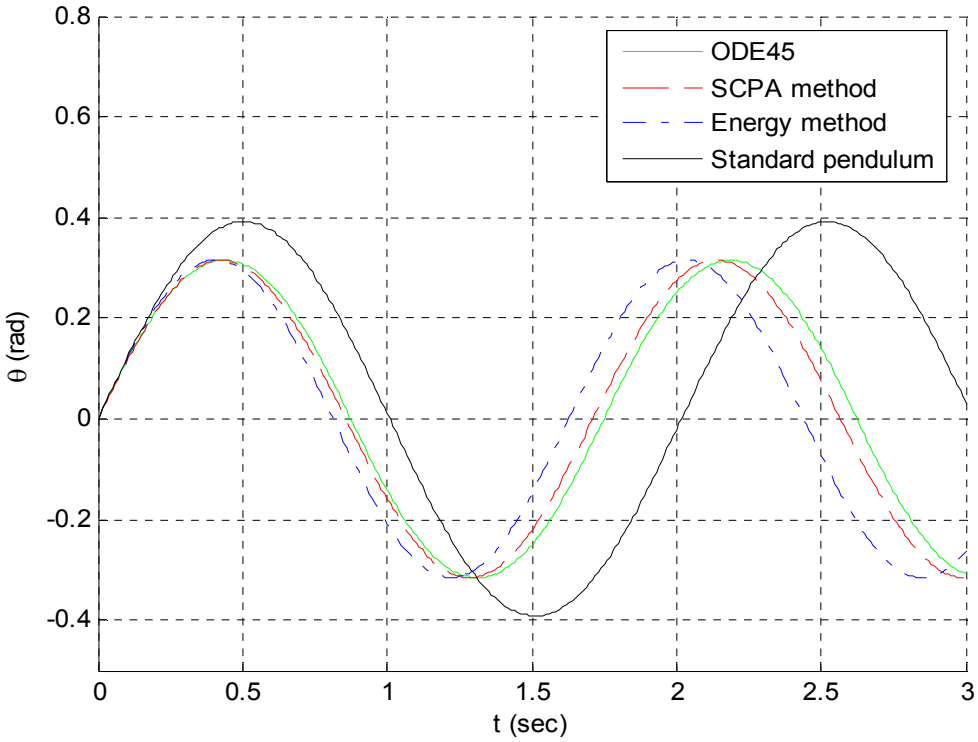

Figure 25. $\alpha=\pi/36$ with initial velocity

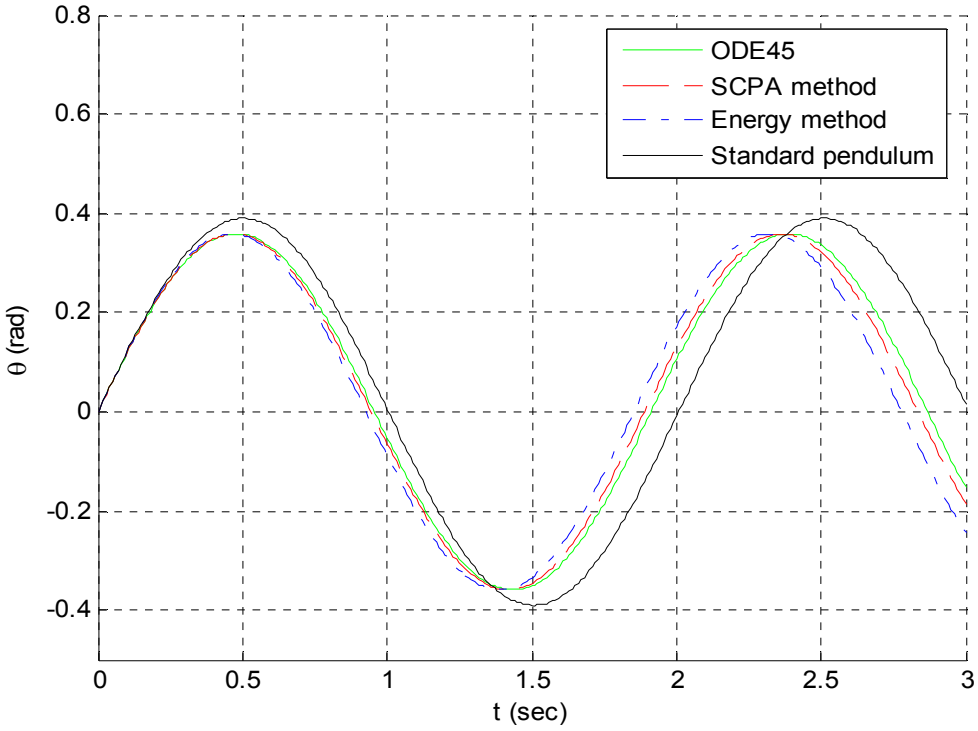

Figure 26. $\alpha=\pi/90$ with initial velocity

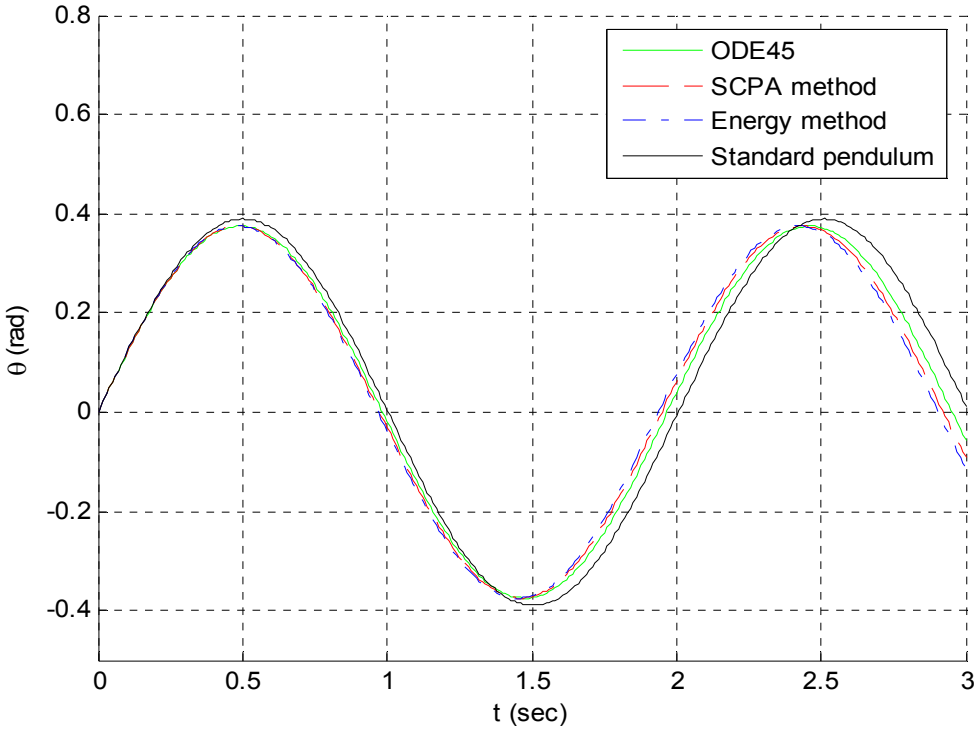

Figure 27. $\alpha=\pi/180$ with initial velocity

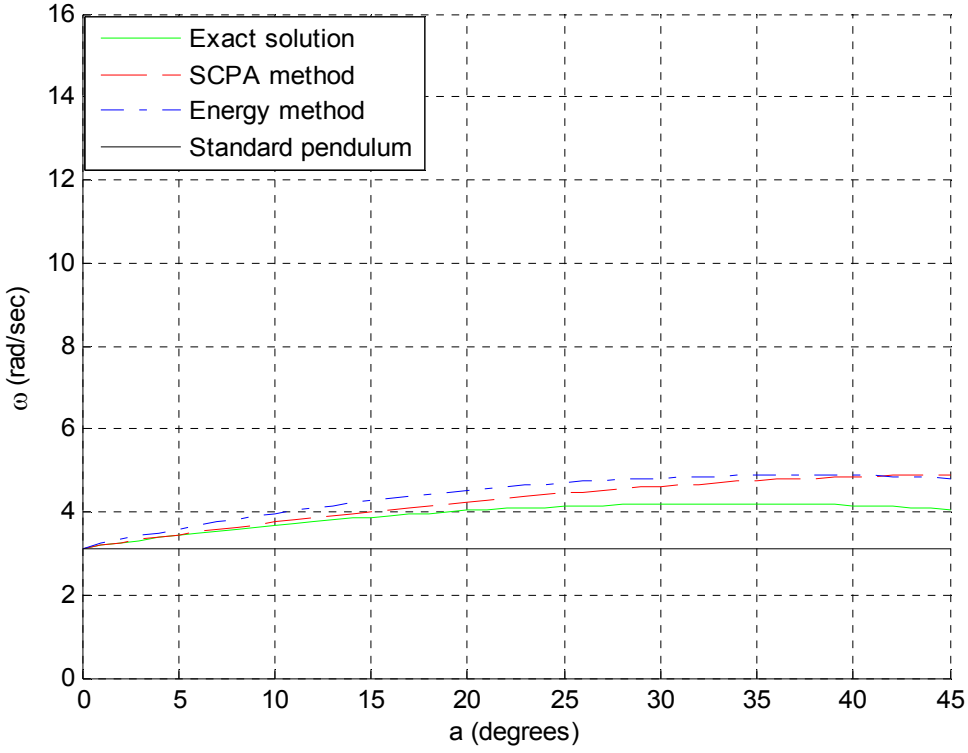

Figure 28. $\theta_0=\pi/6$

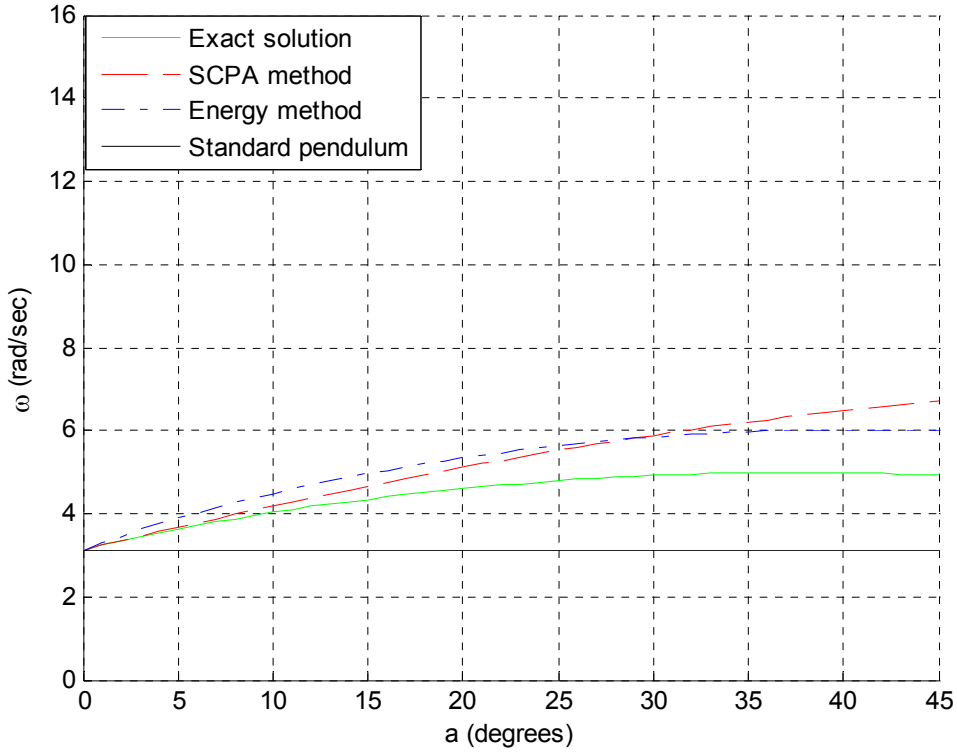

Figure 29. $\theta_0=\pi/10$

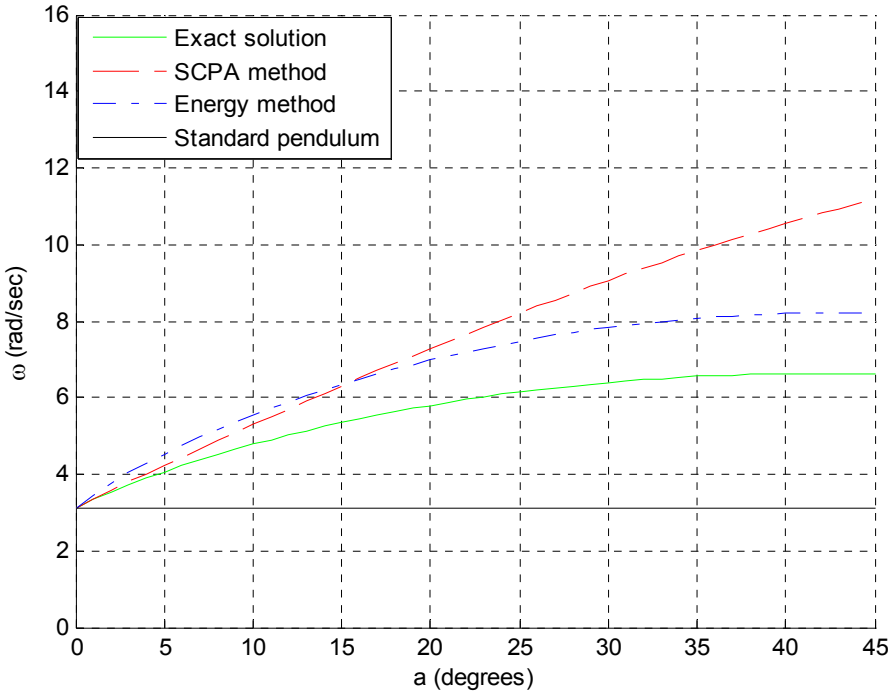

Figure 30. $\theta_0=\pi/20$

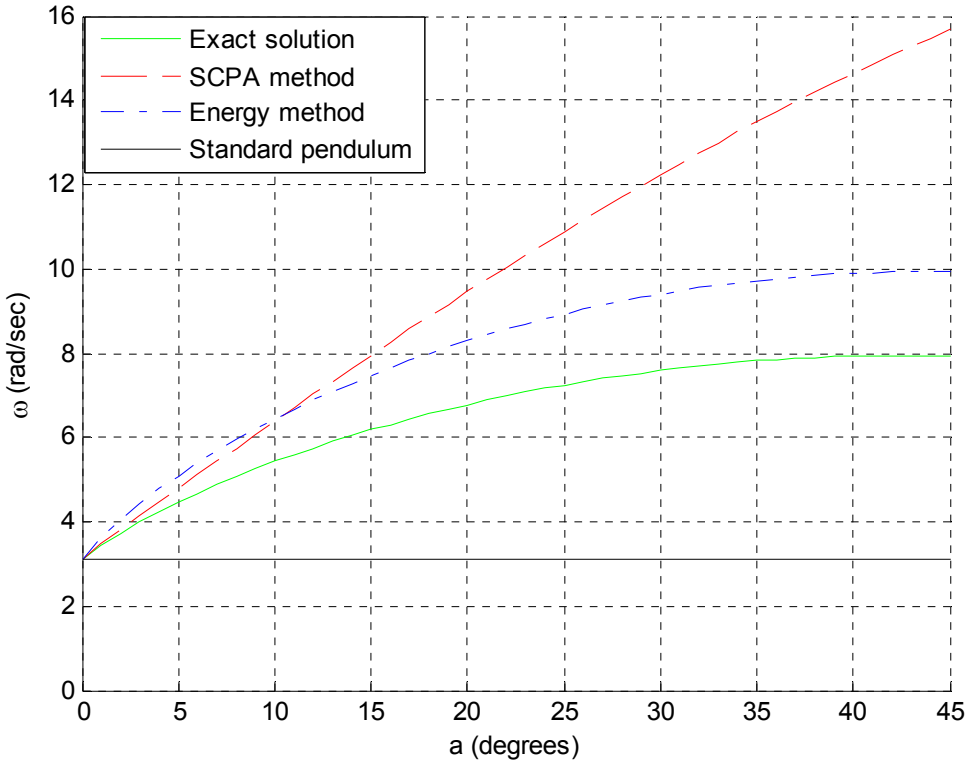

Figure 31. $\theta_0=\pi/30$

In Figures 28, 29, 30, and 31, we can evaluate the accuracy of the response prediction method with respect to the initial displacement θo and value of the characteristic angle α. According to equations (2.28), (2.35), and (2.41), the oscillation angular frequency depends on both parameters. Therefore, the four plots consider four arbitrary values for the initial angular displacements. This allows us to better appreciate the accuracy of the two prediction methods, SCPA and Energy, with respect to the main attribute of the 2-pendulum, which is angle α. We should note that the three equations are valid only for the linear approximations of the equations of motion. In addition, the graphs consider $\alpha \leq 45^0$, a restriction we already mentioned in the beginning of the analysis.

According to the plots, we conclude the following:

- The angular frequency ω of the 2-pendulum is greater compared to the frequency of the standard pendulum which has the same equivalent string length ℓ .
- A smaller maximum angular displacement for the 2-pendulum compared to the standard pendulum results from applying the same initial angular velocity.
- The discrepancy between the two predictions, and the exact calculations, is very low for small values of α, but increases for larger ones. More specifically, while the Energy method follows the exact solution slope trend (although providing higher predicted values), the SCPA method increases almost linearly.
- The SCPA method tends to provide more accurate predictions for larger values of θ_0. If θ_0 becomes too small, the discrepancy from the exact solution grows and, therefore, the predictions are incorrect.

9. Horizontal and Vertical Displacements

Despite the obvious advantage that the 2-pendulum possesses in terms of increased angular frequency of oscillation, increased restoring force, and reduced maximum angular displacements, it is worth mentioning a disadvantage: the differences of both horizontal and vertical displacements associated with angular displacements. The following figure depicts the relationship that governs the maximum horizontal and vertical displacements for $\theta_0=\pi/18$ and a range of α. This figure depicts that, for each angular displacement of the 2-pendulum, the horizontal and vertical displacements are smaller and greater respectively when compared to the standard pendulum. This is due to the two pendula's different reference systems used to measure their angular displacements. Therefore, to obtain a better appreciation of the comparison between the standard and the 2-pendulum, the previous examples of *a* will be plotted in terms of linear displacements instead of angular displacements (Figure 33).

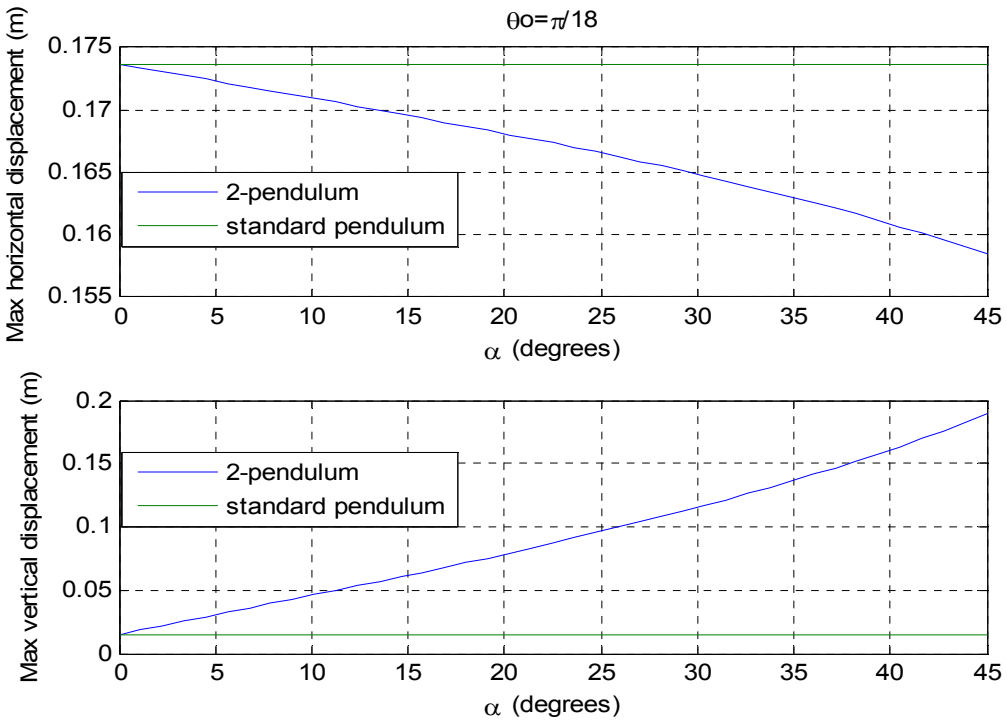

Figure 32. Variation of maximum vertical-horizontal displacements wrt characteristic angle *α*

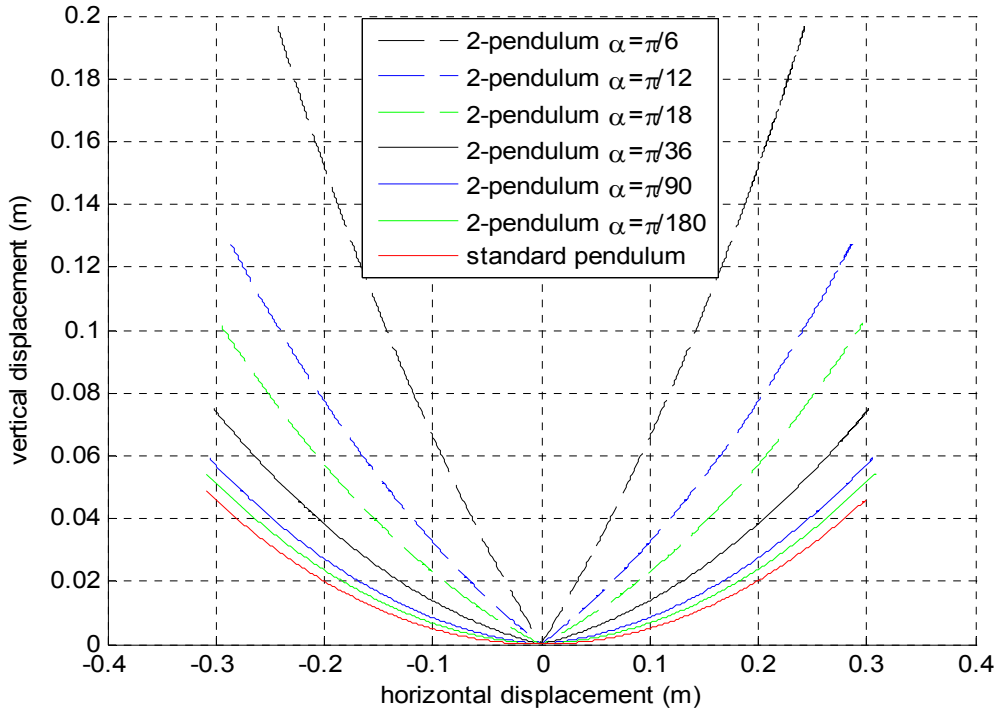

Figure 33. 2-pendulum's mass trajectories during oscillation

B. STRING TENSION INVESTIGATION

1. Analytical Formulation

Another important concept that requires further investigation is the tension applied on the string of the 2-pendulum. As already seen in equations (2.15) and (2.2), the restoring moment on the mass *m* is larger compared to the standard pendulum. Contrarily, the string tension has smaller values since two strings, instead of one, are used to suspend the mass. As pictured in Figure 3, while in equilibrium, positioning the string tension is dependant only on the value of the characteristic angle *α*

$$Ts = \frac{mg}{2\cos\alpha} \tag{2.42}$$

According to Figure 4, during swinging and while the sign of angle *θ* is continuous, the string tension can be computed as follows

$$Ts = Fc + \left\| mg\cos(\alpha + \theta) \right\| \tag{2.43}$$

where $Fc = \frac{mu^2}{l} = m\dot{\theta}^2 l$ is the centripetal force.

Equation (2.43) shows that the magnitude of static Ts ranges from $\frac{mg}{2} \le Ts \le \infty$, for $0 \le \alpha + \theta \le \frac{\pi}{2}$, proving that increasing the characteristic angle does not have only positive results in the overall design.

To determine the dynamic string tension, trigonometric equalities are applied and

$$Ts = m\dot{\theta}^2 l + \left\| mg\cos\alpha\cos\theta - mg\sin\alpha\sin\theta \right\|$$

To attempt to linearize the above equation for *θ*< $\frac{\pi}{10}$,

$$Ts = m\dot{\theta}^2 l + \left\| mg\cos\alpha\, sign\theta - mg\sin\alpha\theta \right\| \tag{2.44}$$

For the standard pendulum, the calculations are easier. Therefore, the tension applied on the string, while in equilibrium position, is

$$Ts = mg \tag{2.45}$$

and during the oscillation is

$$Ts = m\dot{\theta}^2 l + \|mg\cos\theta\| \tag{2.46}$$

or, for small amplitude oscillations,

$$Ts = m\dot{\theta}^2 l + mg \tag{2.47}$$

Since ode45 solves the exact differential equation of motion and, we already evaluated the accuracy of the predictions provided by the SCPA and Energy methods, the string tension simulation will be performed using the results provided by the ode45 method.

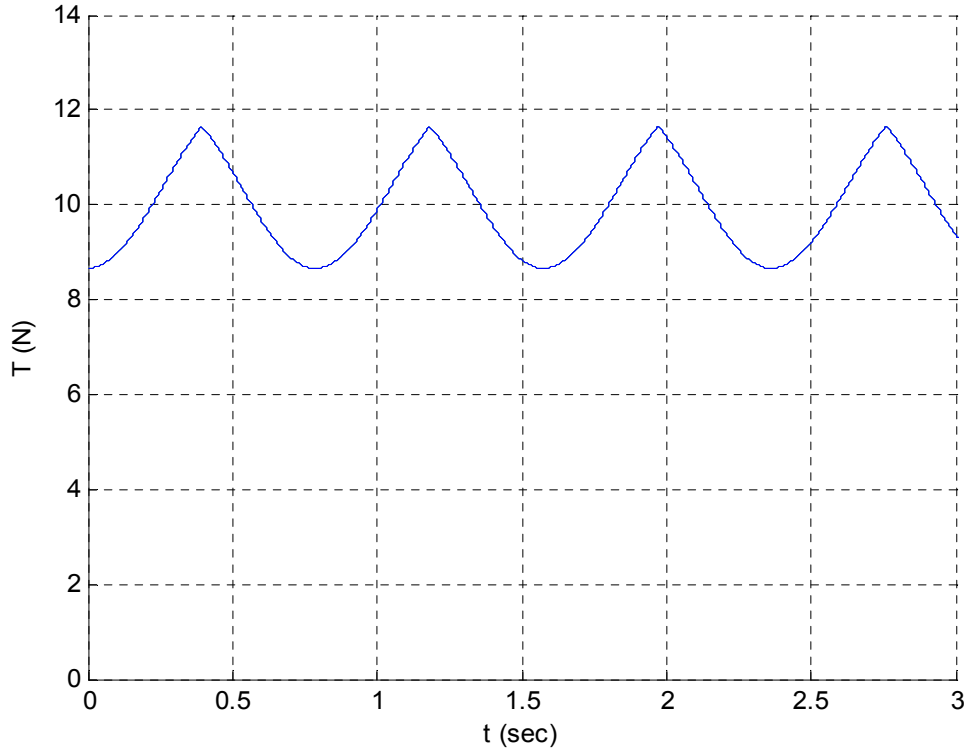

Figure 34. Tension for α=π/18 – θ_0=π/10

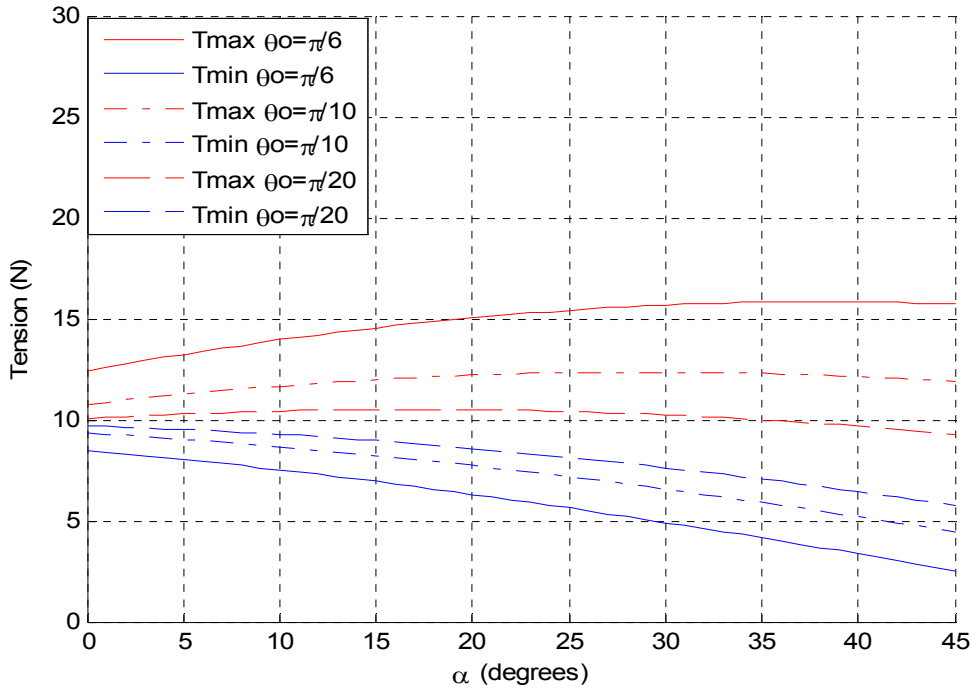

Figure 35. Maximum and minimum tensions

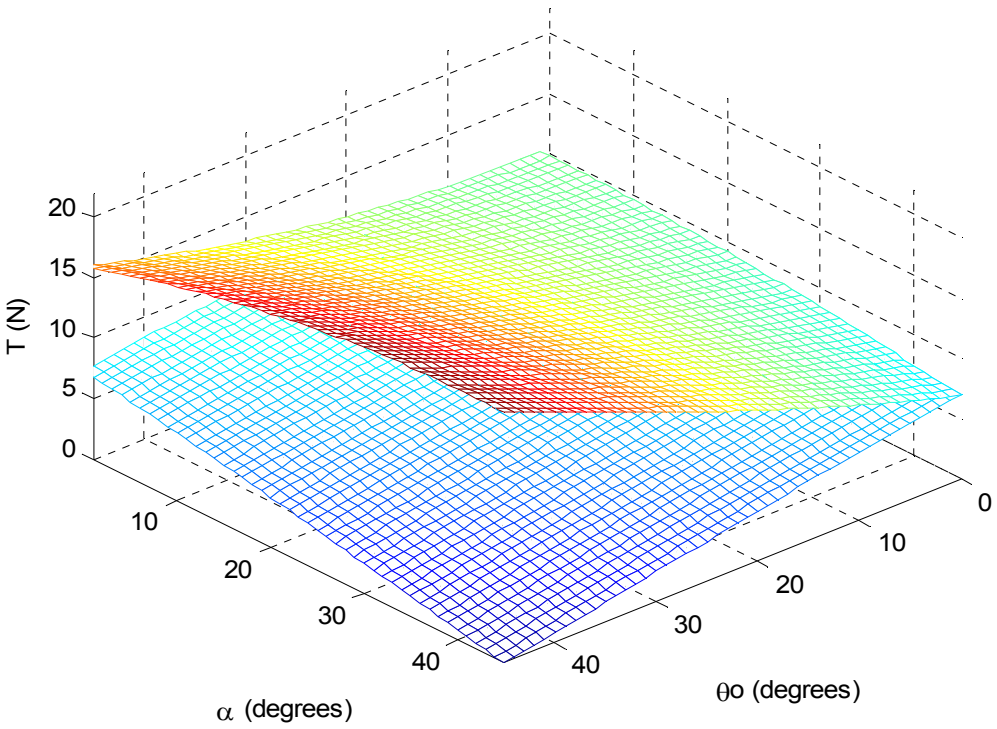

Figure 36. Maximum and minimum tensions 3-D variation

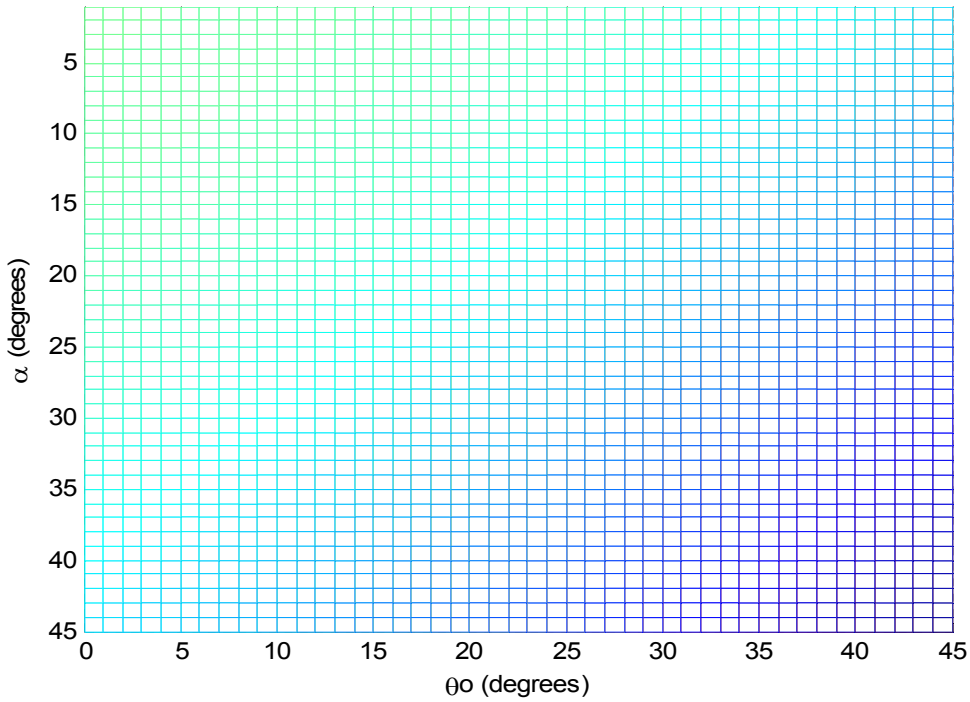

Figure 37. Minimum tension variation

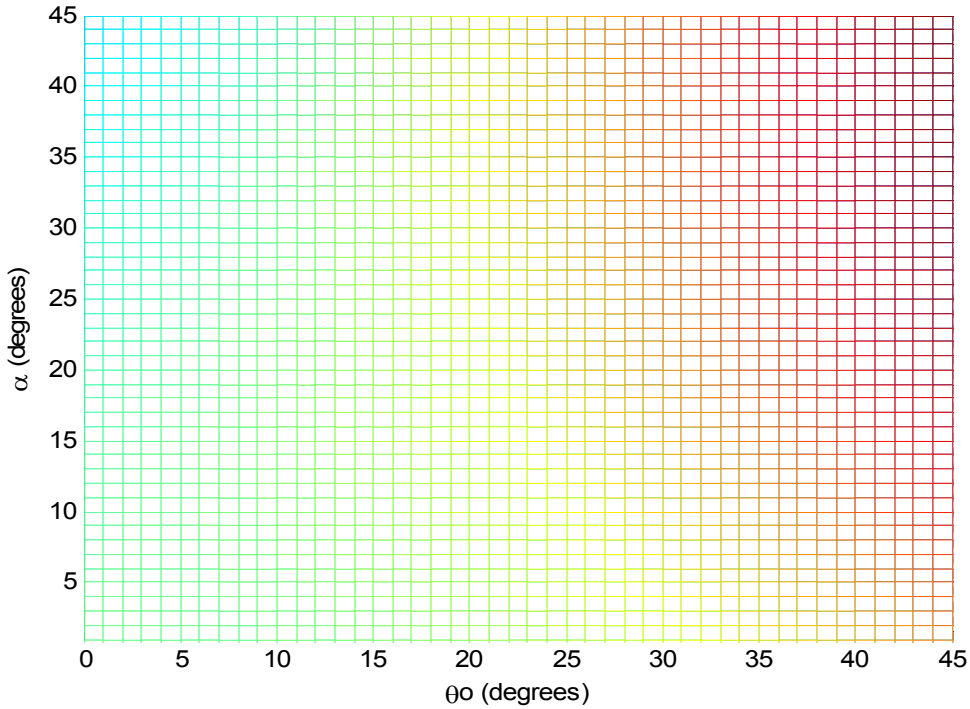

Figure 38. Maximum tension variation

In Figure 34, we should note that this is not the variation of tension in one of the strings, but, rather, the sum of them. Although, each string's tension is zero for every other half period, the fact that we describe the motion of the mass as an equivalent standard pendulum, with altered restoring force, and we do not distinguish the angular displacements with respect to the different strings from each other, leads us to treat the string tension with the same methodology. As a result, in each peak in Figure 34, the mass switches strings, and these exact switches take place when the string tension takes its maximum value.

From Figures 35-38, we can evaluate the variation of maximum and minimum tensions exerted on the strings with respect to both *α* and θo. On the one hand, as expected, increasing *θo* increases the *Tmax* and decreases *Tmin.* On the other hand, increasing *α,* and keeping *θo* constant, steadily decreases *Tmin.* An interesting point is that *Tmax* does not exhibit the same behavior. In Figure 39, we can see for which value of *α we* will have the maximum tension for a range of initial displacements.

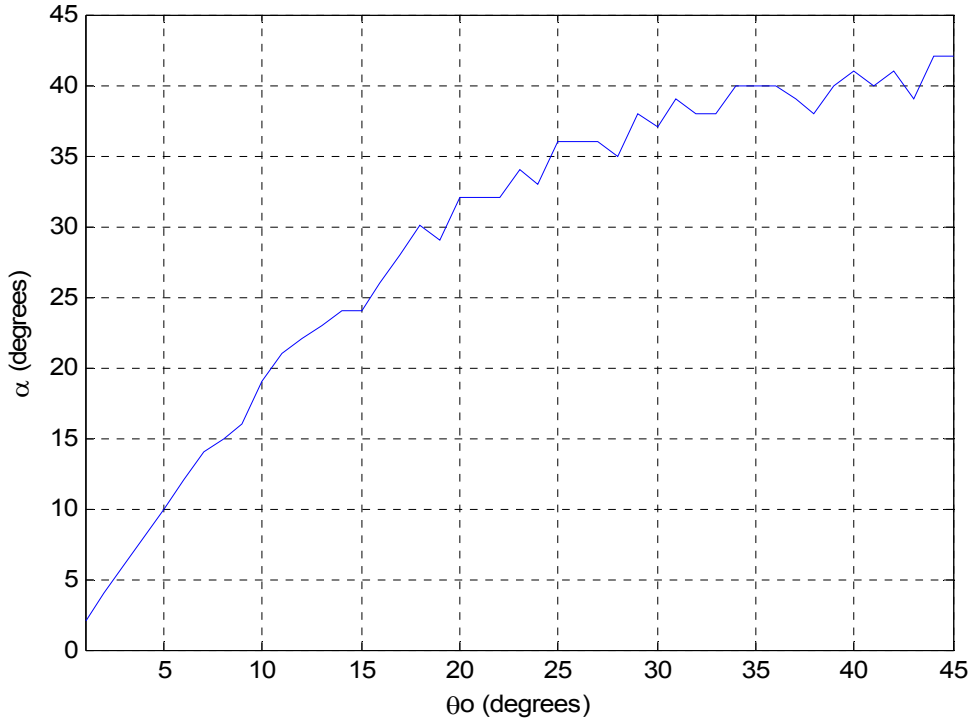

Figure 39. Characteristic angle producing the maximum tension for given θ_0

C. NUMERICAL SIMULATION

A very precise method to simulate the response of the 2-pendulum is with the use of the VISUAL NASTRAN 4-D software. In this section we attempt to validate the methods that we used to predict the 2-pendulum response in Chapter II, Section A, by comparing their results with those produced by VN 4-D.

1. VISUAL NASTRAN Software - SOLIDWORKS

To simulate the response of the 2-string pendulum in real time, a specific procedure had to be followed. This procedure was initiated by designing a model of a 2-string pendulum using SOLIDWORKS. This 3-D design software allows the exact geometrical design of structural models, which are compatible with the VN 4-D software. This model is then transferred into VN 4-D. The distinct attribute of VN 4-D is to solve differential equations in 3-D space and time. The final model used in VN 4-D was comprised of geometrical parts: mass properties -- developed in SOLIDWORKS --, and their assembly -- developed partially in SOLIDWORKS and partially in VN 4-D. The assembly constraints, which resulted in the rigidity of the platform where the 2-pendulum support points were positioned, were developed in SOLIDWORKS. The string constraints were developed in VN 4-D. Before initiating each VN 4-D run, the mass had to be positioned in the exact coordinates. This was the equivalent to a combination of initial angular displacement θ_0 and initial angular velocity $\dot{\theta}_0$ of the VN 4-D. The results of the simulations (in terms of mass position wrt which is the model's global system of axis, linear velocity, and tension of the strings) were then exported into Microsoft Excel spreadsheets. In addition, as defined in Figures 5 and 6, the mass position results were processed to obtain the angular displacement of the pendulum. Finally, all the above results were graphed with the aid of Matlab. This allowed comparing them with our analysis results.

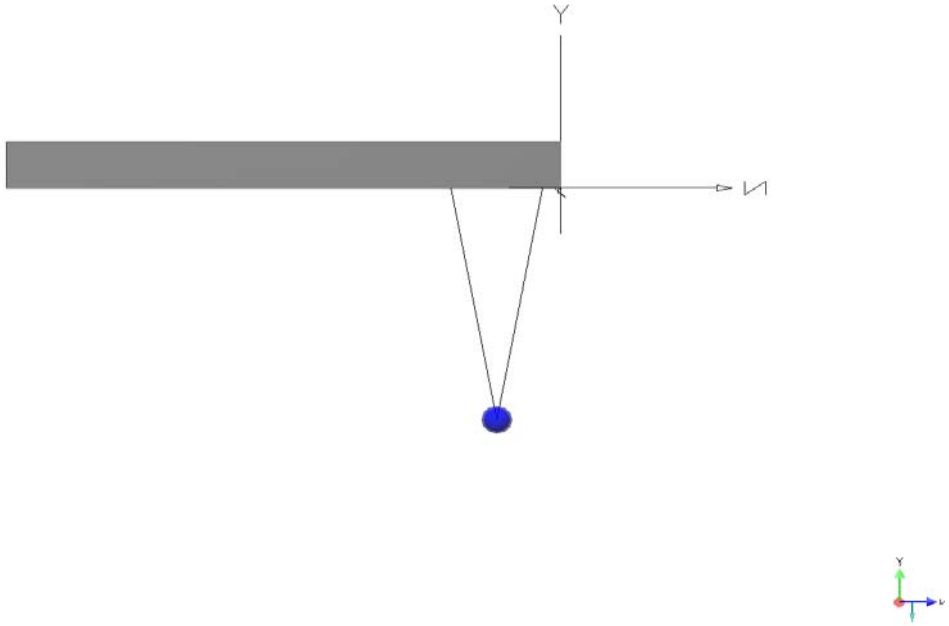

Figure 40. Front view of 2-pendulum VN 4-D model

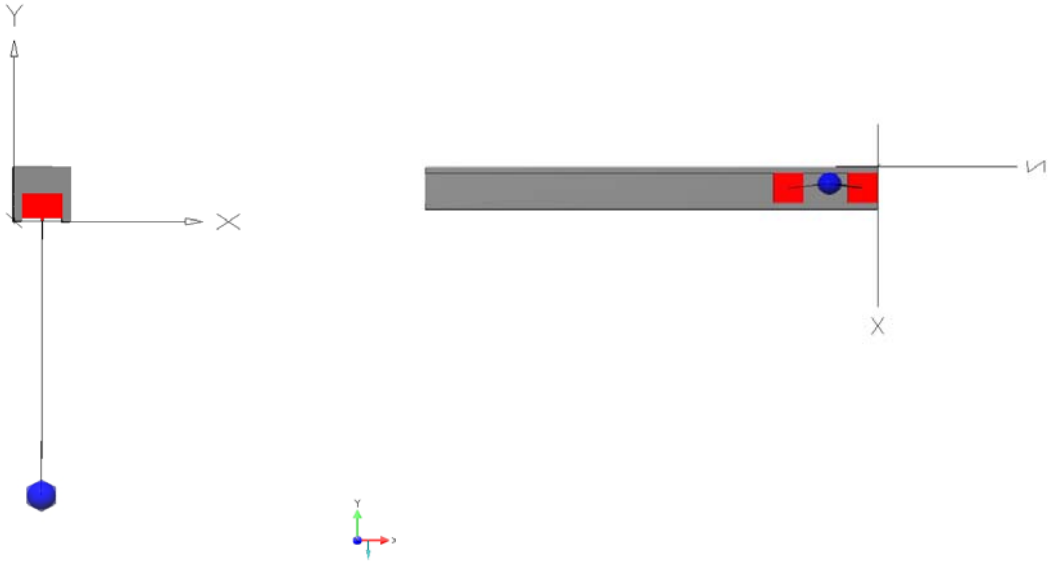

Figure 41. Side and bottom view of 2-pendulum VN 4-D model

The front, side, and bottom views of the model that were used for the VN 4-D simulations can be visualized in Figures 40 and 41. In this model, one can

adjust the mass of the mass (blue sphere) and the characteristic angle by altering the length of the strings (black lines) or the distance between the support points (red cubes). In addition, an initial displacement can be applied to the mass by precisely positioning the mass to a specific position in terms of an exact set of coordinates (X,Y and Z), with respect to the Cartesian global system of axis represented by the black arrows. It should be noted that the exact positioning of the mass is not possible. For a few of the first time steps of the simulation, this results in a slight deviation of the expected results. The numerical integration parameters that were used in all the VN 4-D simulations are:

A/A	Simulation Parameter	Value
1	Integration Method	Kutta-Menson
2	Animation Time Frame	0.001 sec
3	Integration Step	Variable - 0.0005 sec
4	Steps per Frame	2

Table 1. VN 4-D simulation parameters

The above parameter combination yielded results that were tabulated in a time-step size of 0.001sec. This way compatibility was achieved with the previously presented results using the developed Matlab code.

In the following example, we chose to solve the case of the 2-string pendulum of characteristic angle $\alpha = \frac{\pi}{18}$ and initial angular displacement $\theta_0 = \frac{\pi}{10}$. For consistency we used $\ell = 1\text{m}$, while the actual string length was $l = 1.0154\text{m}$.

The VN 4-D results will be compared to the predictions of the three methods described in Chapter II, Section A, numbers 6 and 7, for the same values of ℓ , l ,α and θ_0.

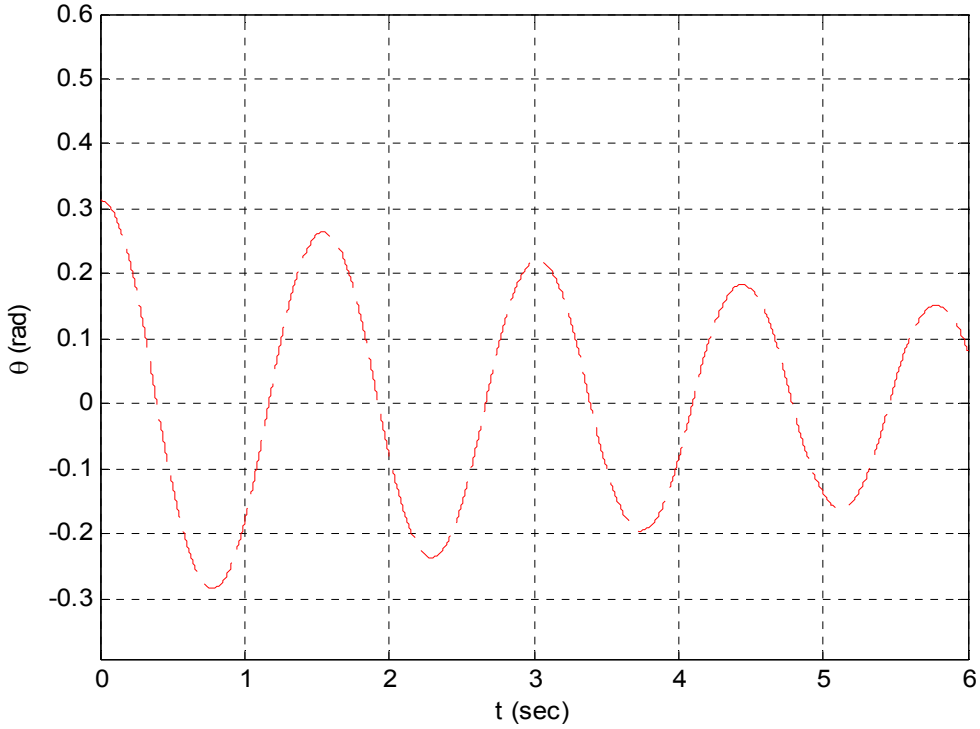

Figure 42. VN 4-D – $\alpha=\pi/18$ – $\theta_0=\pi/10$

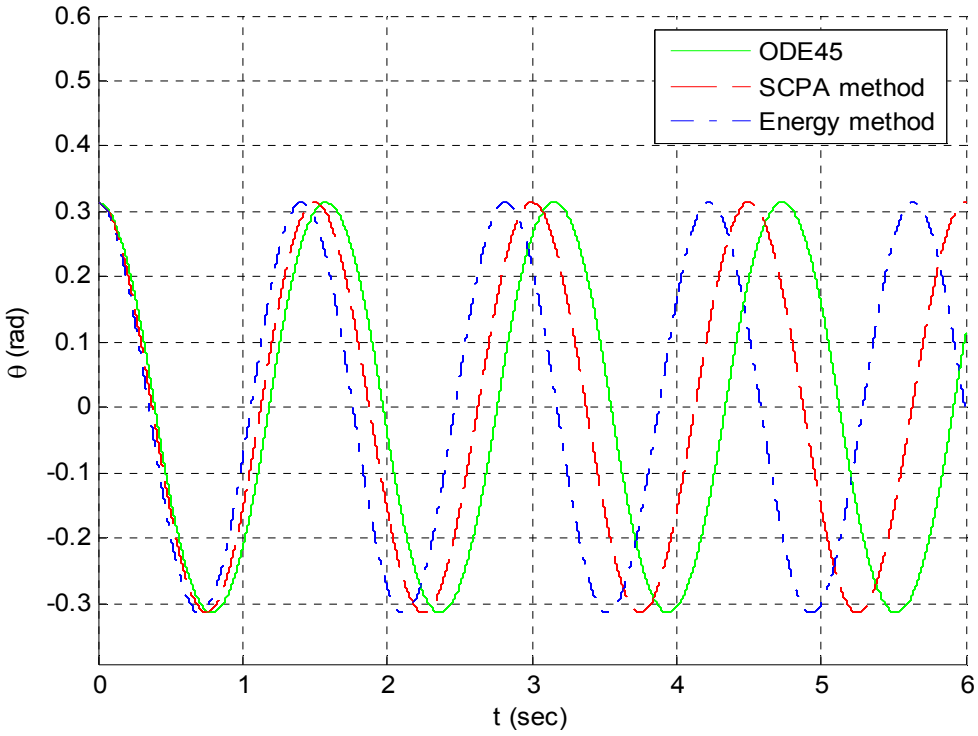

Figure 43. Theoretical predictions for $\alpha=\pi/18$ and $\theta_0=\pi/10$

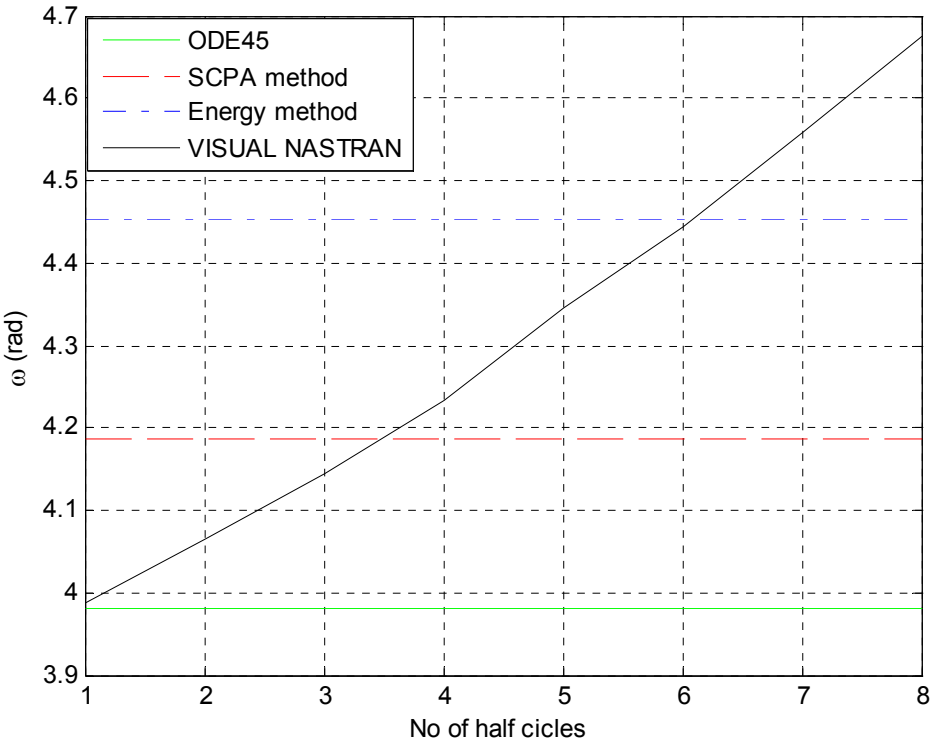

Figure 44. Angular frequency comparison for $\alpha=\pi/18$ and $\theta_0=\pi/10$

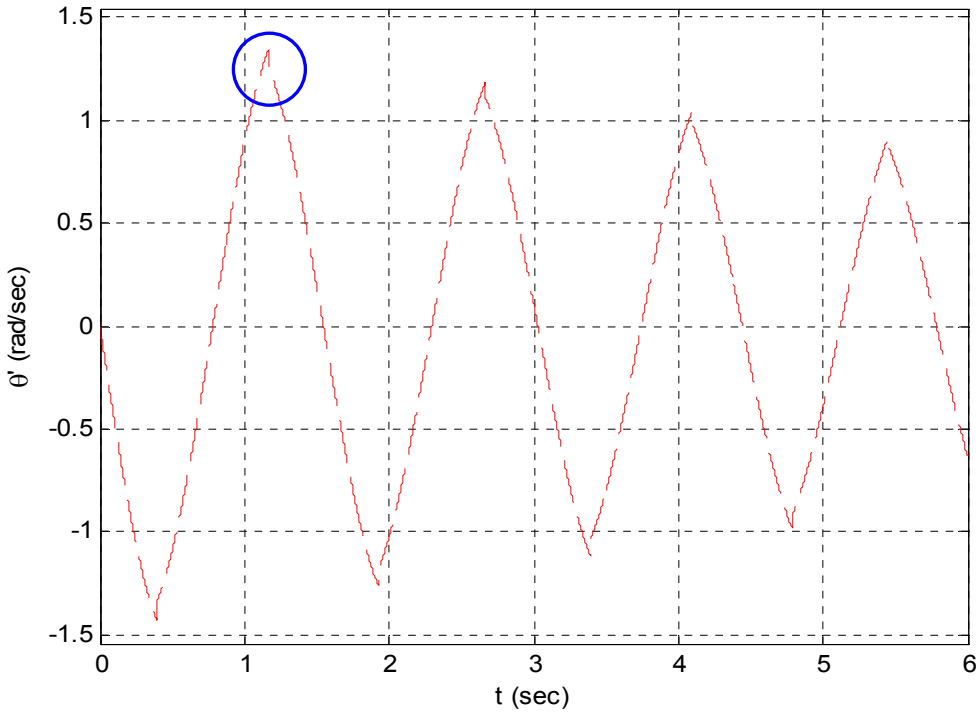

Figure 45. Typical velocity variation for 2-pendulum

2. Evaluation of Results

In Figures 42 and 43, we can see the oscillation prediction using VN 4-D and the analytical methods, respectively. To more precisely appreciate the discrepancies between those methods' predictions, Figure 44 will be used. We can clearly distinguish from Figure 44 that VN 4-D predicts that, with time, the amplitude of oscillation decreases and the angular frequency increases. Further, for angular frequency, the comparison was indispensable. We decided to plot the angular frequency every half-cycle to be able to capture the decrease in ω in the most possible detail. From Figure 44, we can realize that ode45 provided the most accurate prediction for the ω for the first half–cycle, compared to SCPA and Energy methods. Nevertheless, after that point, the ω of VN 4-D started to increase almost linearly. This increase in ω was not captured by the three other methods.

To understand why this increase in ω takes place, we plotted the angular frequency of oscillation predicted by VN 4-D. As seen in Figure 45, for every half-cycle when the mass reached the point where it switched strings about which it oscillated, the velocity magnitude dropped by a certain amount. This discontinuity, just before and after the switch point in velocity magnitude, raises questions about energy conservation. In the following sections, we are going to investigate in more details the dynamics that surface at this point and their effect in terms of energy loss of the oscillation mass.

D. THE REAL 2-PENDULUM

1. Velocity and Force Vector Analysis-Impact Dynamics

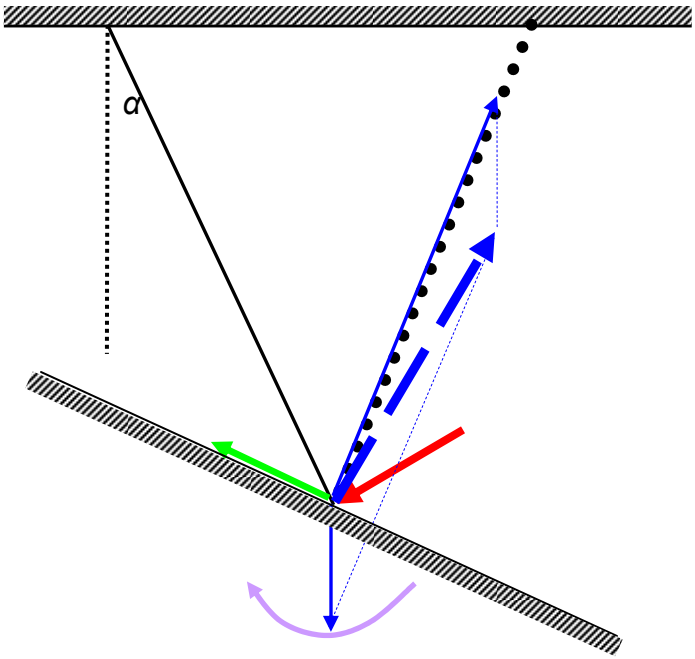

Figure 46. Velocity and force vectors for 2-pendulum at switch point

In Figure 46, we can visualize the forces that act on the mass during this change and contribute to the switch of center of rotation, as already depicted in Chapter II, Section A, number 1 and Figure 7. Nevertheless, in this section we

are going to emphasize the way that the forces change the direction of the linear velocity from $\vec{V}b$ to $\vec{V}a$, as well as other effects, such as energy loss and termination of oscillation for α>45°.

According to Figure 46, the dynamics of our problem strongly resemble the dynamics of a ball colliding with a rigid wall. For α<45°, the only known parameters are: i) vector $\vec{V}b$ (direction, orientation, and magnitude), ii) the direction and orientation of vector $\vec{V}a$, iii) the weight of the mass, and, finally, iv) the direction and orientation of T_{inst}. Based on these parameters, we will attempt to predict the response of the real 2-string pendulum.

2. The Real 2-Pendulum with α<45

In our initial analysis, we are going to assume that the string is stiff enough and allows no elongations even under large values of tension forces. Therefore, we are not considering displacements along the direction of the string. Nevertheless, we are going to assume that an amount of energy is lost during this switch of velocity direction. Following the discussion of Chapter II, Section A, for this case the pendulum will oscillate ideally in a manner that was already analyzed in that section. In addition to the previous analysis, we are going to take into account the energy losses that occur at the switch point due to the introduction of nonlinearity. For this purpose, we will apply the equation of motion of oscillation between two arbitrary consecutive switch point impacts, i and $i+1$, which is equation (2.18), $\ddot{\theta}+\frac{g}{l}\sin\theta\cos\alpha+\frac{g}{l}\cos\theta\sin\alpha\,\mathrm{sign}\,\theta=0$, and the simple impact rule at the switch point i, for instance. The simple impact rule states that the impacts are instantaneous and the energy loss would be represented by a reduction in the velocity magnitude. That is,

$$\dot{\theta}_{+i}=r\dot{\theta}_{-i} \tag{2.48}$$

where r is the coefficient of restitution at impact [3].

Referring to Figure 46, we could be more specific and precise while calculating the energy absorption during impacts described by equation (2.48). As already mentioned, the impact exerted on the mass by the string can be described by a collision of a rigid ball with a rigid wall. Since the weight of the mass is a conservative force, it does not absorb any energy during the collision. Therefore, T_{inst} is the only force that contributes to energy absorption, which equals the work done by force *W* during the period of contact [4]. Moreover, the sole velocity components that are affected by *W* are those parallel to the direction of *Tinst*. Dealing this time with linear velocities (instead of angular), we can see that the components of $\vec{V}b$ and $\vec{V}a$, which are parallel to the direction of the string causing the impact, (heavy dotted line in Figure 46), are $\vec{V}b_{aff}$, with a magnitude of $\left\|\vec{V}b_{aff}\right\| = \left\|\vec{V}b\right\|\cos(90-2a)$, and $\vec{V}a_{aff}$, with a magnitude of $\left\|\vec{V}a_{aff}\right\| = \left\|\vec{V}a\right\|\cos(90-2a)$. Finally, using the notation $\vec{V}a = \vec{V}_{+i}$, $\vec{V}b = \vec{V} - i$,:$\vec{V}a_{aff} = \vec{V}_{aff} + i$ and $\vec{V}b_{aff} = \vec{V}_{aff} + i$

$$W = \frac{\Delta T_{inst}\Delta t[V_{aff-i} + V_{aff+i})]}{2} \tag{2.49}$$

where

$$\Delta T_{inst} = T_{e-i} - T_{c+i} = \frac{\Delta p}{\Delta t} = p_{e-i} - p_{c-i} \tag{2.50}$$

and Δt is the infinitesimally small time duration of the impact.

In equation (2.50), T_{e-i} is the impact force exerted by the mass *m* on the string causing instant elongation. T_{c+i} is the impact force exerted by the string contracting and releasing its strain energy on the mass *m.* p_{e-i}, p_{c-i} are the respective impulses. Consequently, in the circumstance where $T_{c+i} = T_{e-i}$, there would be no energy loss during impact and we would deal with a completely elastic collision.

In addition to the above, from the point of view of the conservation of momentum and considering, once more, only the velocity components that are parallel to the string direction, during the phase of the instantaneous elongation of the string

$$MV_0 = MV_{aff-i} + p_{el} \tag{2.51}$$

where V_0 is the velocity of the mass at the end of the elongation phase, p_{el} is the reaction impulse force that is exerted on the mass, and M is the effective mass which equals $M = \frac{mm'}{m+m'}$. In this case, m' is the fictitious mass of the object onto which the mass *m* collides. Since this object is represented by a rigid wall whose momentum is infinite, we assume that $m' = \infty$. Therefore, $M = m$ and, since $V_0 = 0$, the magnitude of the impulse force is

$$p_{el} = mV_{aff-i}$$

or

$$p_{el} = mV_{-i}\cos(90-2\alpha) = T_{e-i}\Delta t \tag{2.52}$$

where Δt is the infinitesimally small time duration of the impact [3].

The next step should be to calculate the $p_c = T_{c+i}\Delta t$. If we conduct a similar analysis, we would see result

$$p_c = mV_{+i}\cos(90-2\alpha) = T_{c+i}\Delta t \tag{2.53}$$

Looking more closely at equation (2.53), we realize that if $T_{c+i} \neq 0$ after the string-change point, there would be a linear velocity component parallel to the string's direction in addition to the linear velocity component perpendicular to the new string's direction. The second component promotes the smooth circular motion of the mass, while the first component would push the mass to deviate from the circular orbit. Consequently, if we want to predict the path of the mass that would not deviate from the regular pendulum's oscillation path we will assume that

$$T_{c+i} = 0$$
$$V_{+i}\cos(90-2\alpha) = 0 \tag{2.54}$$

Thus, equation (38) should be manipulated and corrected as follows

$$\dot{\theta}_{+i} = \frac{V_{+i}}{l} = \sqrt{\frac{(V_{+i}\sin(90-2\alpha))^2 + (V_{+i}\cos(90-2\alpha))^2}{l^2}} =$$

$$\sqrt{\frac{(V_{-i}\sin(90-2\alpha))^2 + (rV_{-i}\cos(90-2\alpha))^2}{l^2}} =$$

$$\frac{V_{-i}}{l}\sqrt{(\sin(90-2\alpha))^2 + (r\cos(90-2\alpha))^2} \Leftrightarrow$$

$$\dot{\theta}_{+i} = \dot{\theta}_{-i}\sqrt{(\sin(90-2\alpha))^2 + (r\cos(90-2\alpha))^2} \tag{2.55}$$

where, considering (2.55), the coefficient of restitution should be $r = 0$.

The cancellation of the parallel component of the velocity during impact is not only an assumption that facilitates the work of predicting the response of a real 2-pendulum, but, also, a very good approximation. The sudden impulse shock that is applied on the string from the mass produces a compressive wave that propagates throughout the length of the string. This wave will finally die out under the effect of damping. Damping in almost inextensible strings may be caused by several factors, such as viscosity of the air and internal friction. The velocity of elastic wave propagation within the string mass is similar to the speed of sound [5][6]. Therefore, by comparing this velocity with the time scale associated with the periodic motion of the pendulum, the time required for the completion of the energy loss related to this shock is negligible. All the above support the validity of the assumption that the coefficient of restitution, associated with the impact of the mass on the string, is zero.

Finally, from equations (2.54) and (2.55), the amount of energy loss at the switch point is

$$E_{loss} = \frac{1}{2}mV^2{}_{i-1}((1-r)\cos(90-2\alpha))^2 \tag{2.56}$$

The system of equations (2.18) and (2.48) or (2.55) can be solved numerically using a constant time step of $\Delta t = 0.001\text{sec}$ and the forward difference scheme. This takes into account equation (2.48) or (2.55). The Matlab code, Program_3.m, provides the solution to the system of equations for predetermined number of periods.

In the following sections, we are going to compare the prediction of the 2-pendulum response in terms of angular displacement, angular velocity, and string tension. We will use the above m-file (solving equations (2.18) and (2.55)) combined with those obtained from VISUAL NASTRAN. Additionally, we will plot the phase diagrams for each method, as well as the discrepancy between the prediction and the VISUAL NASTRAN simulation results. This will better validate the precision of the Matlab code.

a. Angular Displacement and Velocity Comparison

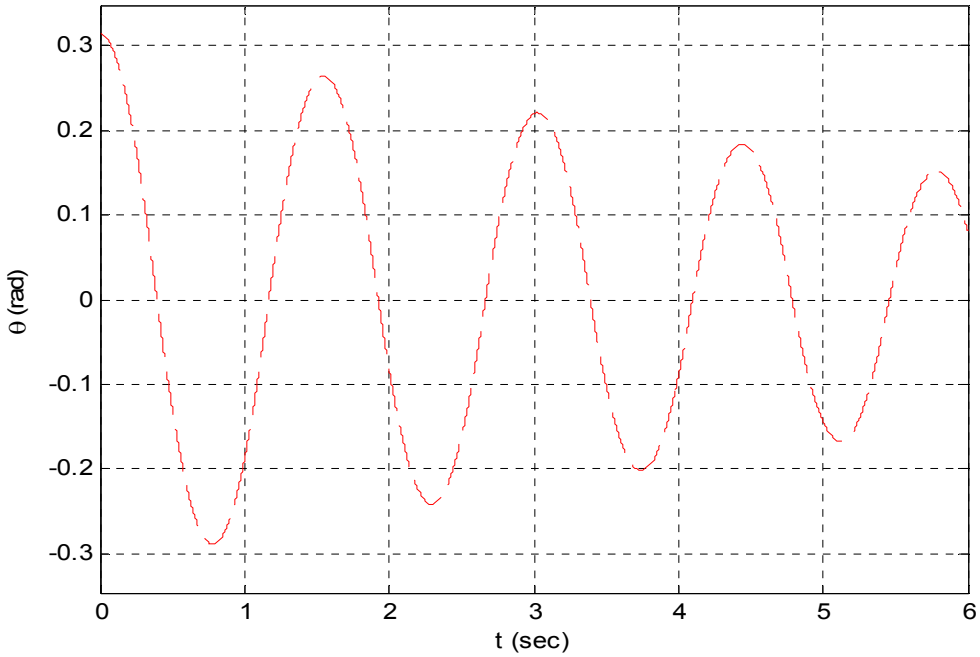

Figure 47. VISUAL NASTRAN - $\alpha=\pi/18$ – $\theta_0=\pi/10$

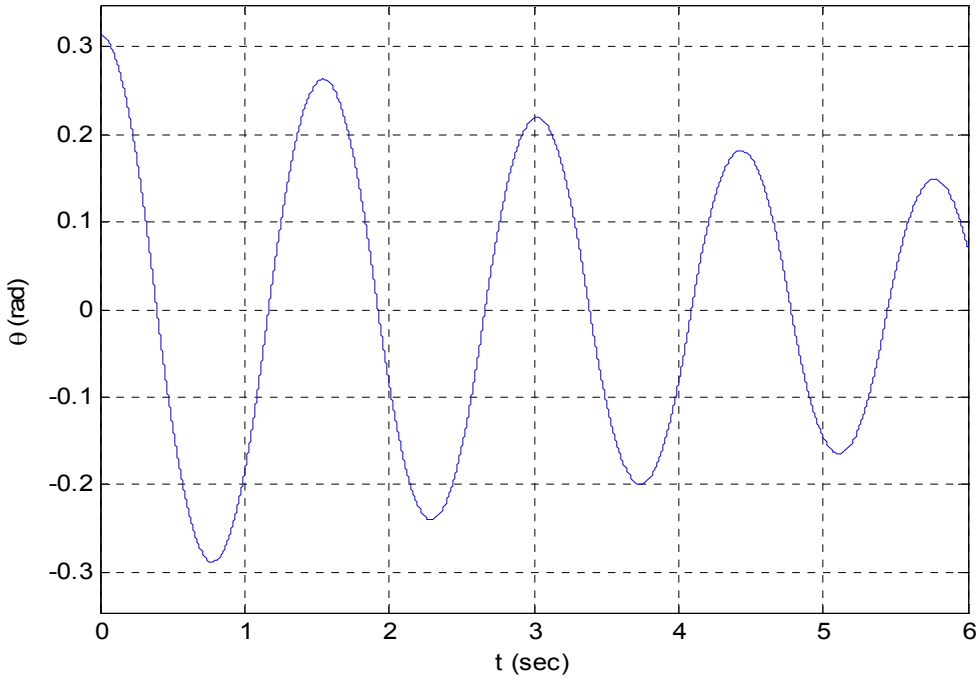

Figure 48. MATLAB - $\alpha=\pi/18$ - $\theta_0=\pi/10$

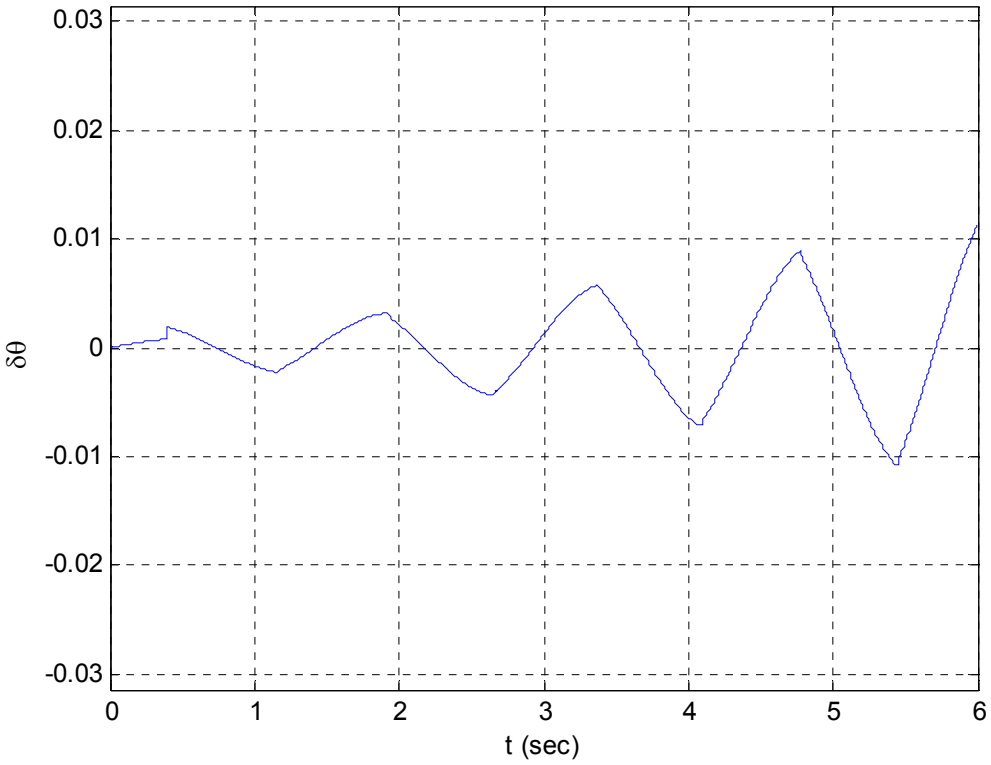

Figure 49. Prediction discrepancy

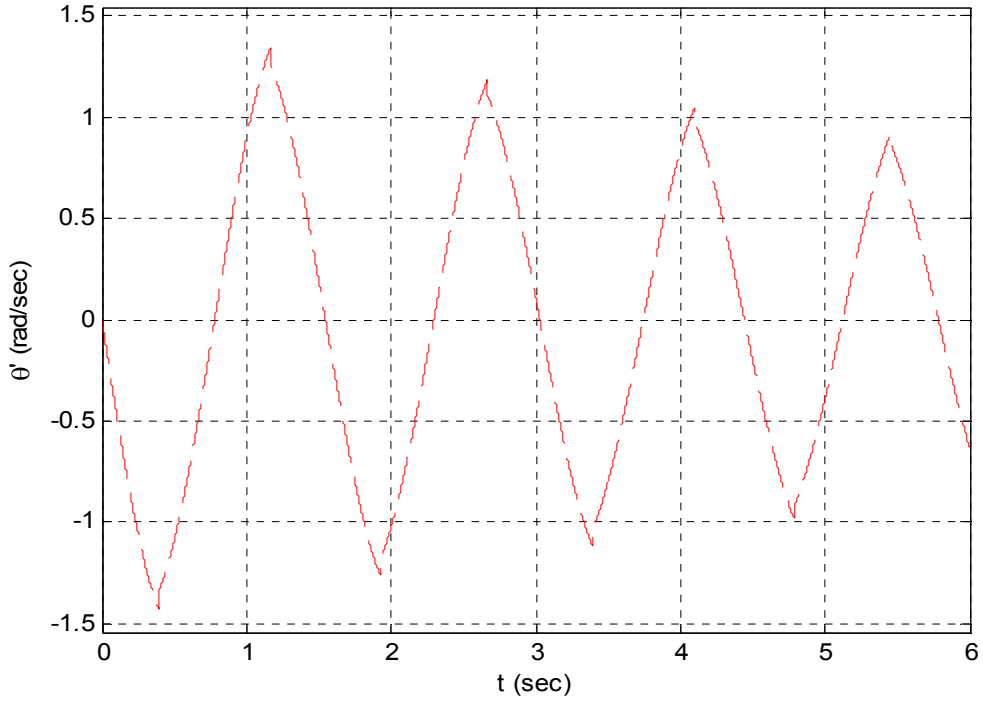

Figure 50. VISUAL NASTRAN - $\alpha=\pi/18$ - $\theta_0=\pi/10$

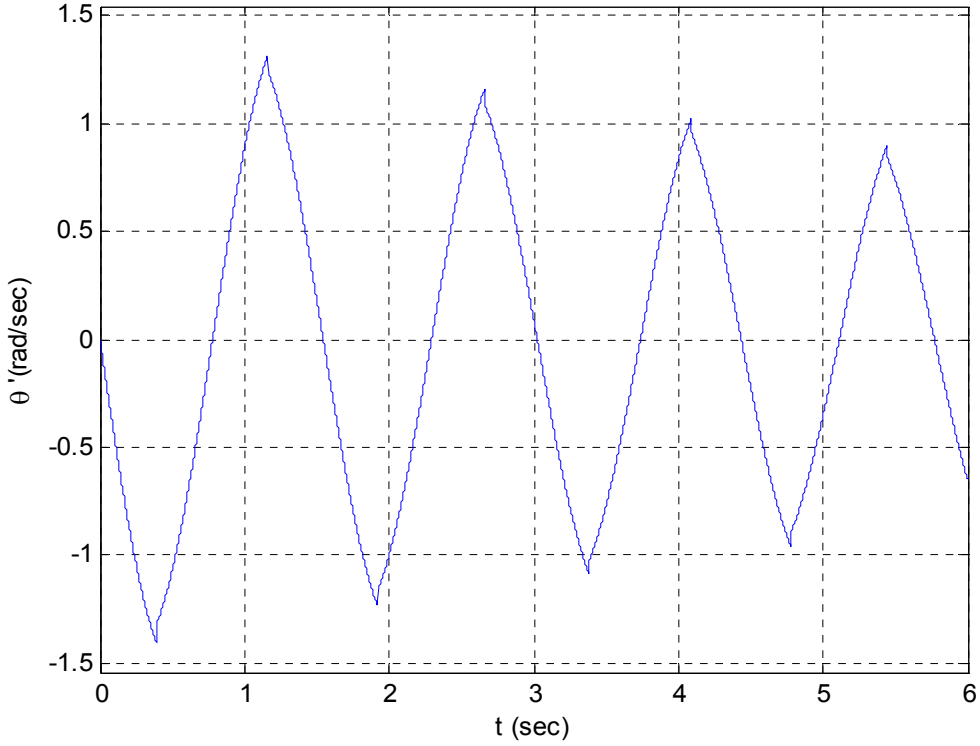

Figure 51. MATLAB – $\alpha=\pi/18$ – $\theta_0=\pi/10$

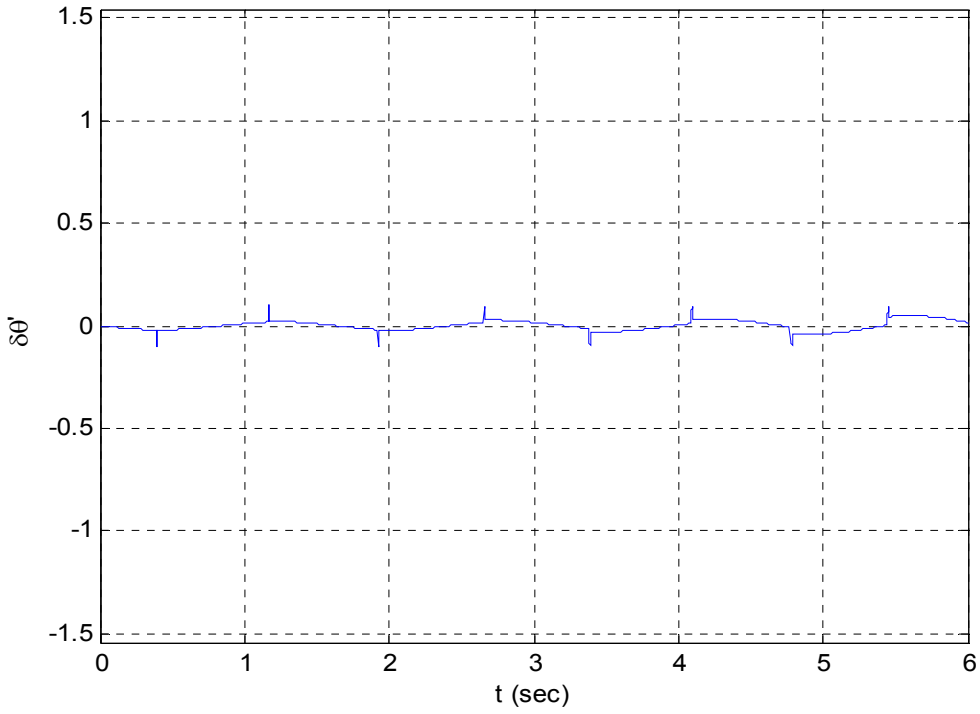

Figure 52. Prediction discrepancy

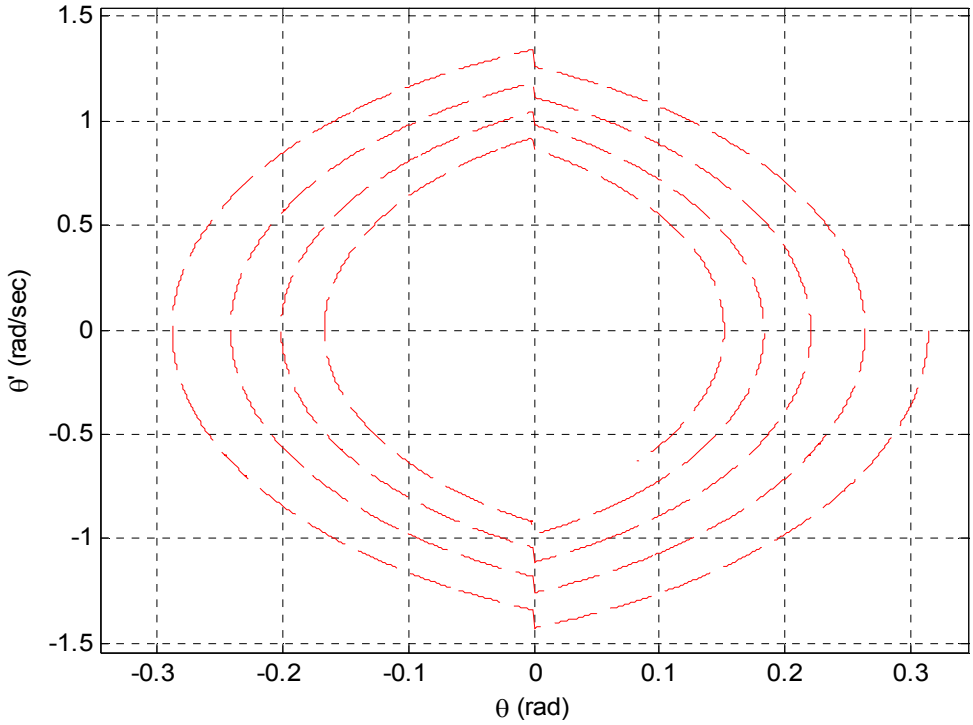

Figure 53. VN 4-D - Phase diagram – $\alpha=\pi/18$ – $\theta_0=\pi/10$

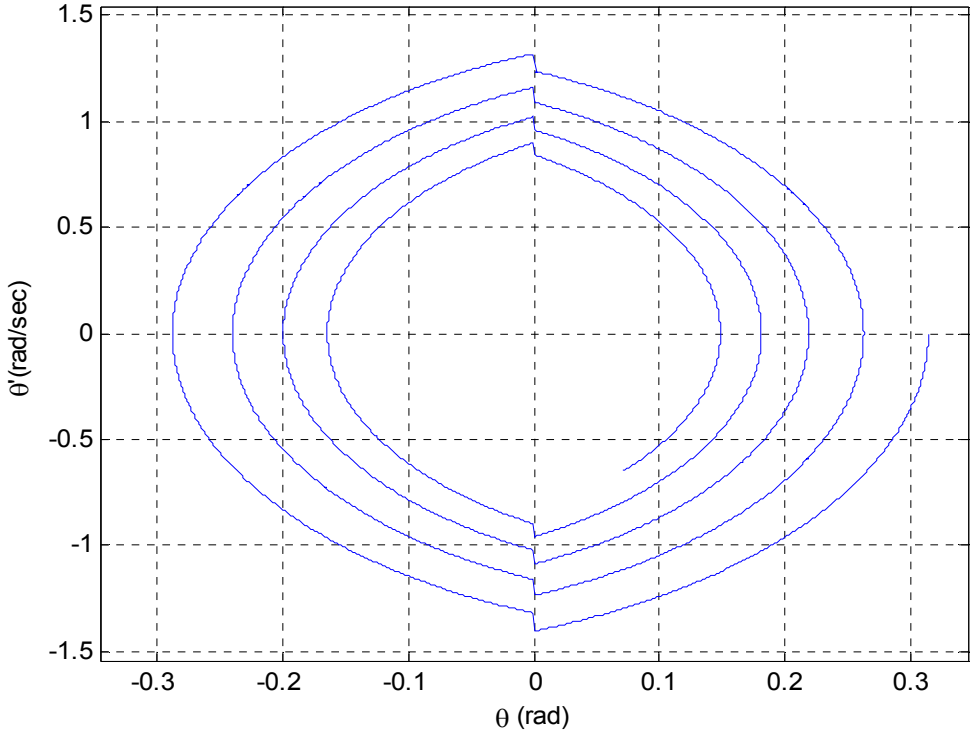

Figure 54. MATLAB – Phase diagram – $\alpha=\pi/18$ – $\theta_0=\pi/10$

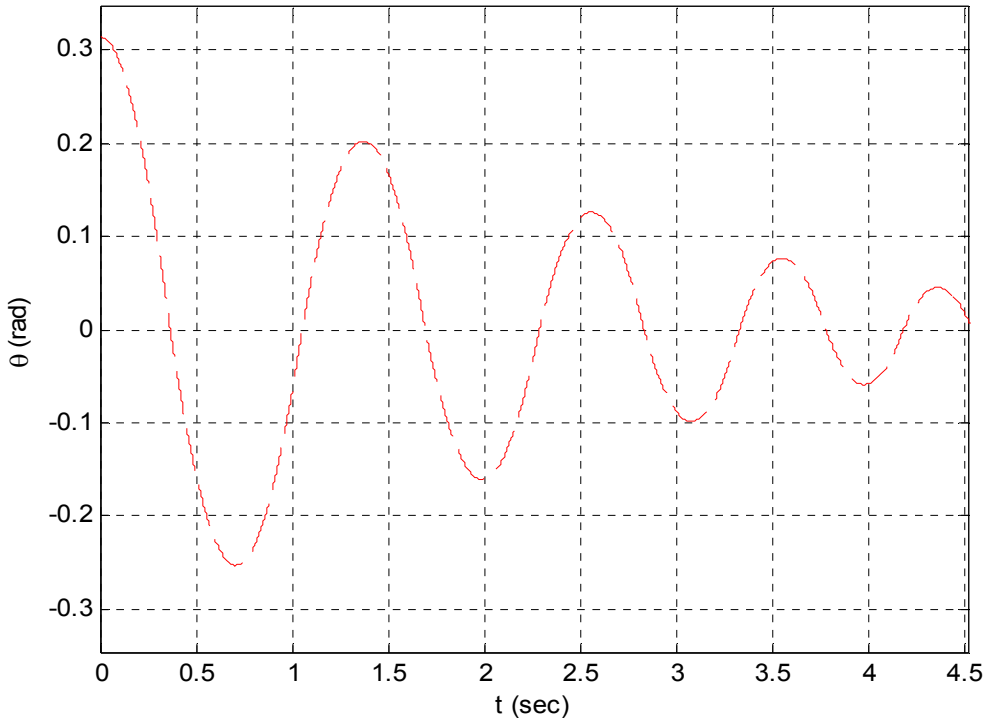

Figure 55. VISUAL NASTRAN - $\alpha=\pi/12$ - $\theta_0=\pi/10$

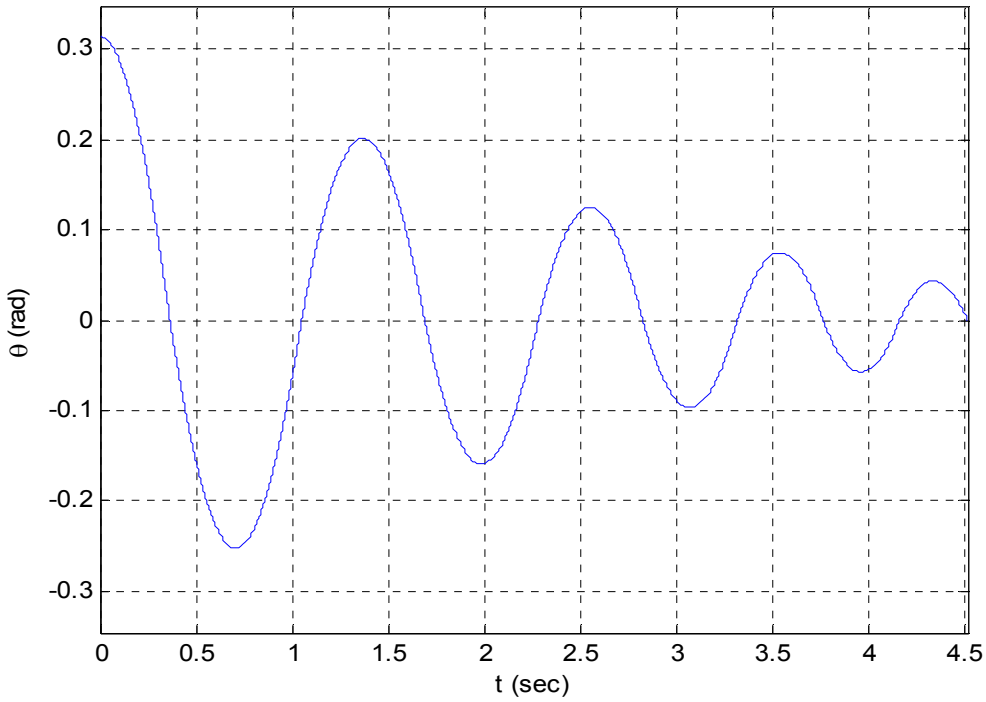

Figure 56. MATLAB simulation - $\alpha=\pi/12$ - $\theta_0=\pi/10$

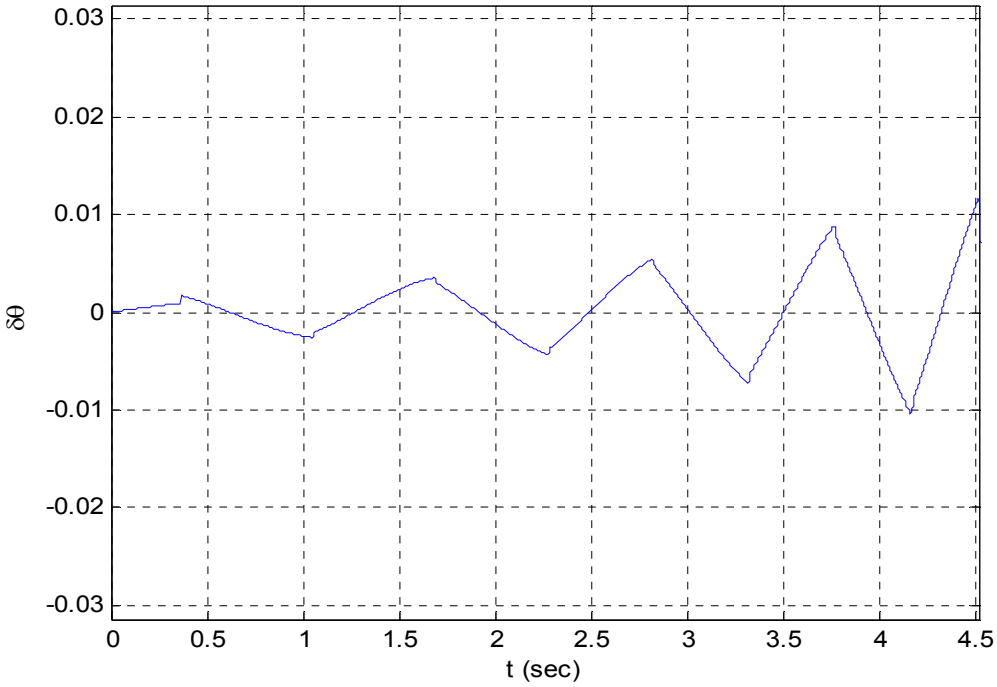

Figure 57. Prediction discrepancy

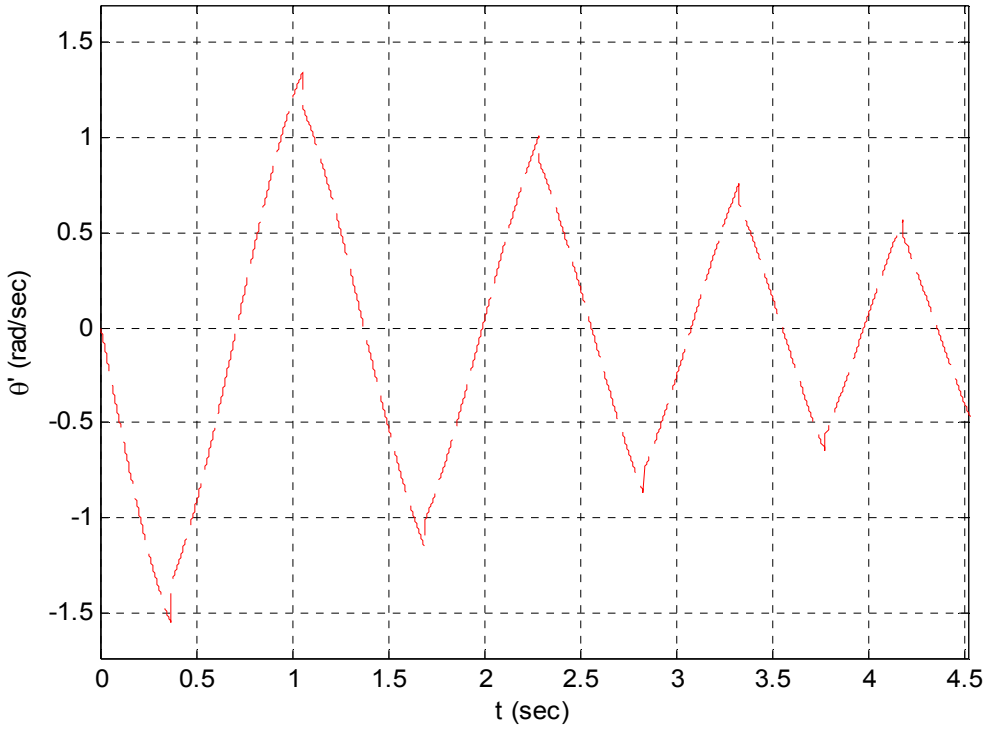

Figure 58. VISUAL NASTRAN - $\alpha=\pi/12$ - $\theta_0=\pi/10$

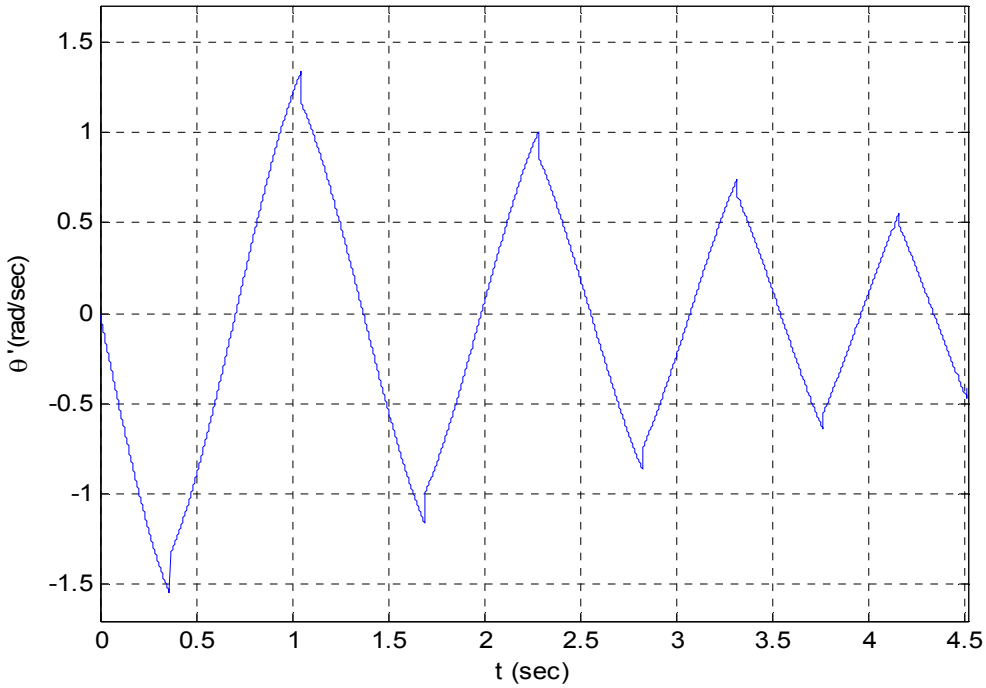

Figure 59. MATLAB simulation - $\alpha=\pi/12$ - $\theta_0=\pi/10$

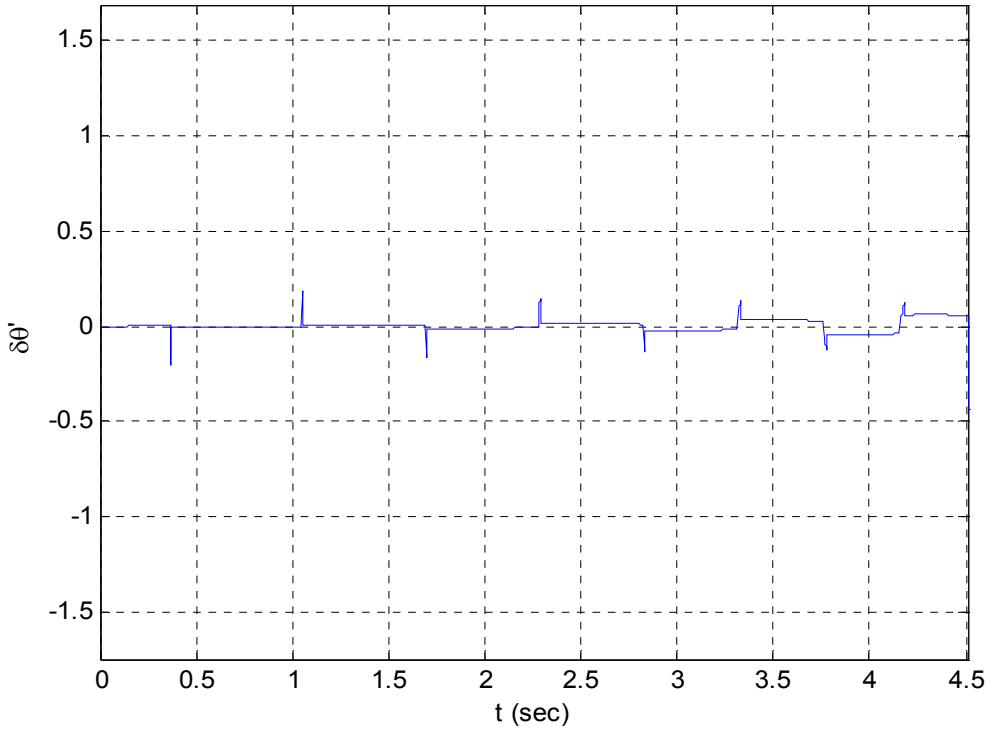

Figure 60. Prediction discrepancy

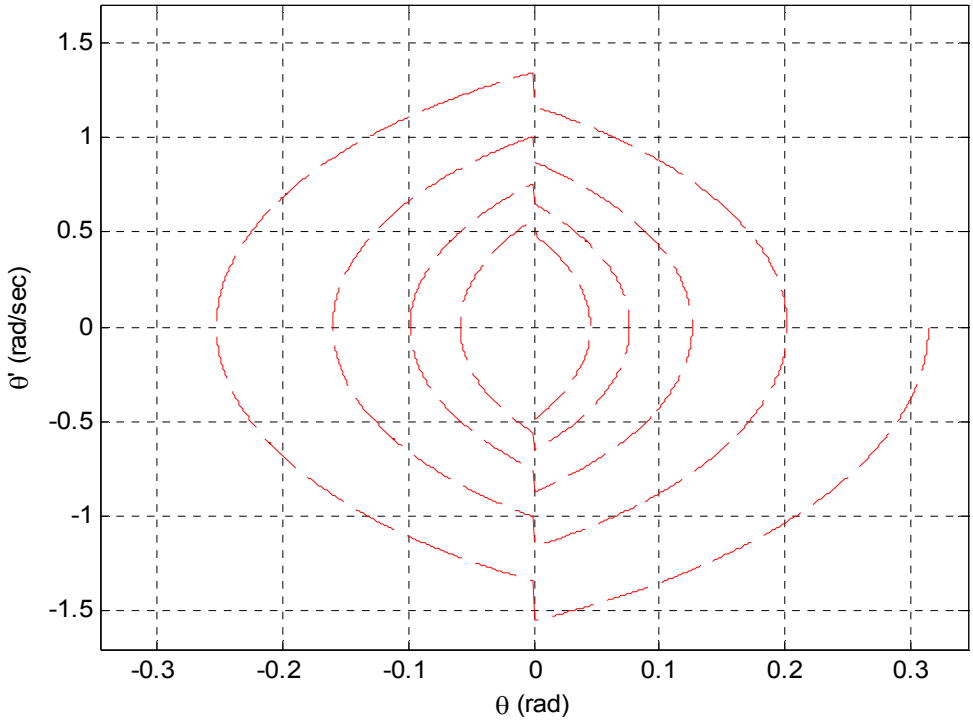

Figure 61. VISUAL NASTRAN Phase diagram

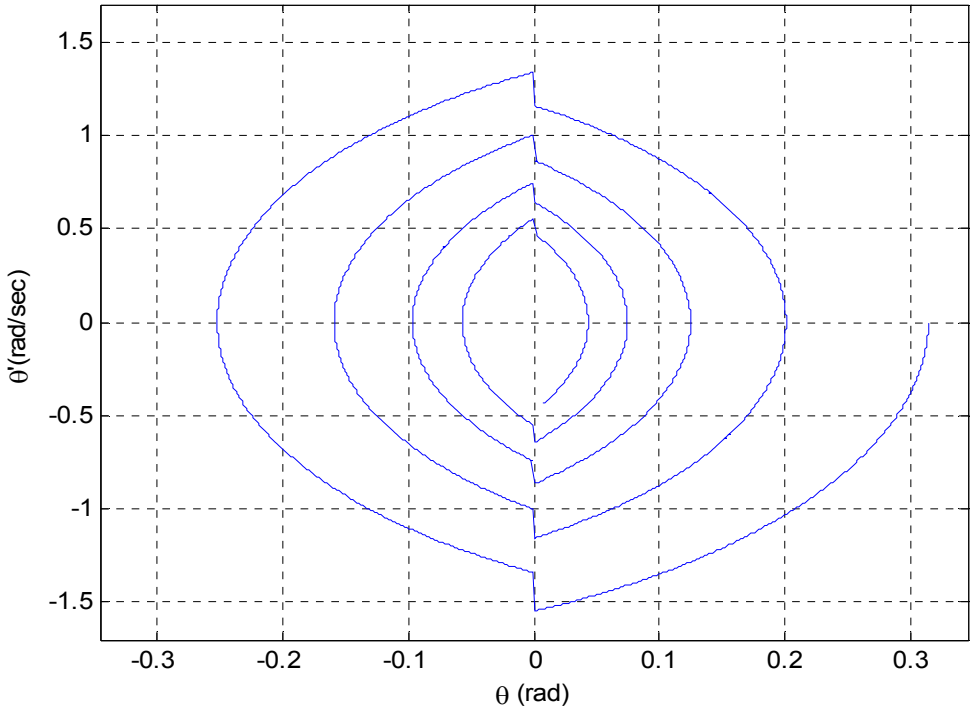

Figure 62. MATLAB prediction Phase diagram

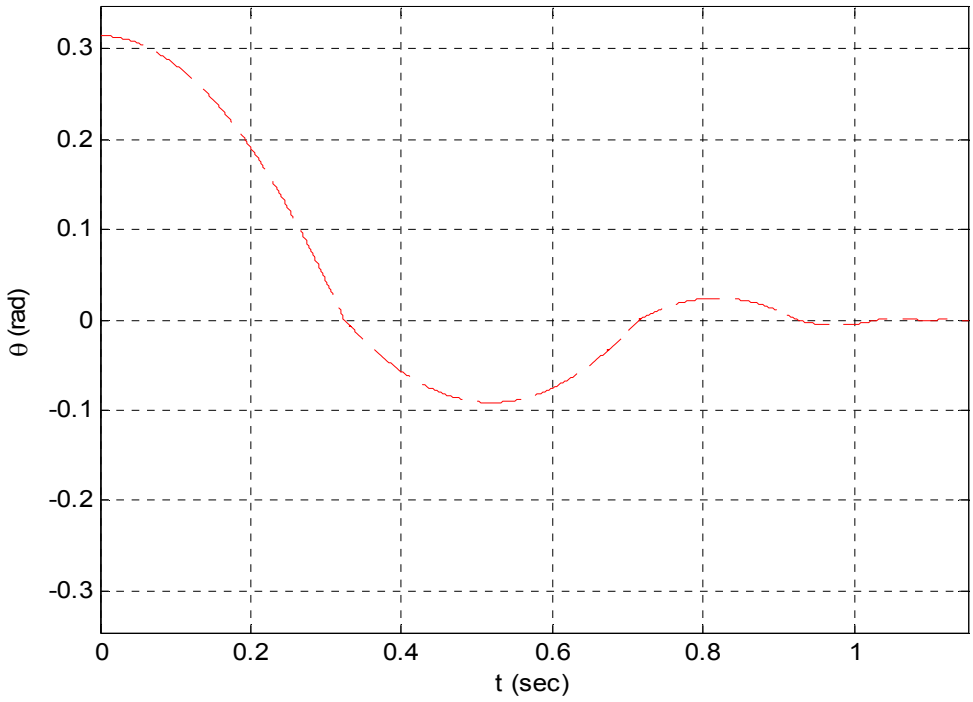

Figure 63. VISUAL NASTRAN - $\alpha=\pi/6$ - $\theta_0=\pi/10$

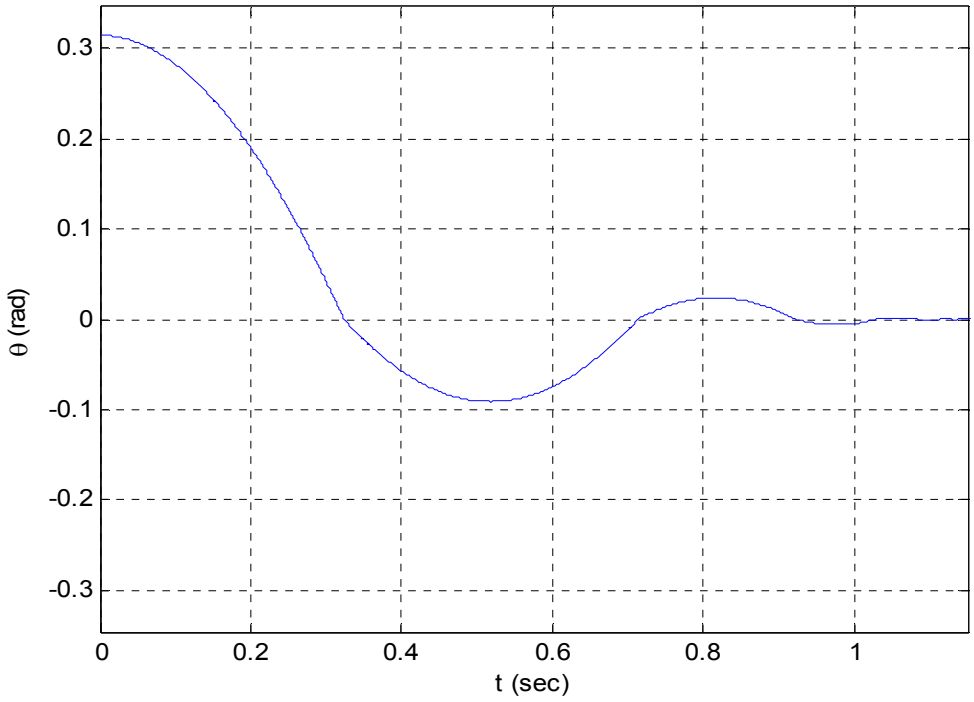

Figure 64. MATLAB simulation – $\alpha=\pi/6$ - $\theta_0=\pi/10$

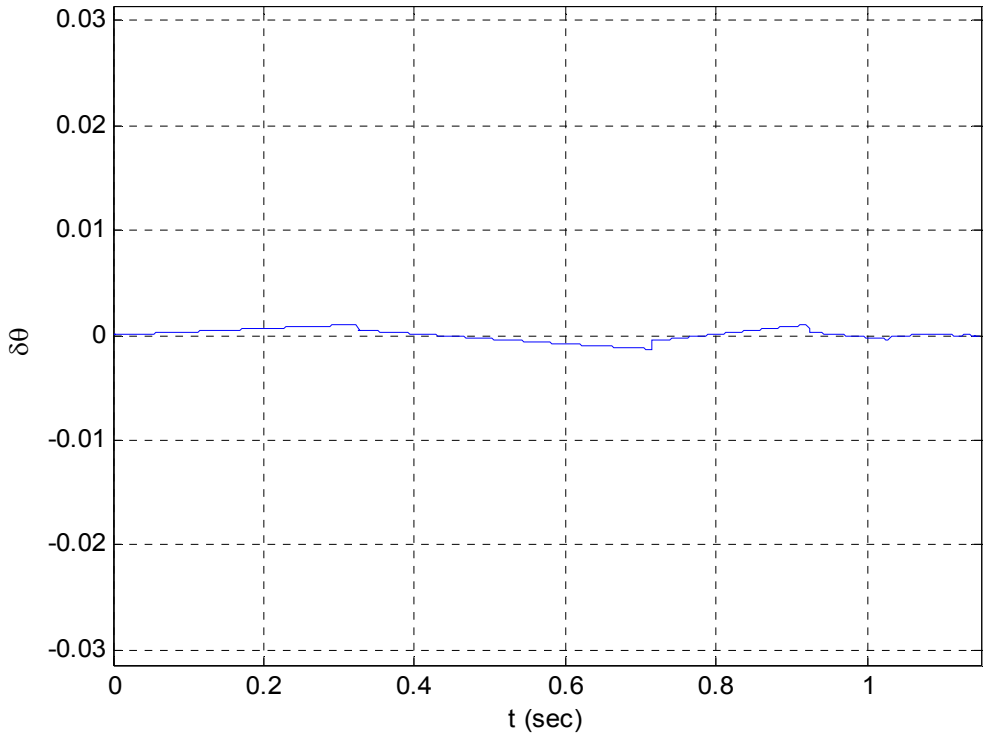

Figure 65. Prediction discrepancy

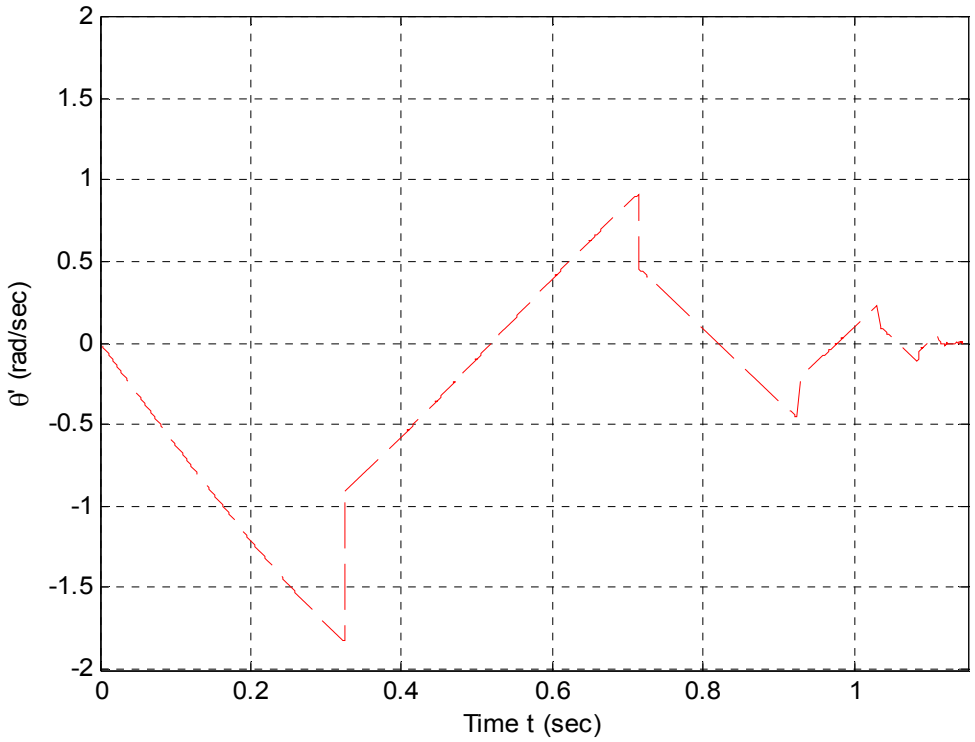

Figure 66. VISUAL NASTRAN - $\alpha=\pi/6$ - $\theta_0=\pi/10$

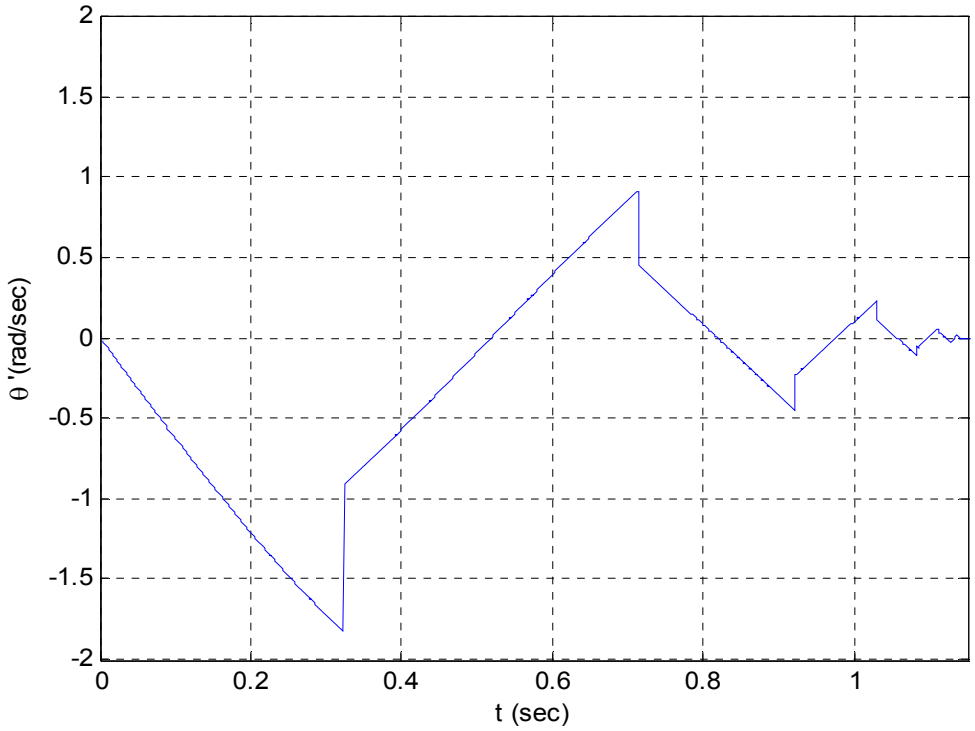

Figure 67. MATLAB simulation - $\alpha=\pi/6$ - $\theta_0=\pi/10$

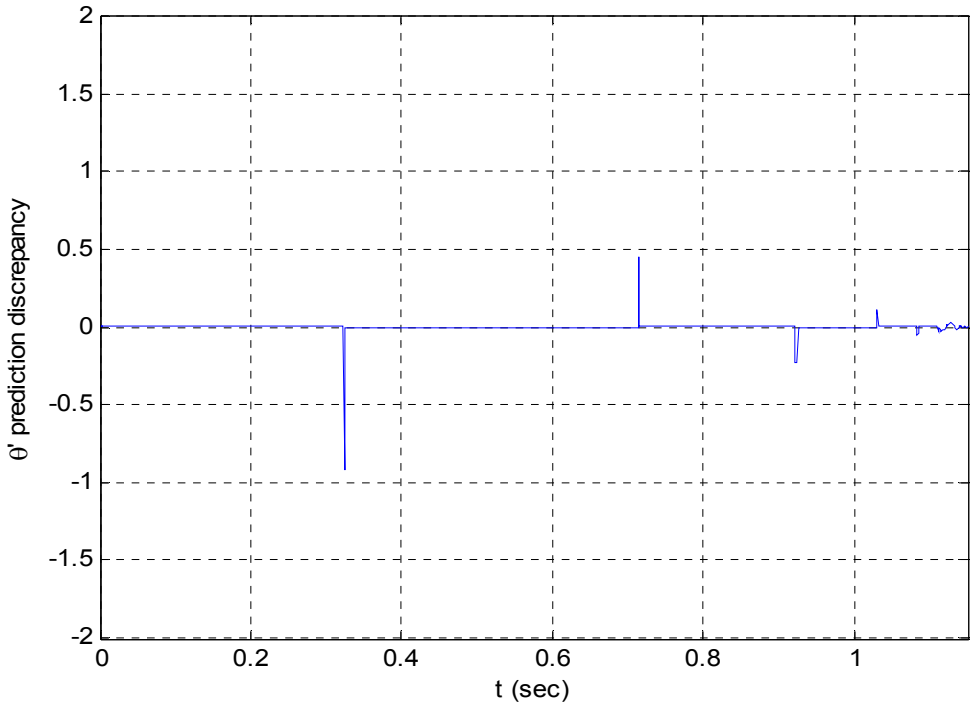

Figure 68. Prediction discrepancy

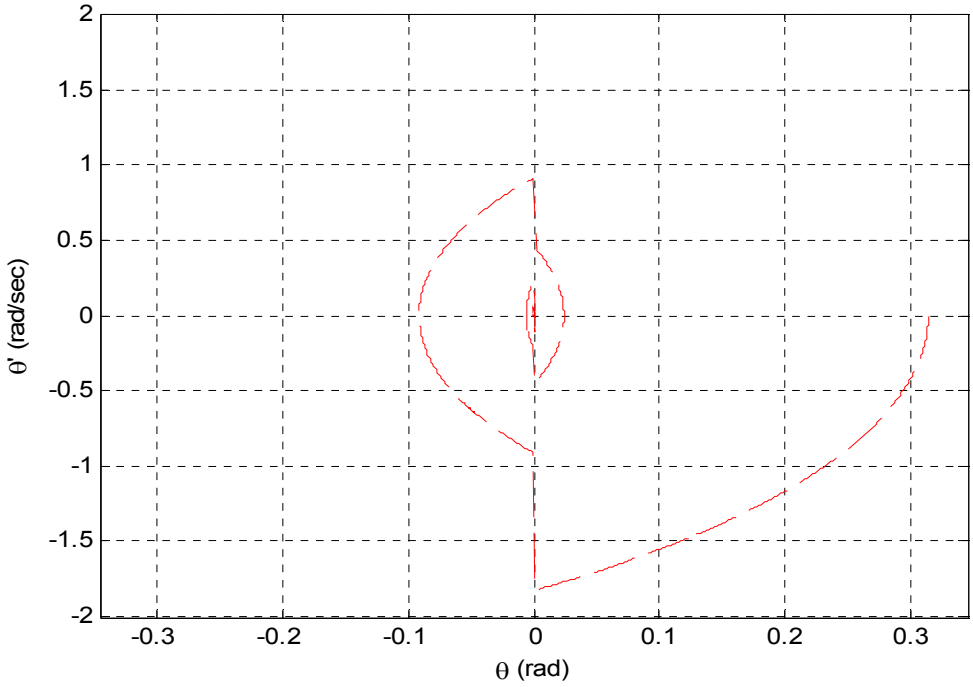

Figure 69. Phase diagram

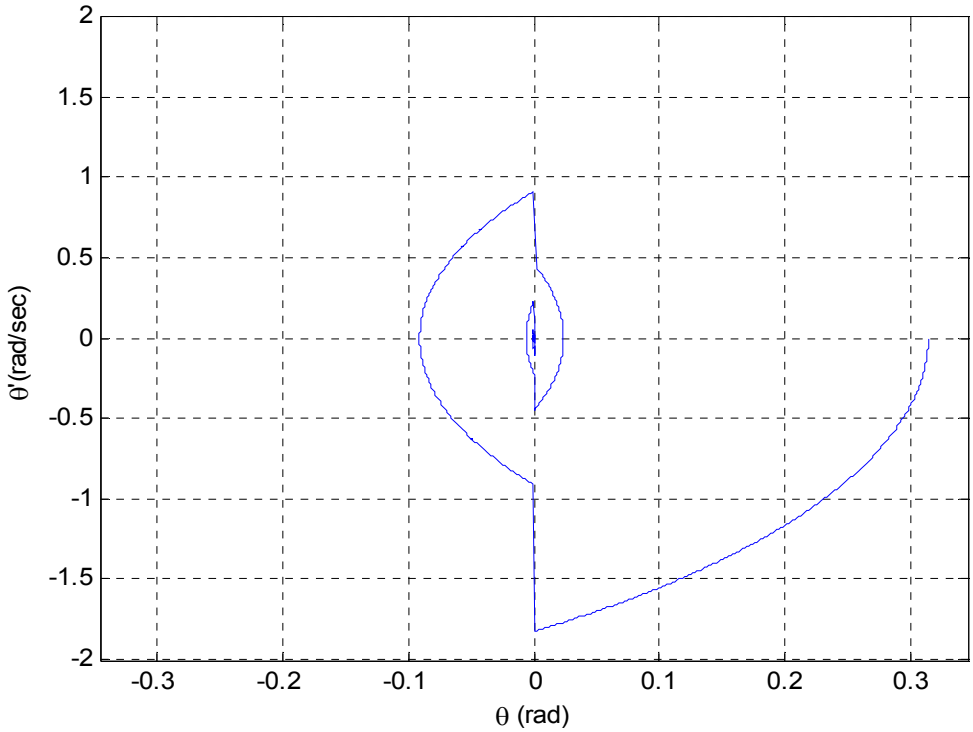

Figure 70. Phase diagram

Evaluating the above set of figures, we conclude the following:

- The variable frequency of oscillation, as well as when the string switch takes place, is relatively well predicted. The error between the predicted and actual performance causes spikes in the angular velocity discrepancy plots.
- In terms of the prediction of the angular displacement and velocity of the oscillation, the discrepancies are caused, on the one hand, by the failure to precisely predict both the location in time of the switch points and the energy loss at every one of them. On the other hand, it was not possible to obtain the exact equations used in VN 4-D to calculate these parameters. Therefore, a comparison with the VN 4-D software results does not provide a precise appreciation of the actual accuracy of the results.
- For smaller values of characteristic angle α, which equals less energy loss at the switch point, the prediction discrepancy is minimized.

b. String Tension Comparison

For the string tension prediction, equation (2.46) was used. The Matlab code had already computed the angular velocity and displacement inputs.

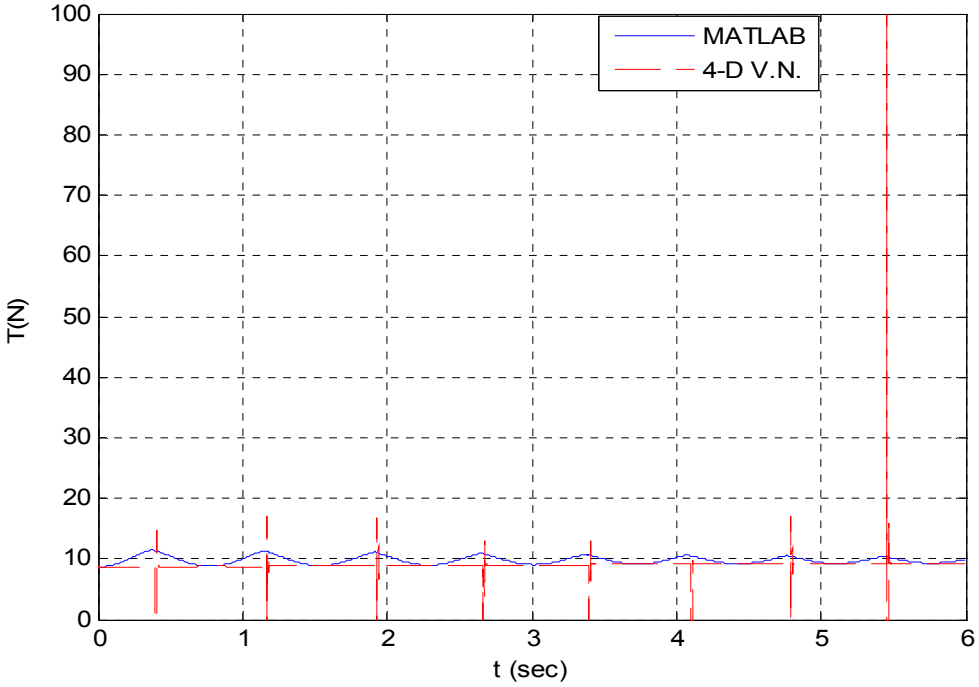

Figure 71. Tension comparison $\alpha=\pi/18$ – $\theta_0=\pi/10$

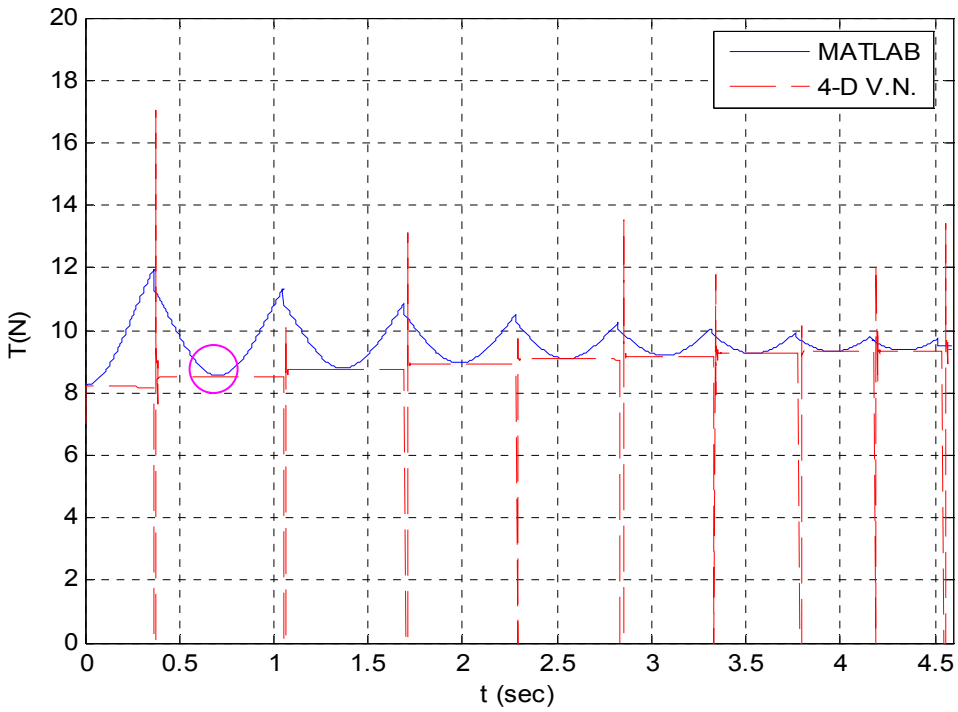

Figure 72. Tension comparison $\alpha=\pi/12$ – $\theta_0=\pi/10$

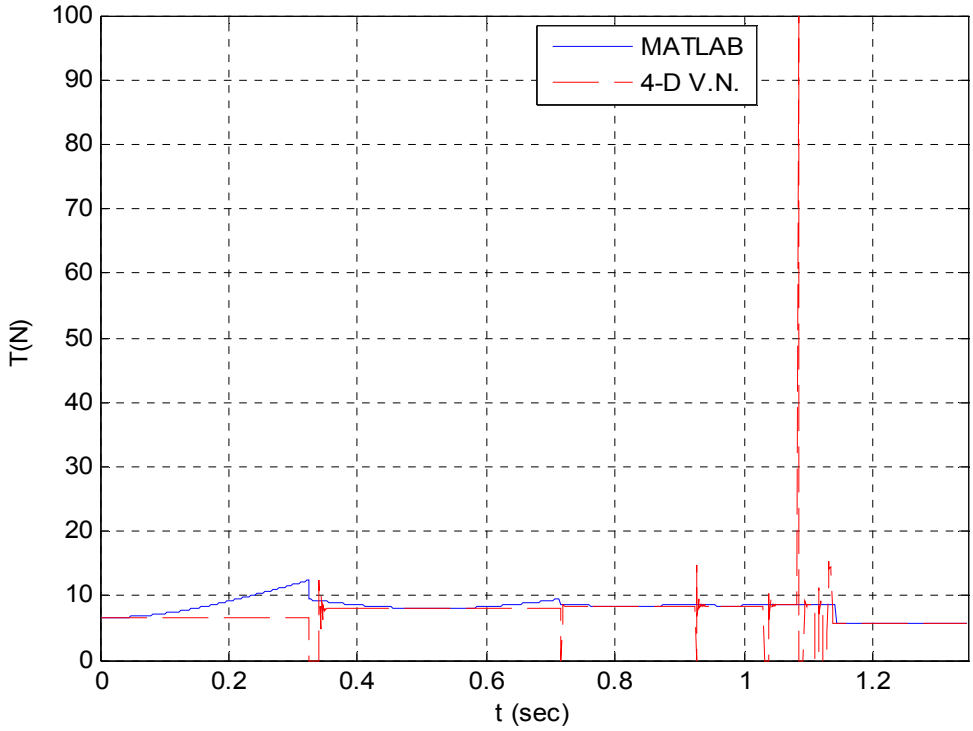

Figure 73. Tension comparison $\alpha=\pi/6$ – $\theta_0=\pi/10$

The above plots lead to the following conclusions:

- It can be seen that, for larger values of α, which correspond to extensive energy loss at the switch point, VN 4-D reveals time periods when the tension on both strings is zeroed. This corresponds to an instantaneous jump. Because the mechanism of energy restitution of the ropes used in VN 4-D is not known and that there is the possibility that the previously assumed zero parallel velocity component is not completely eliminated, the resulting jump after impact could be expected.
- The tension predicted by VN 4-D shows spikes of irregular magnitude at the switch points. The existence of these features can be related to the previously presented explanation. Although they do not show a pattern, the fact that a previously slack string becomes taught within an infinitesimally small time duration can provoke this peak tension magnitude. This corresponds to the impulse, which zeroes the parallel velocity component.

- The Matlab code tension prediction coincides with the VN 4-D only at the instances when the mass velocity is zero (indicated with a purple circle in Figure 72). Therefore, the VN 4-D tension prediction is not in accordance with equation (2.46). To understand this unexpected result, a model of two standard pendula -- one with a string and the other with a massless rod -- was used to calculate the tension during free oscillation with an arbitrary initial displacement. The results revealed that the standard rod pendulum's tension agrees with equation (2.46), while the standard string pendulum's tension does not. Moreover, an effort was made to understand the pattern that provided the string tension results. After some trial and error efforts, the equation that provided an almost identical tension prediction was

$$T = \frac{-m\dot{\theta}^2 l}{2} + mg\cos\theta \tag{2.57}$$

Efforts were made to understand the above equation, but, unfortunately, the MSC Software no longer supported the specific software. Consequently, further tension comparisons with VN 4-D will not be performed and, also, the Matlab results will be presented without validation from the VN 4-D results.

3. The Real 2-Pendulum with *a*≥45

In the case that α=45^o, when applying equation (2.55), we realize that for $r = 0$ all the kinetic energy of the pendulum would be absorbed by the string during impact. Thus, the oscillation would be terminated. The above can be visualized from the following graphs, where VISUAL NASTRAN and MATLAB simulations are used to provide the response of the 2-string pendulum with α=45^o.

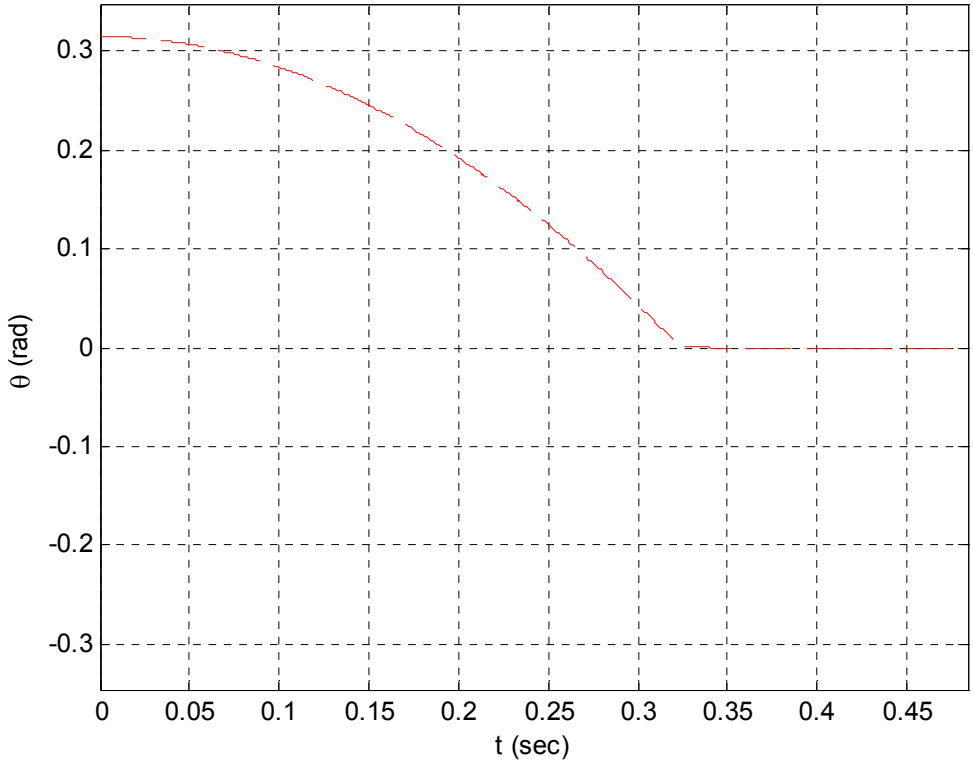

Figure 74. VISUAL NASTRAN - $\alpha=\pi/4$ - $\theta_0=\pi/10$

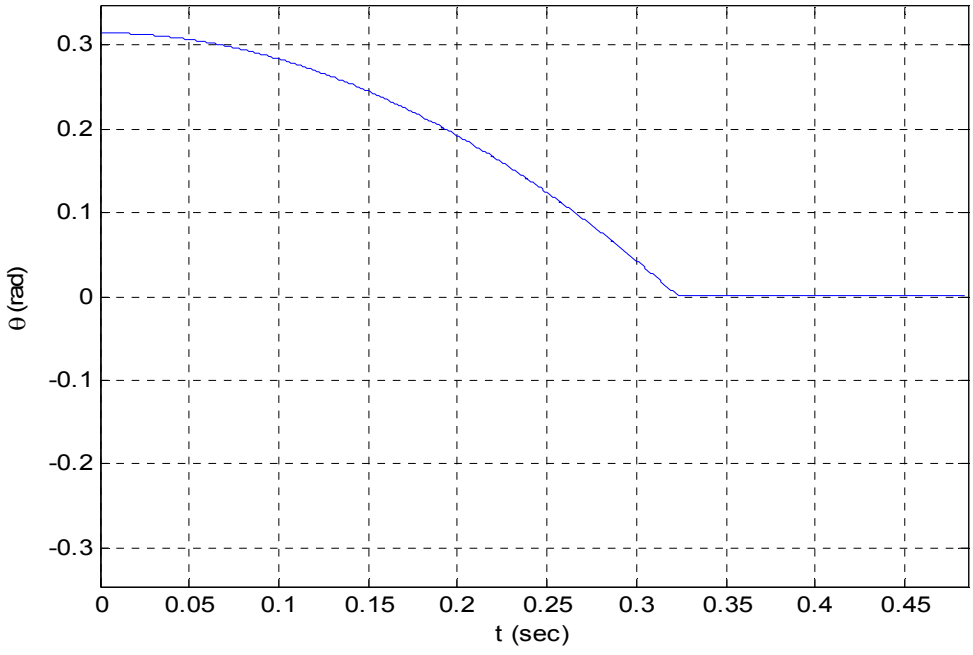

Figure 75. MATLAB simulation - $\alpha=\pi/4$ - $\theta_0=\pi/10$

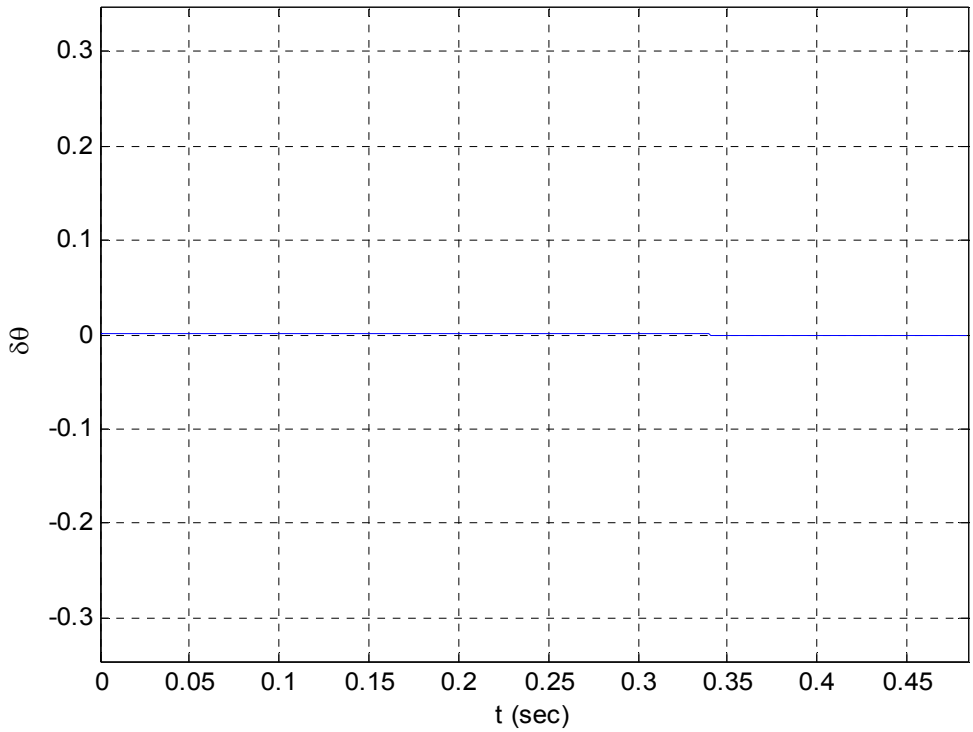

Figure 76. Prediction discrepancy

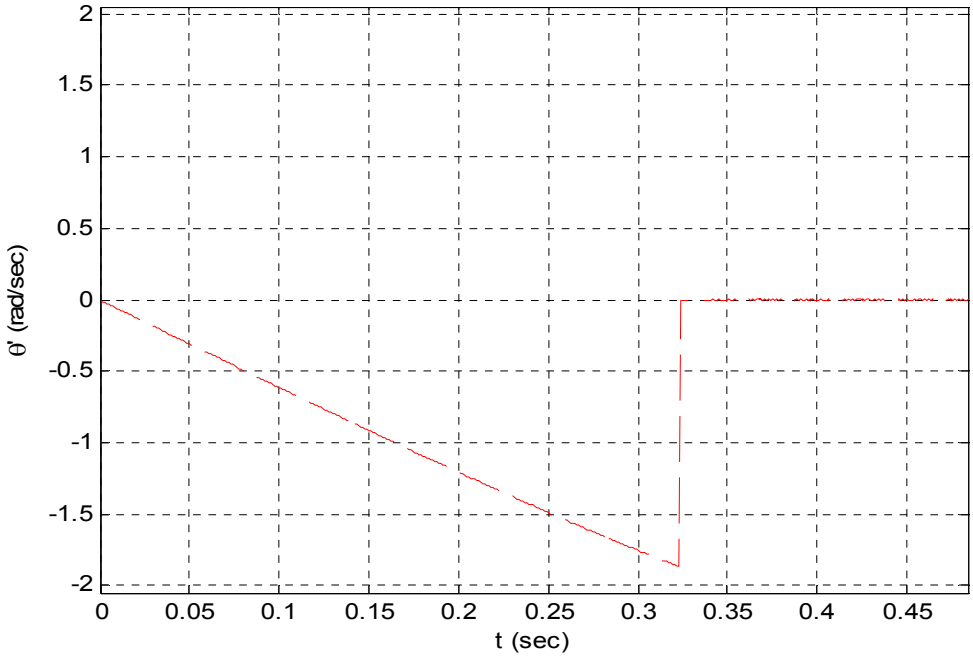

Figure 77. VISUAL NASTRAN - $\alpha=\pi/4$ - $\theta_0=\pi/10$

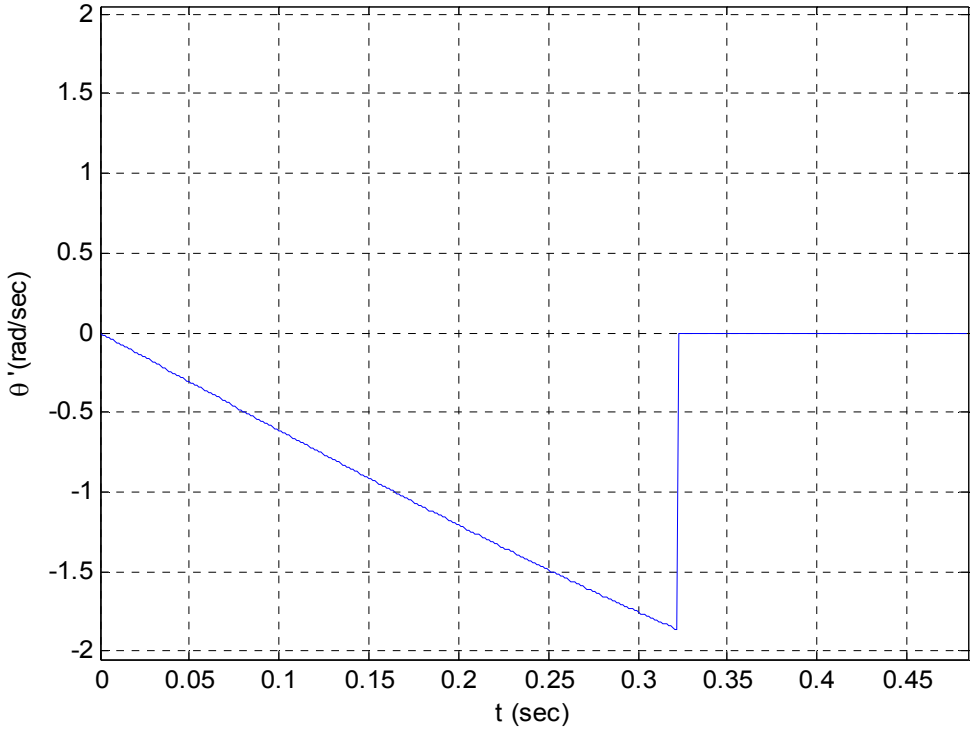

Figure 78. MATLAB simulation - $\alpha=\pi/4$ - $\theta_0=\pi/10$

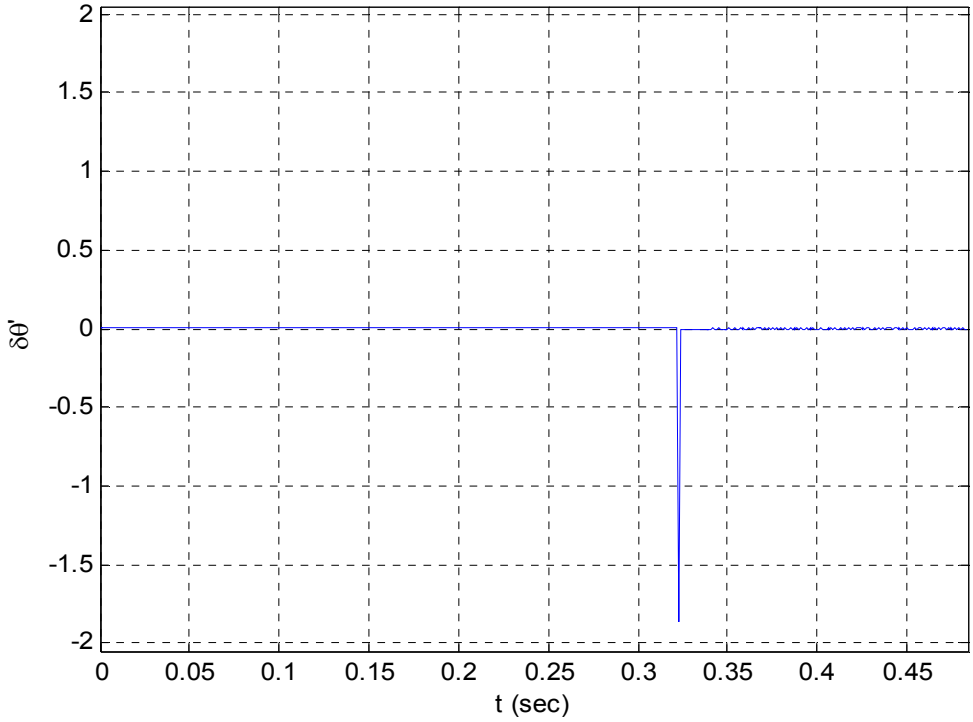

Figure 79. Prediction discrepancy

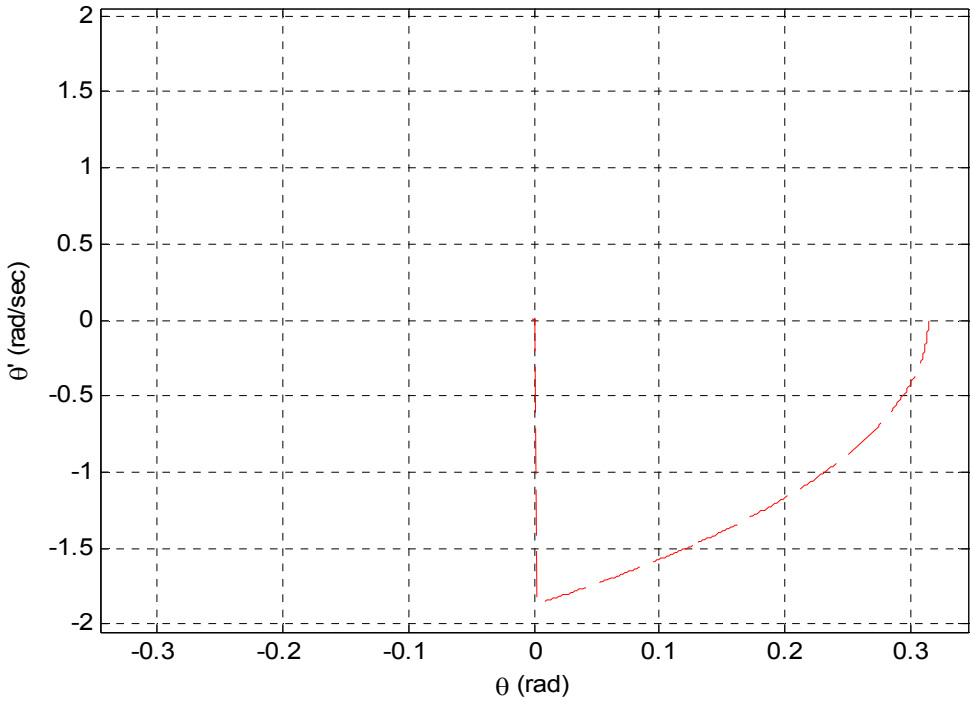

Figure 80. VISUAL NASTRAN – $\alpha=\pi/4$ – $\theta_0=\pi/10$

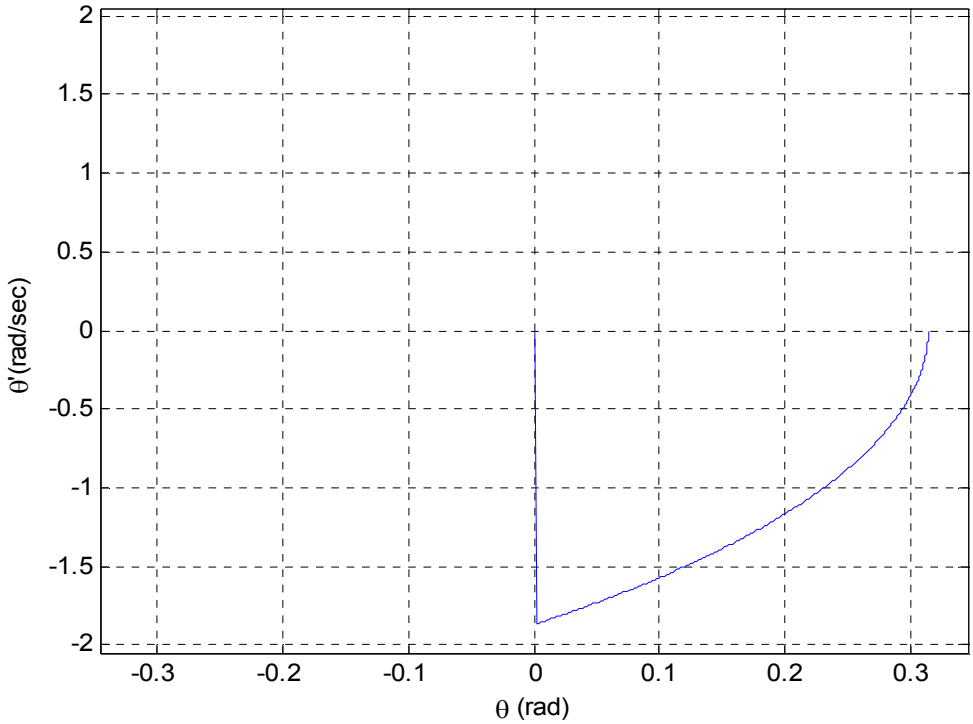

Figure 81. MATLAB $\alpha=\pi/4$ – $\theta_0=\pi/10$

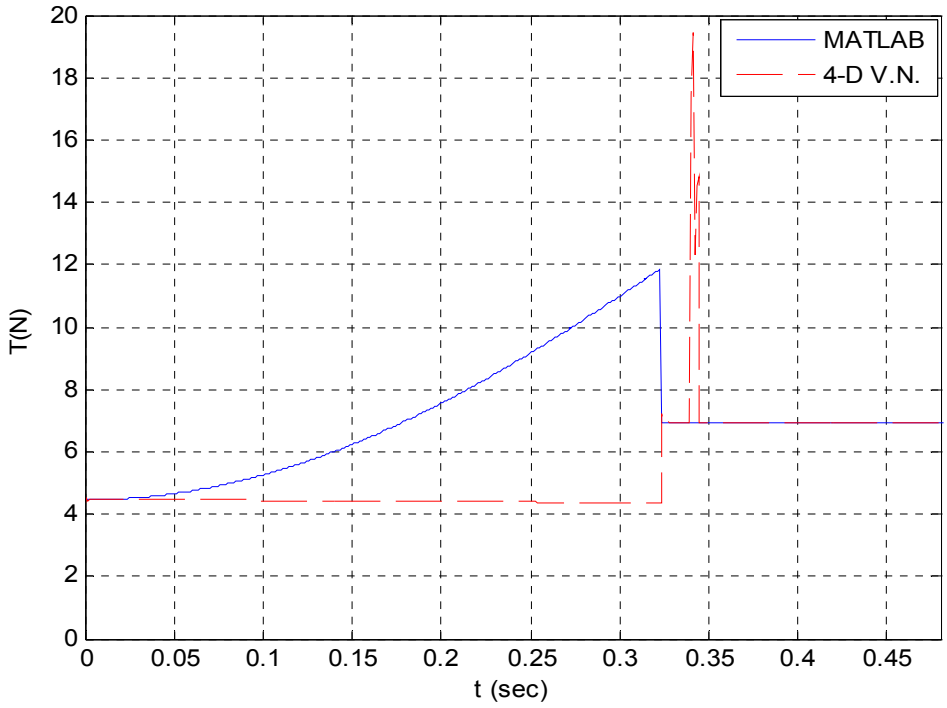

Figure 82. Tensions $\alpha=\pi/4$

Although the limiting case of $\alpha=45^{o}$ can be described by equations (2.18) and (2.55) (assuming only that $r=0$) if $\alpha>45^{o}$, the motion of the mass will not be governed by linear or nonlinear equations of motion, but only by its interaction with the strings.

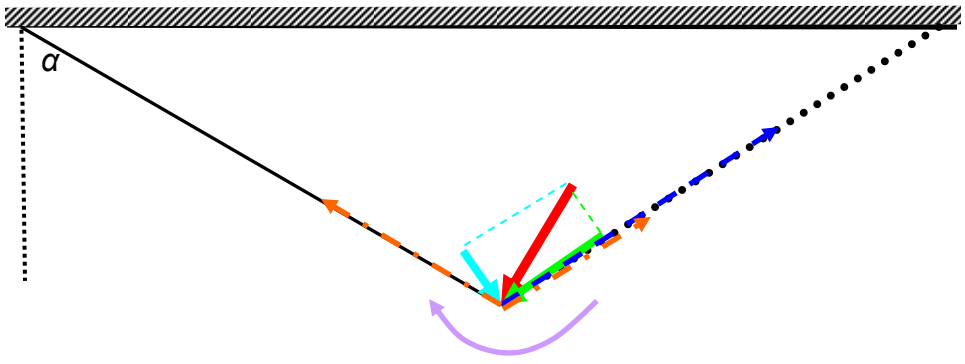

Figure 83. Force and velocity diagram for $\alpha>45^{o}$

According to Figure 83, the linear velocity before the switch point $\vec{V}b$ (red vector) is composed of two components, $\vec{V}b_1$ and $\vec{V}b_2$ (turquoise and green vectors, respectively). At the instance when the right string becomes tight, the tension of the string (blue vector) exerts an impulse affecting $\vec{V}b_2$. Irrespective to the value of the restitution coefficient that governs this impact, $\vec{V}b_1$ cannot promote the circular motion of the mass with respect to the right string due to its direction. Contrarily, the left string, which becomes slack after the switch point for $\alpha<45^{o}$, continues to be tight and exerts, along with the right string, an impulse on the mass opposing $\vec{V}b_1$ (orange vectors). Thus, either the mass will bounce or it will come to rest. This depends on the restitution coefficient. Consequently, if we preserve the assumption that $r=0$ for all mass-string impact interactions, after the mass reaches the switch point, it comes to rest.

E. THE DRIVEN PENDULUM

Extending the analysis performed in the previous sections, we should include the case of the pendulum in which the supporting point, or points, undergoes motion due to forcing. The moving support induces complexity to the response of the pendulum that may not end in oscillatory behavior [6].

1. The Standard Driven Pendulum

Consider a standard pendulum which, at an arbitrary moment of the oscillation, has an angular displacement θ, where $-\frac{\pi}{2}\le\theta\le\frac{\pi}{2}$. We define a world system of axis where x-axis points to the right and y-axis points upwards. An arbitrary motion drives the support point of the pendulum, whose acceleration at that moment has both a horizontal and a vertical component.

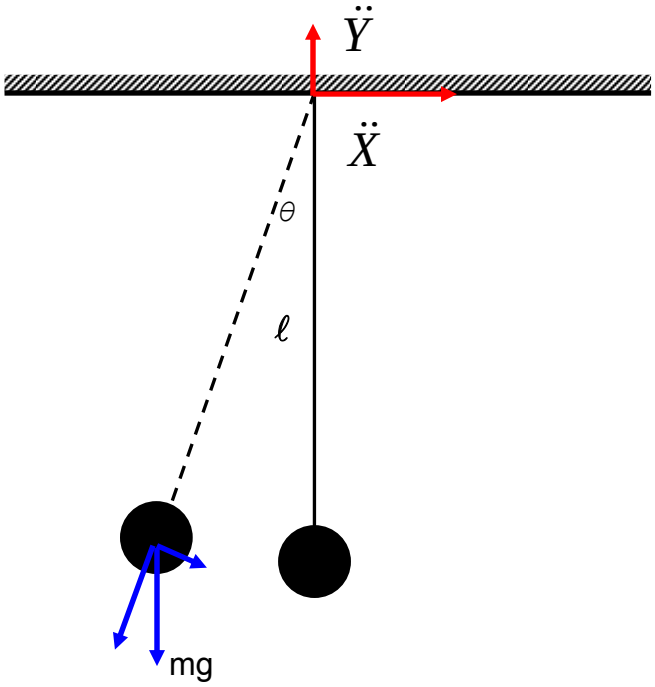

Figure 84. The standard driven pendulum

According to the previous analysis, the equation of motion for the undriven standard pendulum is either equation (2.6) or (2.2). The effect of the horizontal component of the support acceleration is an inertial force on the mass $Fx = -m\ddot{X}$. Similarly, for the vertical component, the inertial force is $Fy = -m\ddot{Y}$. We notice that Fy has the same direction and orientation as gravity. These two forces contribute to restoring force with two additional components depending on angle θ. Therefore, the new restoring force is

$$Fr = (mg + m\ddot{Y})\sin\theta - m\ddot{X}\cos\theta \tag{2.58}$$

Therefore, the equation of motion becomes

$$\ddot{\theta} + \frac{(g+\ddot{Y})}{l}\sin\theta - \frac{\ddot{X}}{l}\cos\theta = 0 \tag{2.59}$$

Finally, from equation (2.59) we can draw the conclusion that, due to the horizontal acceleration, the pendulum will initiate oscillations even without the existence of initial displacement or initial velocity. Thus, for $\theta=\theta_0=0$, equation, (2.59) becomes $\ddot{\theta}=\frac{\ddot{X}}{l}$. Finally, the above equation is valid for the range of θ already mentioned with one exception: when a jump occurs. The jump behavior of the driven pendulum will be analyzed in a subsequent section.

2. The Driven 2-Pendulum

Based on the previous analysis and equation (14), we can derive the equation of motion for the driven 2-pendulum as follows for $-\frac{\pi}{2}\le\theta+\alpha\le\frac{\pi}{2}$:

$$\ddot{\theta}+\frac{(g+\ddot{Y})}{l}\sin(\theta+\alpha)-\frac{\ddot{X}}{l}\cos(\theta+\alpha)=0$$

$$\ddot{\theta}+\frac{(g+\ddot{Y})}{l}(\sin\theta\cos\alpha+sign\theta\cos\theta\sin\alpha)-\frac{\ddot{X}}{l}(sign\theta\cos\theta\cos\alpha-\sin\theta\sin\alpha)=0$$

$$\ddot{\theta}+(\frac{(g+\ddot{Y})}{l}\cos\alpha+\frac{\ddot{X}}{l}\sin\alpha)\sin\theta+(\frac{(g+\ddot{Y})}{l}\sin\alpha-\frac{\ddot{X}}{l}\cos\alpha)sign\theta\cos\theta=0 \quad (2.60)$$

Again, the validity of equation (2.60) is questioned when a jump occurs.

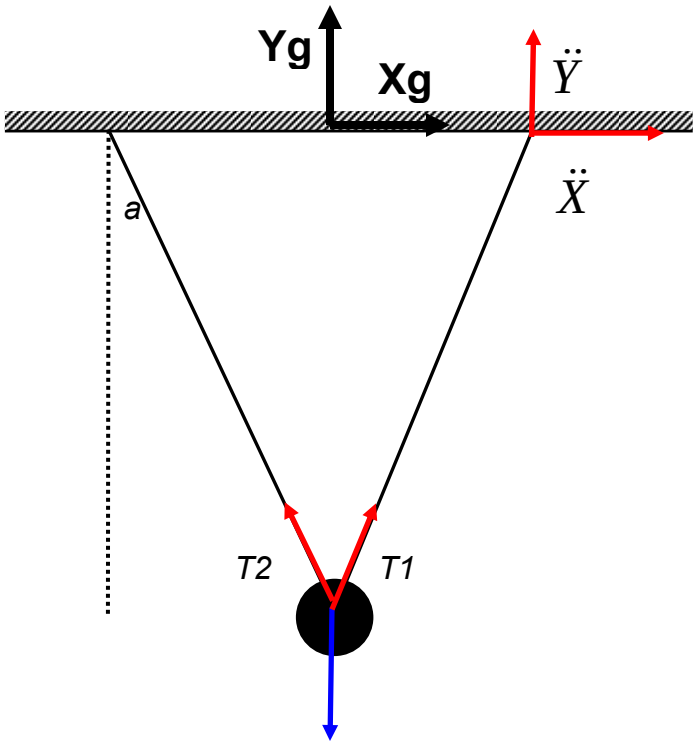

Figure 85. The driven 2-pendulum

a. String Tension Investigation of the Driven 2-Pendulum

Assuming that the support of the 2-pendulum is accelerated in the direction shown in Figure (85), the mass will leave the equilibrium position only if *T2*=0 N. For this to occur, the vertical component of *T1* should be able to withstand the virtual weight of the mass, which is $Wv = m(\ddot{Y} + g)$. We can easily prove that the magnitude of the string tension about which the mass will oscillate is

$$T = m(\dot{\theta}^2 l + \ddot{X}\sin(\theta+\alpha) + \ddot{Y}\cos(\theta+\alpha) + g\cos(\theta+\alpha)) \qquad (2.61)$$

which is valid for all $-\frac{\pi}{2}+\alpha \le \theta \le \frac{\pi}{2}-\alpha$. Nevertheless, close attention should be given in terms of the sign of angles *θ* and *α*. If inconsistencies are to be avoided, angle *α* should always have the same sign as angle *θ*. A quick look at

Figure 86 shows us that a positive $\ddot{X}$ would increase the tension on the string while a negative $\ddot{X}$ would decrease it. Nevertheless, if the mass were oscillating about the other string, a negative $\ddot{X}$ would increase the string tension, and so on. The above facts are predicted by equation (2.61).

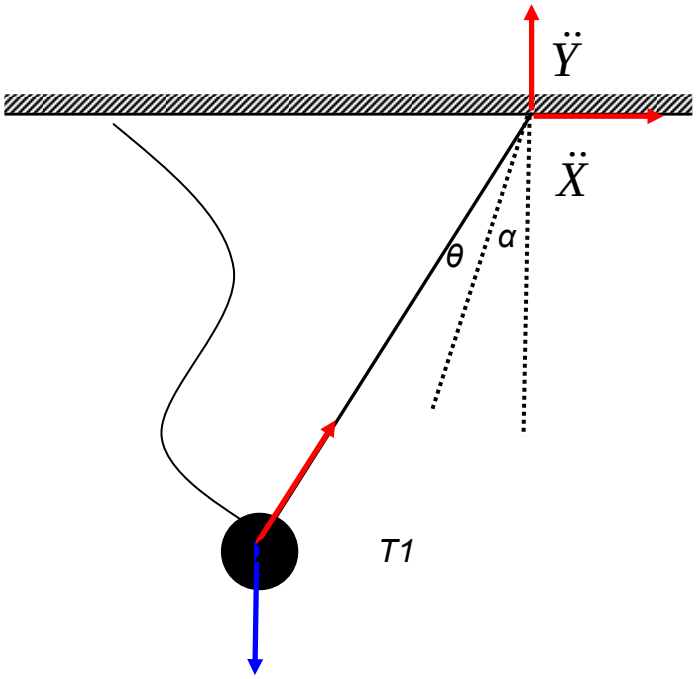

Figure 86. 2-pendulum's force and acceleration diagram during oscillation

Nevertheless, equation (2.61) has one limitation: the tension can only take positive values. When the string tension is zeroed, a jump occurs. That behavior will be analyzed in a subsequent section.

In addition, it would be useful to know the magnitude of the tension exerted on the strings while the mass remains in its equilibrium position. While the mass is in that position, the sum of the vertical components of *T1* and *T2* should be equal to the virtual weight of the mass Wv, while the difference of their horizontal components should be equal to $m\ddot{X}$

$$\cos\alpha(T1+T2)=m(\ddot{Y}+g) \text{ and } \sin\alpha(T1-T2)=m\ddot{X}$$

solving the above system of two equations

$$T1=\frac{m}{2}\left(\frac{(\ddot{Y}+g)}{\cos\alpha}+\frac{\ddot{X}}{\sin\alpha}\right)$$
$$T2=\frac{m}{2}\left(\frac{(\ddot{Y}+g)}{\cos\alpha}-\frac{\ddot{X}}{\sin\alpha}\right) \quad (2.62)$$

b. Stability of the 2-Pendulum

While equation (2.60) describes the 2-pendulum's oscillation in the absence of non-zero initial conditions, the oscillation will not be initiated under any value of horizontal acceleration.

Manipulating equation (2.60) with zero initial conditions, results in $\ddot{\theta}=-\frac{(g+\ddot{Y})}{l}\sin\alpha+\frac{\ddot{X}}{l}\cos\alpha$. The vertical components of the restoring force tend to drive the mass to move downwards. This motion is constrained in this situation since the mass is supported by both the taught string (an exception exists for the case that $\ddot{Y}$ is negative and $g+\ddot{Y}<0$). Therefore, an angular acceleration will be induced only if the horizontal component manages to overcome the condition and

$$\frac{\left\|\ddot{X}\right\|}{\tan\alpha}-\ddot{Y}>g \quad (2.63)$$

is fulfilled.

Another approach, which would lead us to the same conclusion, is analyzing the string tension. Assuming that the support of the 2-pendulum is accelerated in the direction shown in Figure 86, the mass will leave the equilibrium position only if *T2*=0 N. For this to occur, the vertical component of *T1* should be able to withstand the virtual weight of the mass, which is

$Wv = m(\ddot{Y} + g)$. In the case of the 2-pendulum, which is about to leave its equilibrium position $\theta = 0$ and from (2.61), for the mass to be lifted up we must have

$$T\cos\alpha = m(\ddot{X}\sin\alpha + \ddot{Y}\cos\alpha + g\cos\alpha)\cos\alpha > m(\ddot{Y} + g)$$

$$\ddot{X}\sin\alpha\cos\alpha > g\sin^2\alpha + \ddot{Y}\sin^2\alpha$$

$$\frac{\ddot{X}}{\tan\alpha} - \ddot{Y} > g$$

Finally, from equation (2.63), we can draw the conclusion that choosing larger values for α would make the 2-pendulum more stable. Nevertheless, this advantage has a considerable drawback: the increase in string tension associated with larger characteristic angles. In Figure 87, one can observe both the limiting value of horizontal acceleration, which allows the 2-pendulum equilibrium, and the maximum tension associated with this horizontal acceleration for a range of characteristic angles ($1^o < \alpha < 80^o$).

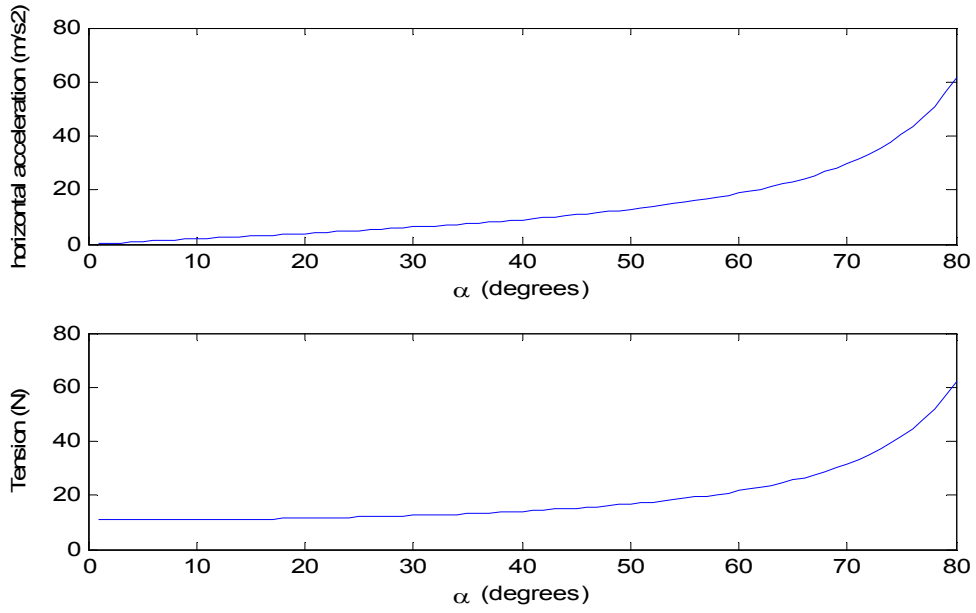

Figure 87. Horizontal acceleration inducing instability versus associated maximum tension

From the above figure, it can be seen that, although the necessary $\ddot{X}$ would break the equilibrium, which increases steadily for the first half of the range of *α*, the related tension increases in a slower pattern. This difference in increasing pattern is caused by the analytical equations that describe them. These equations are

$$\begin{aligned} \ddot{X}_{\lim} &= (g + \ddot{Y}_{\min}) \tan\alpha \\ T_{\max} &= \frac{(g + \ddot{Y}_{\max})}{\cos\alpha} + \frac{\ddot{X}_{\max}}{\sin\alpha} \end{aligned} \tag{2.64}$$

One method to evaluate the optimum choice of *α* would be to define a ratio of acceleration over the maximum attained tension. According to the previous equations, this ratio would be $R = \sin\alpha$.

Nevertheless, this method is not effective. The values of the required $\ddot{X}$ to disturb equilibrium are very large for the second half of the *α* range, and even for some values of the first half. A more realistic approach is to choose a value of *α* (for example 20^o) as a reference value, $\alpha_{ref,}$ and, then, compare the maximum tension, T_{maxref}, with the one exerted on the strings of the 2-pendulums of larger *α,* but still associated with the same $\ddot{X}_{ref}$.

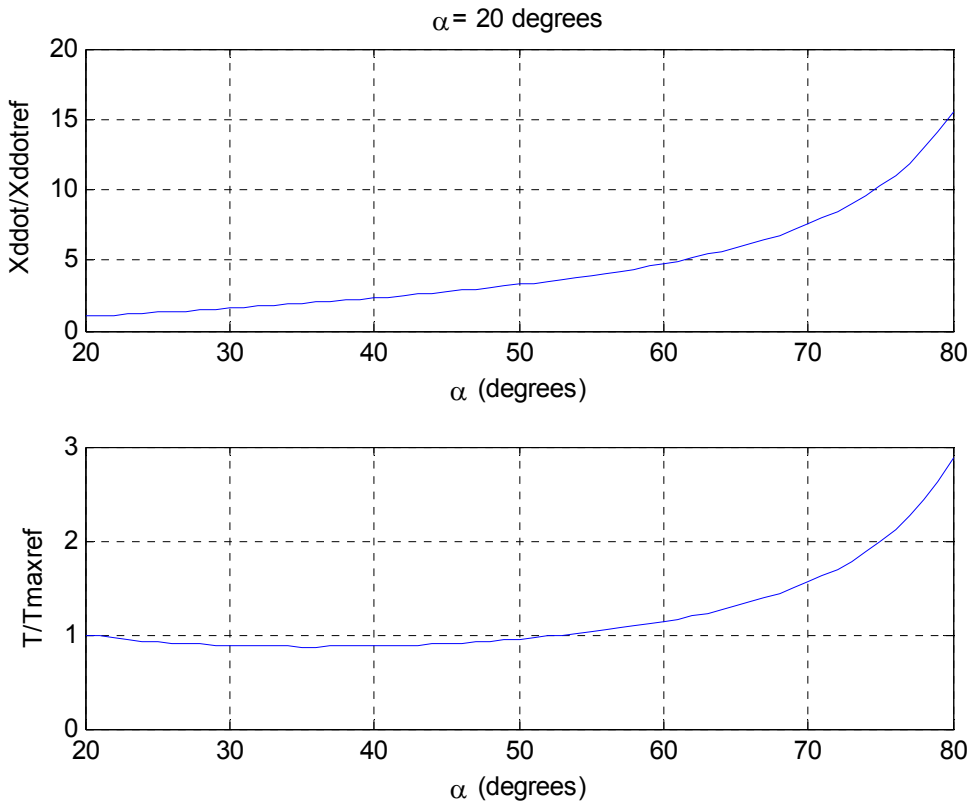

Figure 88. α=20^{o} reference angle

The above plots reveal that, in a choice of a greater, but less than 52^{O}, α would be a better choice.

Another approach is to find the angle α which will result in the minimum exerted tension for a combination of vertical and horizontal accelerations. In the following figures, we can visualize the variation of optimum α when $\ddot{X}$ and $\ddot{Y}$ vary from zero to g along with associated tension. The results are validated with the constraint that the 2-pendulum should be stable for the combination of α, $\ddot{X}$, and $\ddot{Y}$.

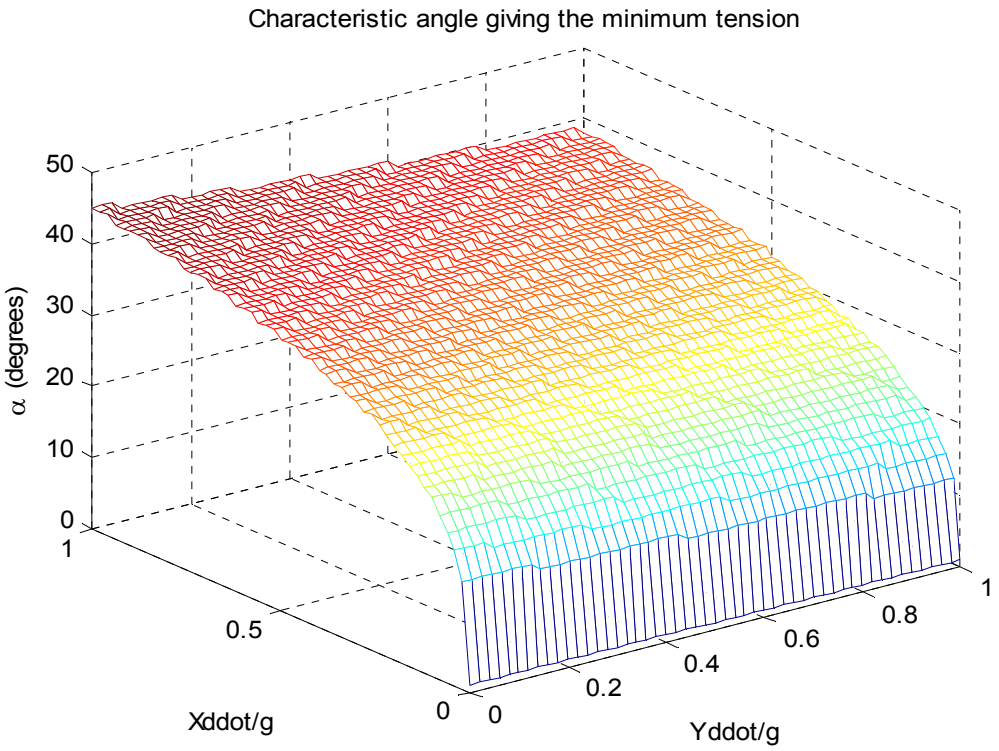

Figure 89. Optimum characteristic angle investigation for combinations of accelerations

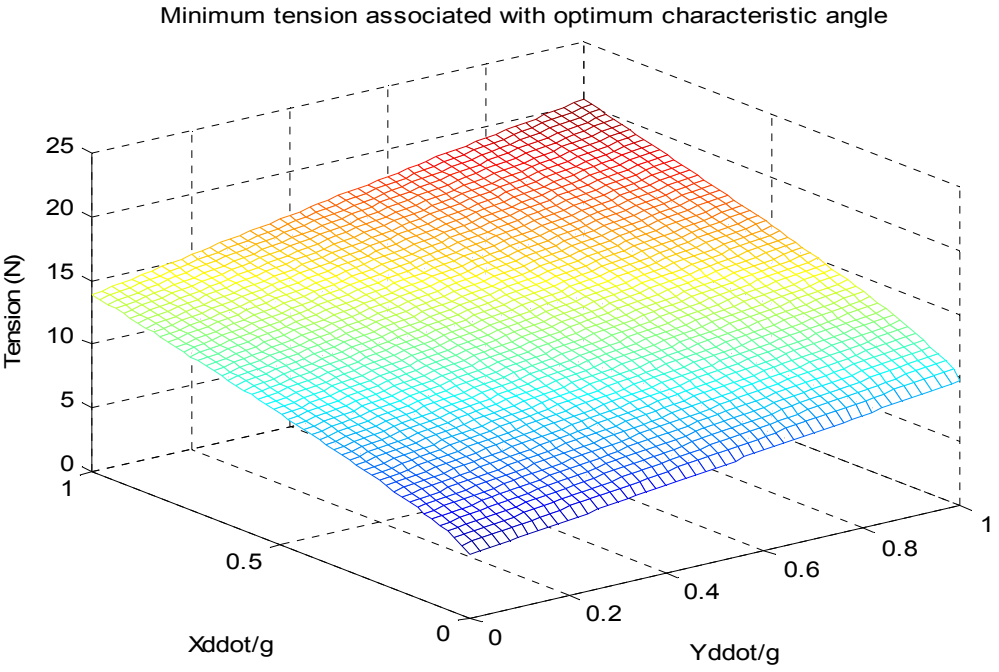

Figure 90. Tension related to optimum *α*

A first step to take advantage of the above plots and analysis would be to choose the maximum expected $\ddot{X}$ and $\ddot{Y}$ for our design and, then, iterate for the optimum *a* in terms of minimum tension. The second step would be to verify that the design would be stable for a new range of $\ddot{X}$ and $\ddot{Y}$ composed of negative values because $\ddot{Y}$ tends to destabilize the 2-pendulum. In the following example, the range of $-0.3g \le \ddot{Y} \le 0.7g$ is chosen to challenge the stability of the selection of α=38° designed to provide the minimum tension for the $\ddot{X} = g, \ddot{Y} = g$ combination of maximum accelerations.

As depicted in the following figure, there exists a range of $\ddot{X}$ and $\ddot{Y}$, where the driving design constraint is not the desired minimum tension, but, rather, the stability for the pendulum. Therefore, for $\ddot{X} = \ddot{Y} = g$, we should select another characteristic angle according to the stability criterion.

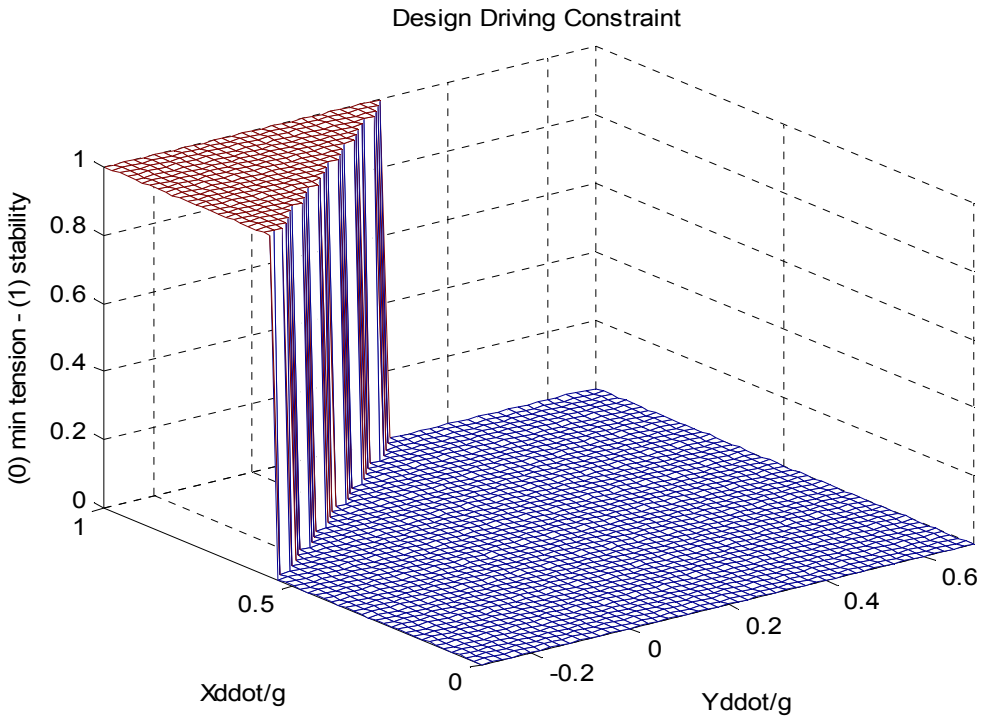

Figure 91. Design driving factor constraint versus objective function minimization

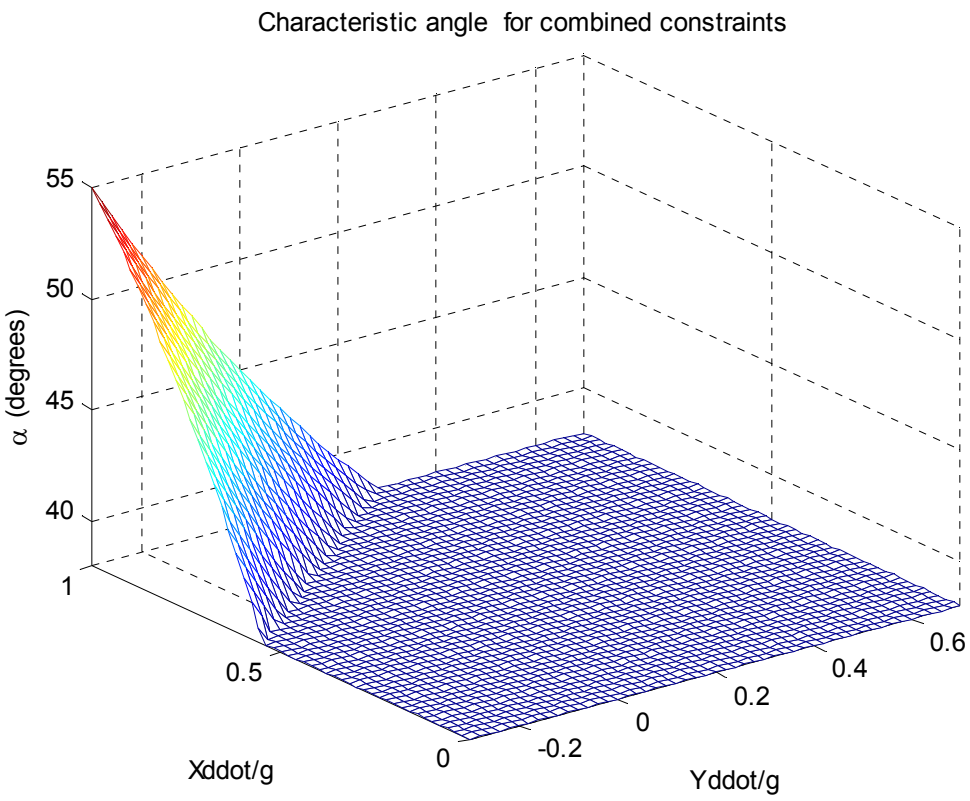

Figure 92. Characteristic angle selection for combined constraint and objective function minimization

Therefore, from Figure 92, we can decide which should be angle *α*. This would be based on the worst expected negative vertical acceleration. For example, a combination of $\ddot{X} = g, \ddot{Y} = -0.3g$ would require *α*=55°.

In addition to the above manipulations, another design method would be the use of basic optimization techniques. In terms of optimization, the problem is a minimization problem, i.e., minimizing the maximum exerted tension ($T_{\max} = \frac{(g + \ddot{Y}_{\max})}{\cos\alpha} + \frac{\ddot{X}_{\max}}{\sin\alpha}$) with one objective variable (characteristic angle *α*) and subject to boundary conditions ($\alpha > 0, \alpha > \arctan(\frac{\ddot{X}}{g + \ddot{Y}_{\min}})$). A Matlab code was developed to yield the optimum characteristic angle for given maximum and

minimum accelerations. In the following figure, we can visualize the results for an arbitrary input combination.

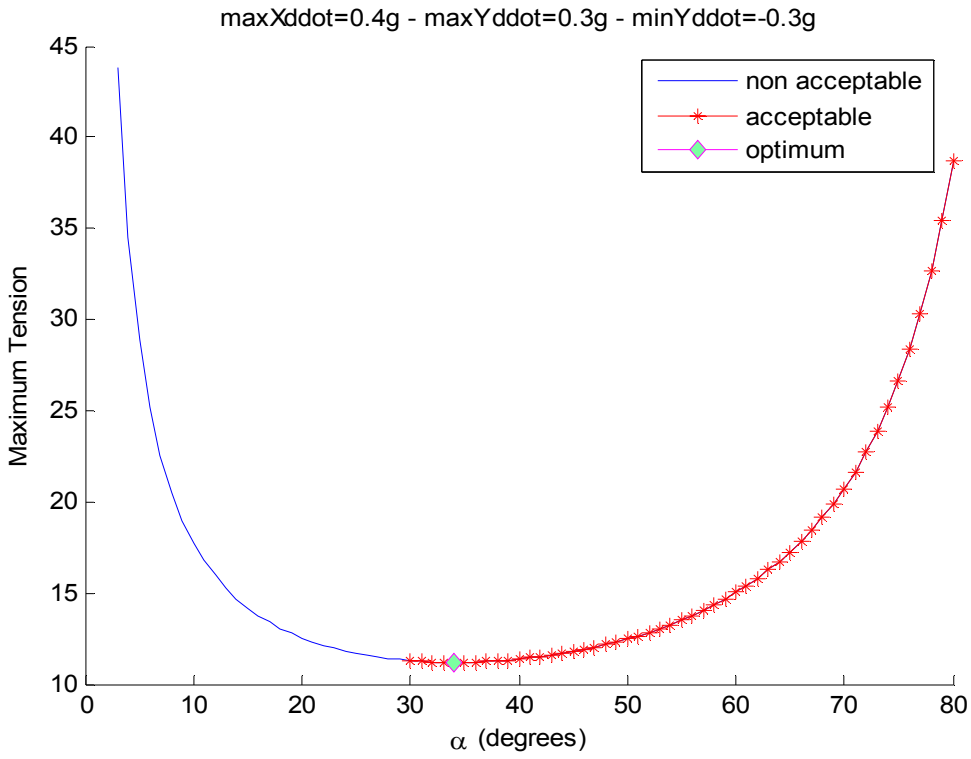

Figure 93. Optimum selection for arbitrary design inputs

c. Jumps of the Driven 2-Pendulum

The tension magnitude provided by equation (2.61) denotes that, under certain conditions, string tension may become zero. Keeping the assumption that $-\frac{\pi}{2}+\alpha \le \theta \le \frac{\pi}{2}-\alpha$, the only terms that can take tension off the string are $\ddot{X}\sin\theta$ and $\ddot{Y}\cos\theta$. Therefore, the restriction that $\|\theta+a\| > \frac{\pi}{2}$ for a jump to occur, which is valid for the unforced 2-pendulum, is unnecessary. To predict the motion of the mass after the jump, we should follow a certain procedure.

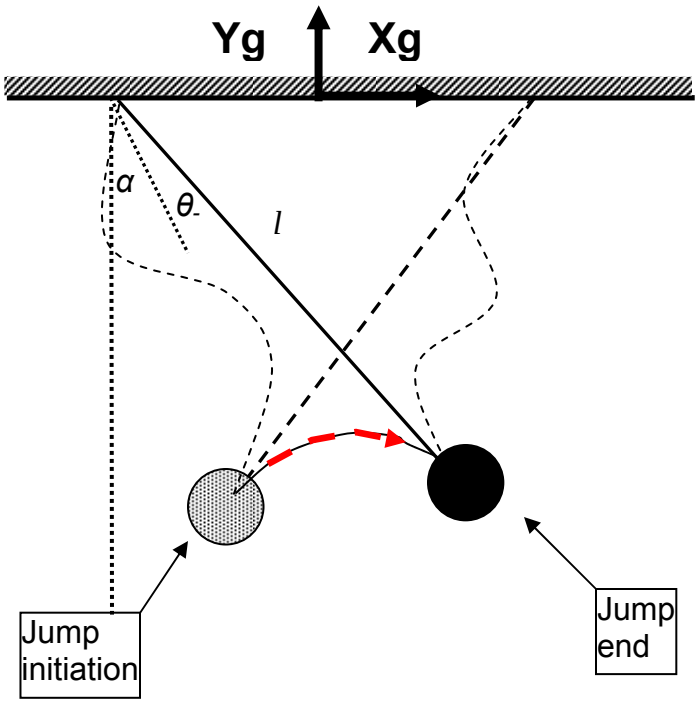

Figure 94. Jump of the 2-pendulum

Firstly, just after the jump, we should track the position with respect to a global coordinate system, x_0 and y_0, and to the linear velocity magnitude, u, of the mass. With the above initial conditions, the mass will follow a projectile path. Thus, the equations of motion are

$$x = x_0 + u_0 t \cos\phi$$
$$y = y_0 + u_0 t \sin\phi - \frac{1}{2} g t^2 \qquad (2.65)$$

Secondly, after the jump, we should track the positions, velocities, and accelerations of the two support points. Depending on the type of motion applied to the support, we should especially track the position of the support points during the jump for each time step.

Finally, we should track the distance between the mass and each one of the support points. When this distance becomes equal to the string length,

it is dynamically possible for the oscillation to proceed again. The methodology used to predict the oscillation characteristics after the end of the jump is similar to the one used while analyzing the pendulum's behavior at the switch points. Firstly, the jump takes place while both the strings lengths are less than l. Consequently, the first step is to identify which string becomes taught first. This determines if angular displacement has occurred after the jump. Secondly, the magnitude of post-jump angular displacement has to be calculated. Knowing the mass positions just before the end of the jump, x and y, as well as each of the string's support point positions, $Z_{left} = Z - l\sin\alpha$ and $Z_{right} = Z + l\sin\alpha$, the total angle defined by the taught string and the vertical, φ is

$$\begin{aligned} \phi &= \tan\left(\frac{\sqrt{Z_{right} - z}}{\sqrt{Y_{right} - y}}\right), \theta > 0 \\ \phi &= \tan\left(\frac{\sqrt{z - Z_{left}}}{\sqrt{Y_{left} - y}}\right), \theta < 0 \end{aligned} \tag{2.66}$$

Therefore,

$$\begin{aligned} \theta &= \phi - \alpha, \theta > 0 \\ \theta &= -\phi + \alpha, \theta < 0 \end{aligned} \tag{2.67}$$

Moreover, at the moment when one of the strings becomes taught one faces again a mass to string impact. Knowing the linear velocities of the mass just before the impact,

$$\begin{aligned} u_x &= u_0 \cos\phi \\ u_y &= u_0 \sin\phi - gt \end{aligned} \tag{2.68}$$

and the horizontal - vertical velocities of the support, $\dot{X}$ and $\dot{Y}$, the mass will undergo impact with the taught string. This is governed by the same restitution coefficient assumption that was explained in Chapter II, Section D, number 2. In

this case, the impact velocity components are the relative velocities between the mass and the support, $Ux_{imp} = u_x - \dot{X}, Uy_{imp} = u_y - \dot{Y}$. Consequently, the following two equations are used to obtain the post-jump angular velocity

$$\begin{aligned} \dot{\theta} &= \frac{1}{l}(-Ux_{imp}\cos\phi + Uy_{imp}\sin\phi), \theta > 0 \\ \dot{\theta} &= \frac{1}{l}(-Ux_{imp}\cos\phi - Uy_{imp}\sin\phi), \theta < 0 \end{aligned} \tag{2.69}$$

Finally, knowing the post-jump angular displacement and velocity initial allows the continuation of the oscillation subject to the new initial conditions.

3. Evaluation of Results

In the following two sets of figures (Figures 95-99 and Figures 100-104), two examples of the response prediction for forced oscillation with jumps are presented. A Matlab code Program_3.m was developed to predict the position of the mass while the supports are subjected to horizontal, for the first set, and to horizontal and vertical motion, for the second set, under conditions that will force a jump to occur. The motion that was applied to the support midpoint can be visualized in Figures 95 and 100. It can be seen that in order to produce a jump, i.e., zero tension on both strings, we applied a sudden stop to a motion that was previously under the effect of variable acceleration. This violent stop was enough to produce a distinguishable jump both in VN 4-D and in Matlab. The blue solid lines represent the Matlab predictions for the mass positions and angular displacement, while the red dashed lines represent the VN 4-D predictions.

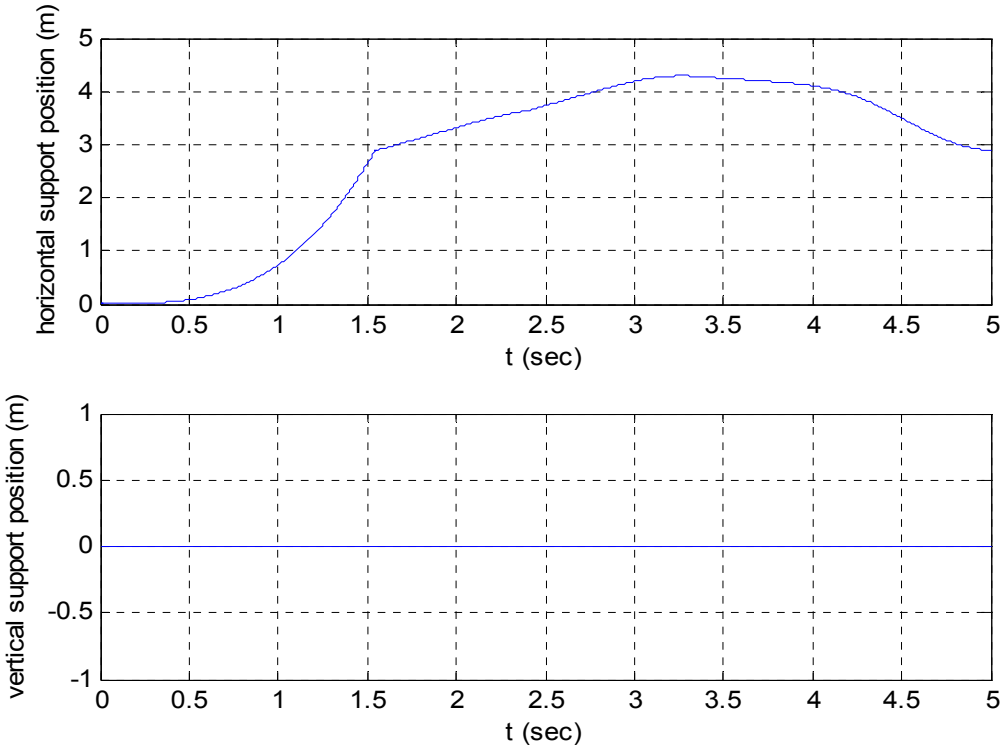

Figure 95. Support midpoint trajectory

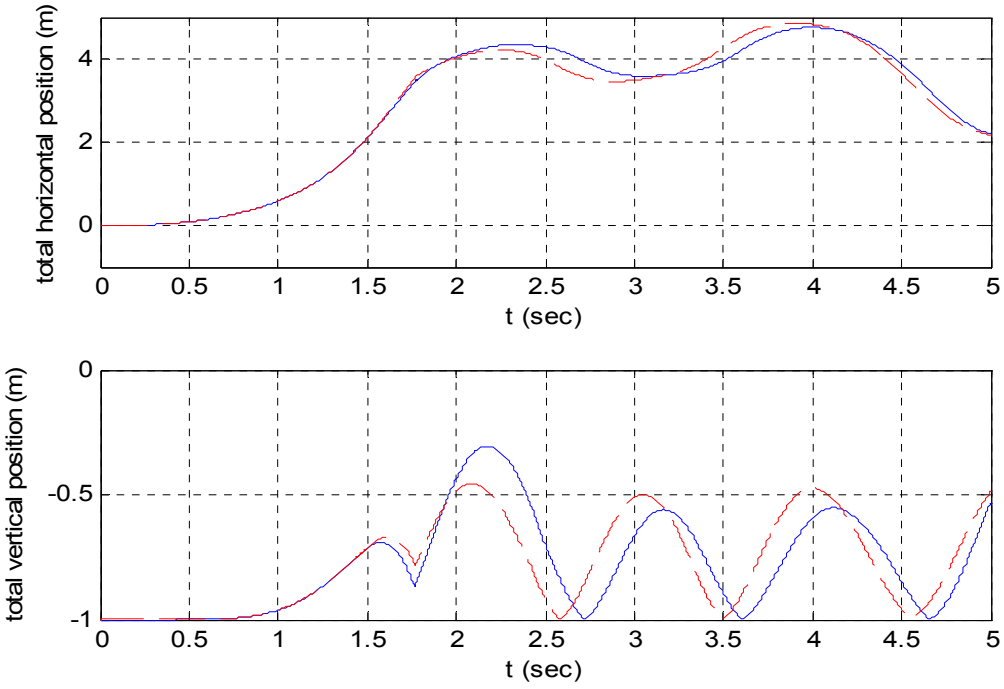

Figure 96. Mass trajectory

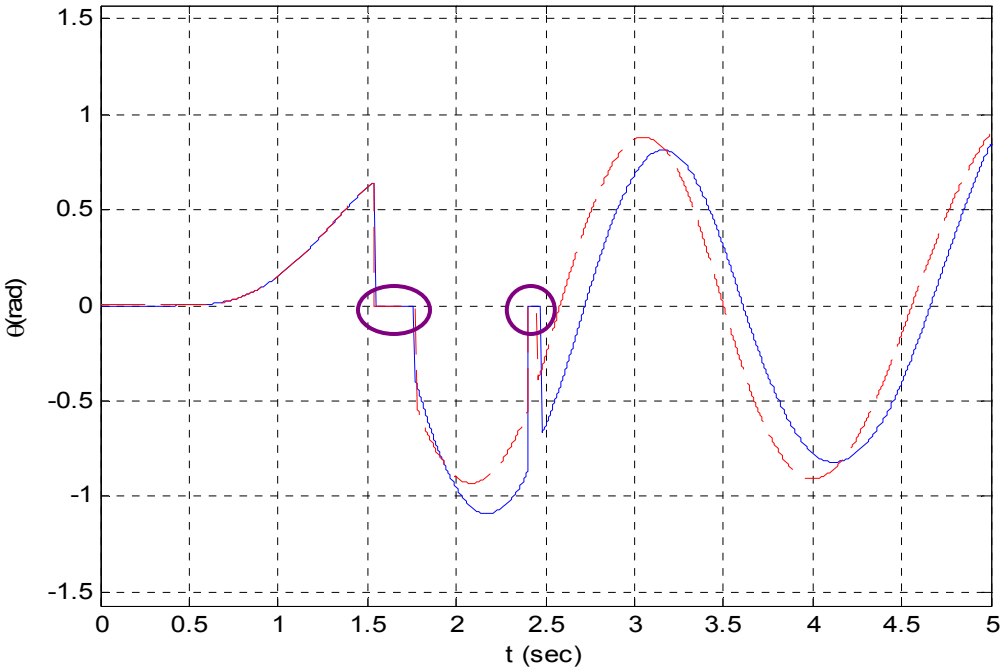

Figure 97. Angular displacement

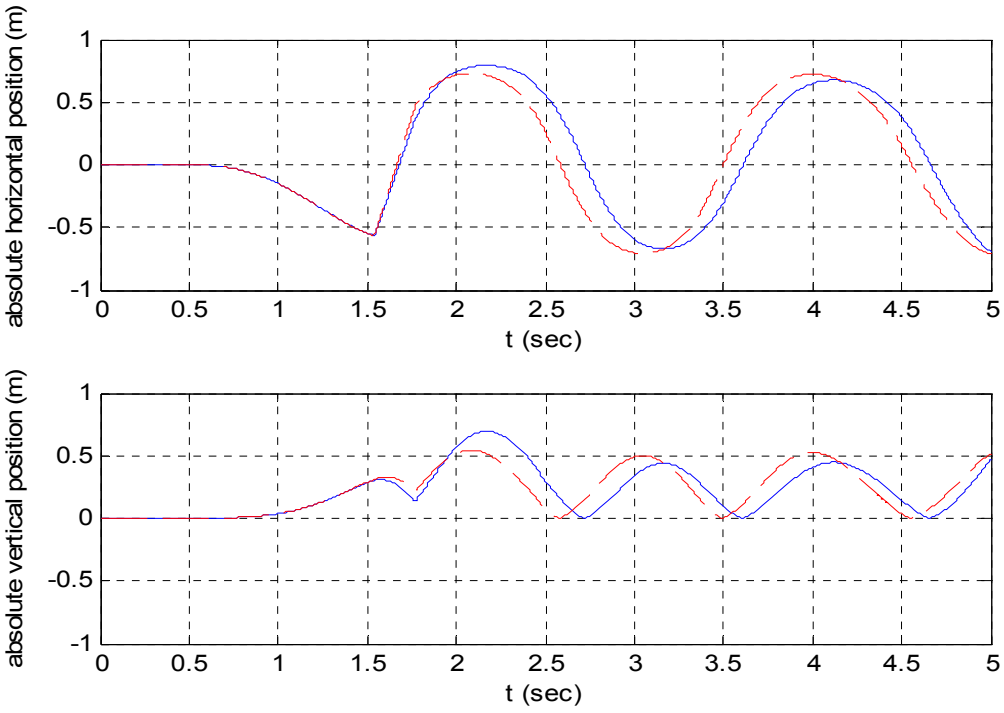

Figure 98. Mass absolute position

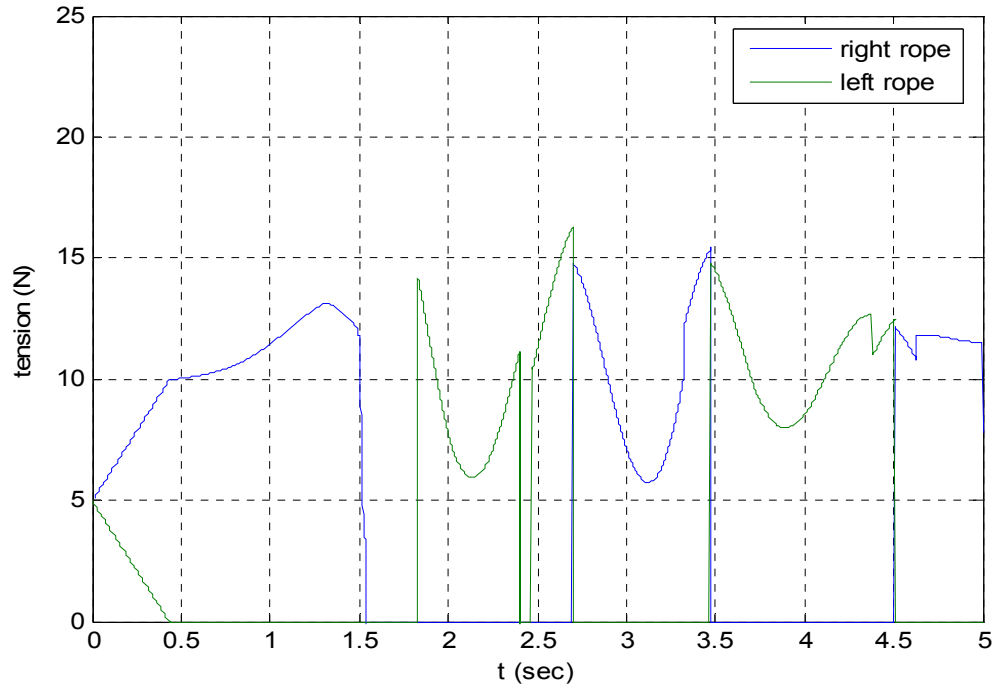

Figure 99. Tension variation

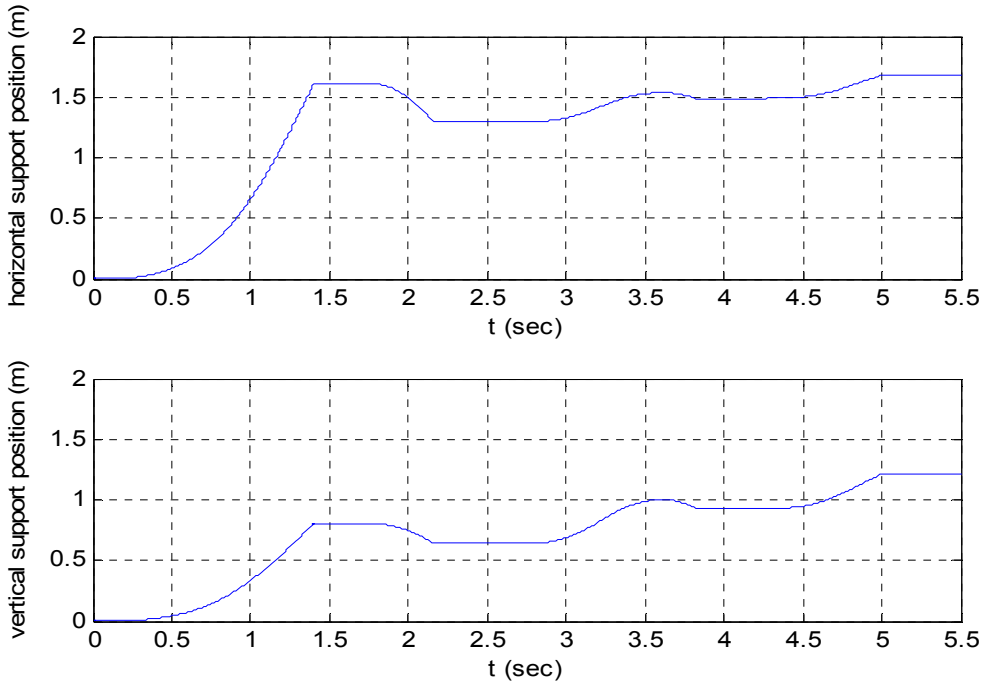

Figure 100. Support midpoint trajectory

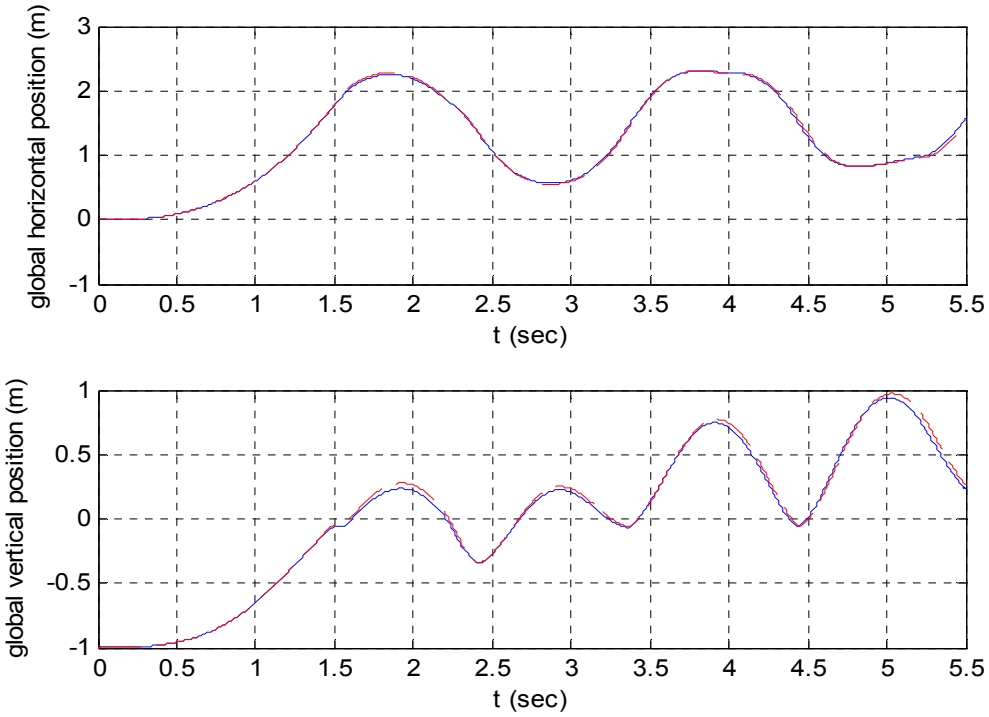

Figure 101. Mass trajectory

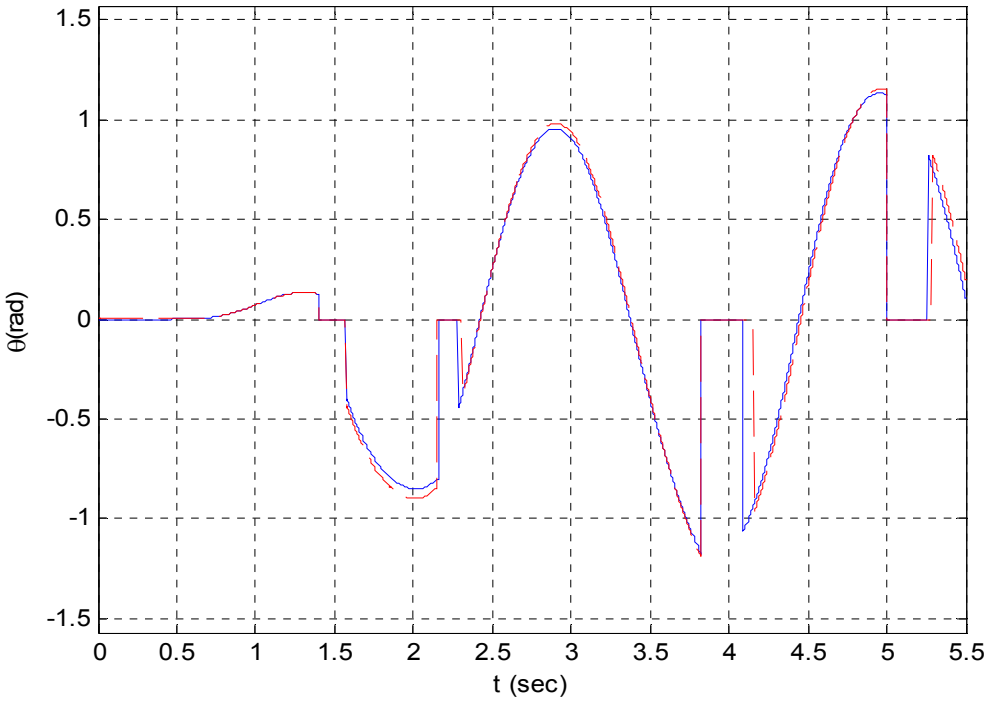

Figure 102. Angular displacement

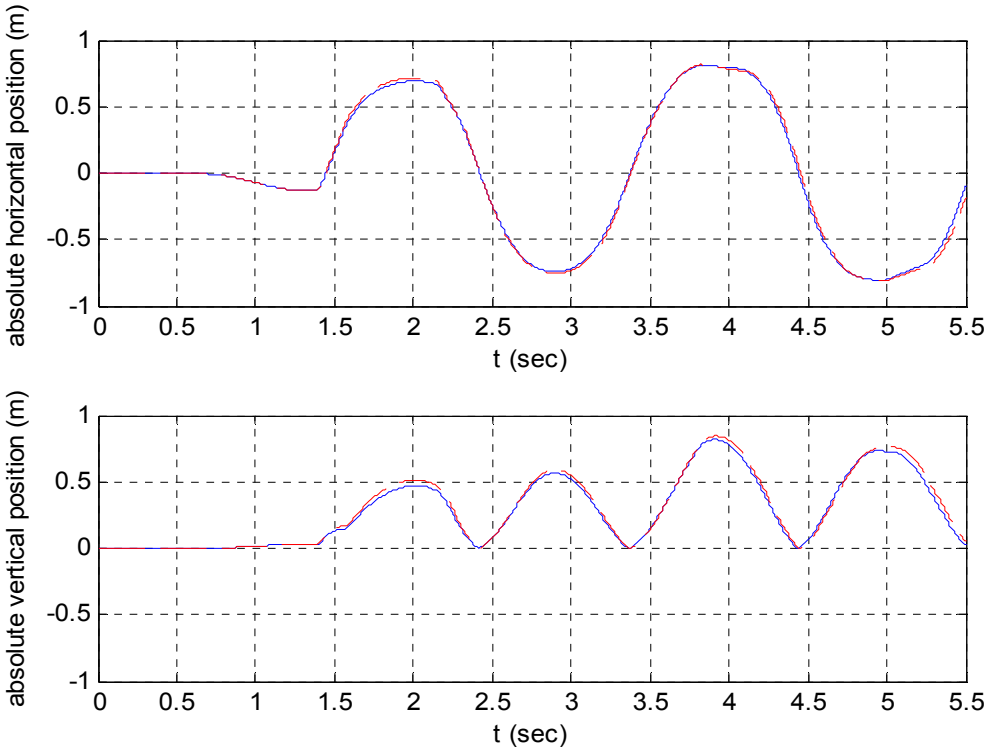

Figure 103. Mass absolute position

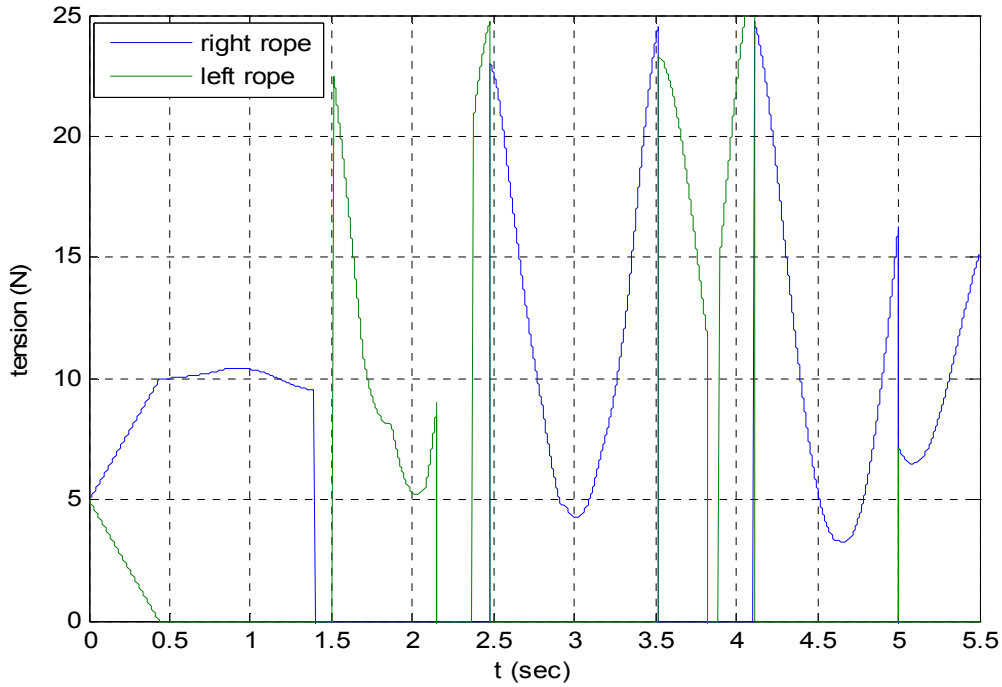

Figure 104. Tension variation

On the one hand, the positions of the support midpoint (Figures 95 and 100) and the total mass positions (Figure 96 and 101) are calculated to coordinate the axis system with its origin positioned on the support midpoint **Xg-Yg**. On the other hand, the absolute mass position is calculated wrt a coordinate axis system with its origin at the equilibrium position of the mass following the support motion (Figures 98 and 103). Moreover, the angular displacement is presented where, during the jumps, the value is set to zero (Figures 97 and 102). Finally, as explained in Chapter II, Section D, number 2.d, the strings' tensions are plotted without including the VN 4-D results.

The discrepancy that can be observed between the Matlab and VN 4-D results does not seem to be related to the complexity of the induced support motion. After a more extensive study of the VN 4-D results (tabulated data exported from the software interface), it can be seen that, in some of the jumps, a nonlinear change in the mass velocity exists at the exact moment of the jump initiation. Introducing this exact nonlinearity in the Matlab code yields the same results with VN 4-D.

4. Convergence Evaluation

An essential and final step that must be performed before ending the analysis of the driven 2-pendulum is to examine the convergence of the results for different choices of time steps. From the initial analysis of the free 2-pendulum to the simulation of the driven 2-pendulum with jumps, the integration time step selected for the numerical solution of the nonlinear equations of motion was dt=0.001 sec. Therefore, a basic evaluation procedure of the examples will be presented to verify that the selected time step offers convergence of results over other choices of larger time steps.

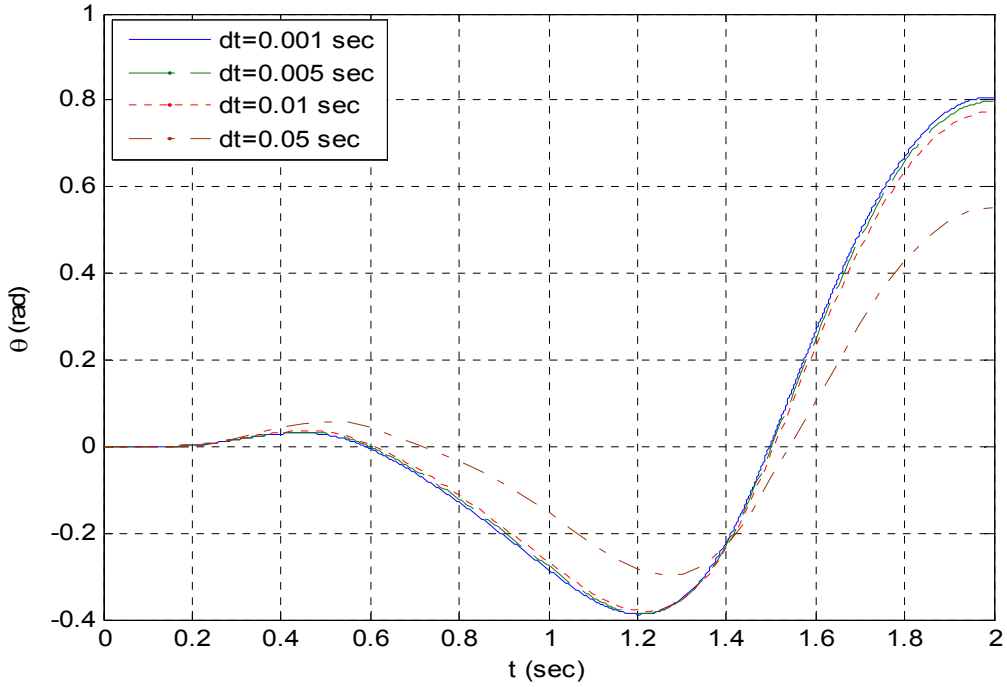

Figure 105. Convergence evaluation for forced oscillation – no jumps

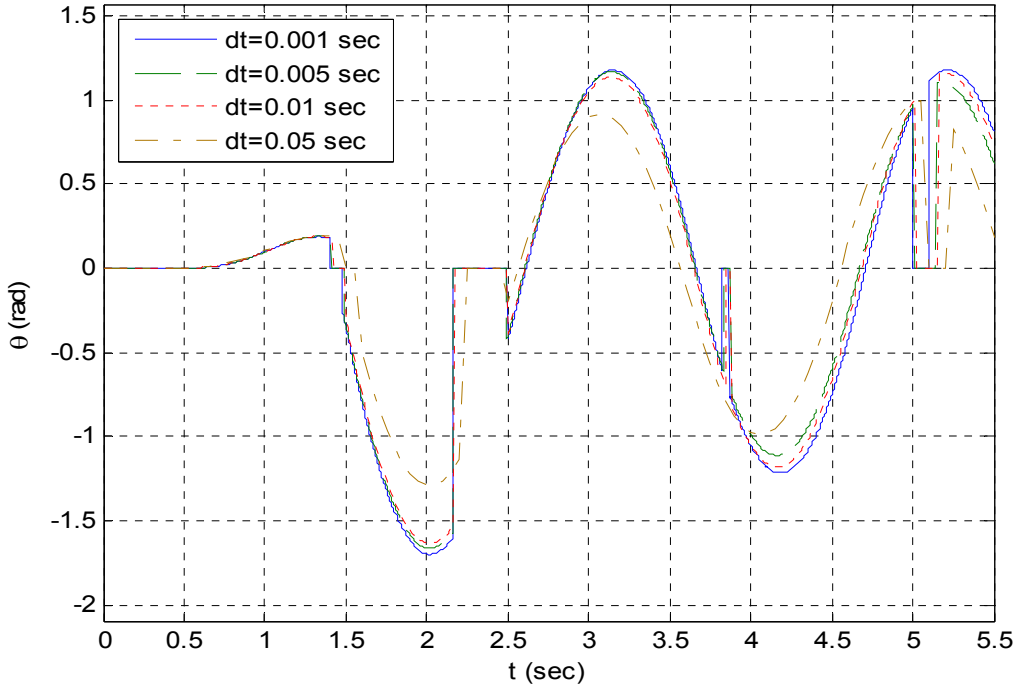

Figure 106. Convergence evaluation for forced oscillation – jumps

In Figure 105, the convergence is tested with both vertical and horizontal support motion. A case with jumps is presented in Figure 106. From both figures, one can easily conclude that gradually increasing the time step *dt* will provoke a solution divergence. While the discrepancy for *dt*=0.005 sec or *dt*=0.01 sec (up to ten times larger than the initial choice) will cause the solution to change slightly, a further increase in the time step size may yield solutions with larger discrepancies than the original. Especially in the jump cases, it can be seen that some jumps are incorrectly predicted (in terms of time of jump initiation and termination) or even skipped if the time step is large enough.

III. THE FOUR-STRING PENDULUM

A. THE 4-PENDULUM DESIGN ANALYSIS

To extend the previous analysis of the 2-pendulum to more complex designs, the performance of a four-string pendulum will be analyzed. The four strings have the same length and their supports are symmetrically placed wrt the mass. All the strings are attached to the center of mass. The following figures represent the model that was used in VN 4-D and offers four views of the design:

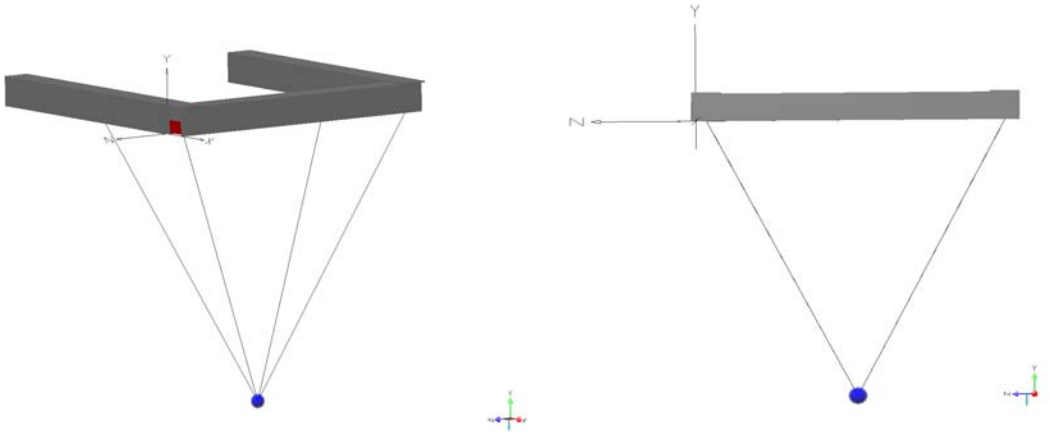

Figure 107. 4-pendulum perspective and front view

Figure 108. 4-pendulum bottom and side view

Such a design is one of the more representative simplifications of the real world suspension designs. Multi-rope suspension designs differ from each other on the number of ropes that are used, the positioning of their support points, and the selection of their attachment positions on the suspended load.

The purpose of this section's analysis will not be to investigate the swinging attitude of such a pendulum, but, rather, to study its ability not to swing when accelerating motion is applied to its support. Moreover, the string tensions will be analyzed to try to draw the most accurate picture of the design characteristics that should be considered to achieve a desirable 4-pendulum design.

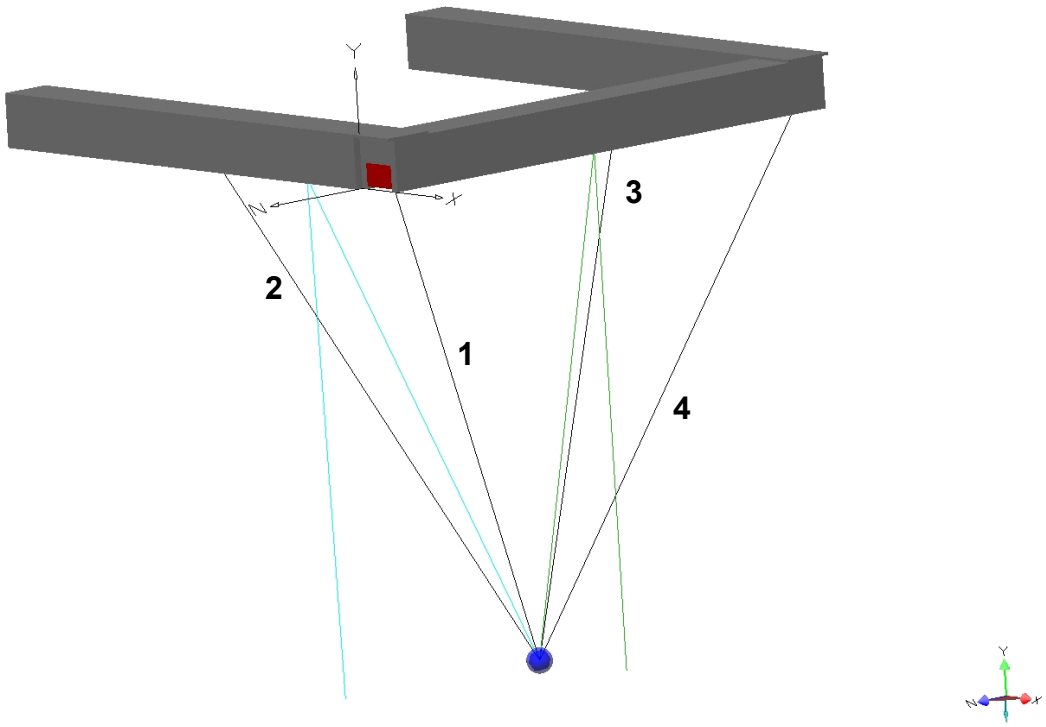

Figure 109. 4-pendulum design characteristics

In the above figure, the black sphere represents a 1kgr mass and the black lines are the strings of the pendulum. The global coordinate system of axis is presented. It dictates that the positive X-axis represents the forward motion;

the positive Z-axis represents the side motion towards the right; and the positive Y-axis represents the upward motion of the support. Since we are now dealing with a 3-D analysis, instead of 2-D for the 2-pendulum, there are two distinct characteristic angles that have to be defined. In Figure 109, the angle defined by the two green lines will be called the forward principal characteristic angle, φ_1, while the angle defined by the two turquoise lines is the side principal characteristic angle, φ_2.

1. String Tension Investigation of the Driven 4-Pendulum

The 4-pendulum is assumed to be subjected to a forward, lateral, and vertical support motion characterized by $\ddot{X}$, $\ddot{Z}$, and $\ddot{Y}$ accelerations, respectively. To formulate the tension equations for each individual string, the superposition rule will be used. Let us name the strings: string **1,** the one closest to the global system of axis; and strings **2**-**4,** counting clockwise looking the pendulum from the top (Figure 109).

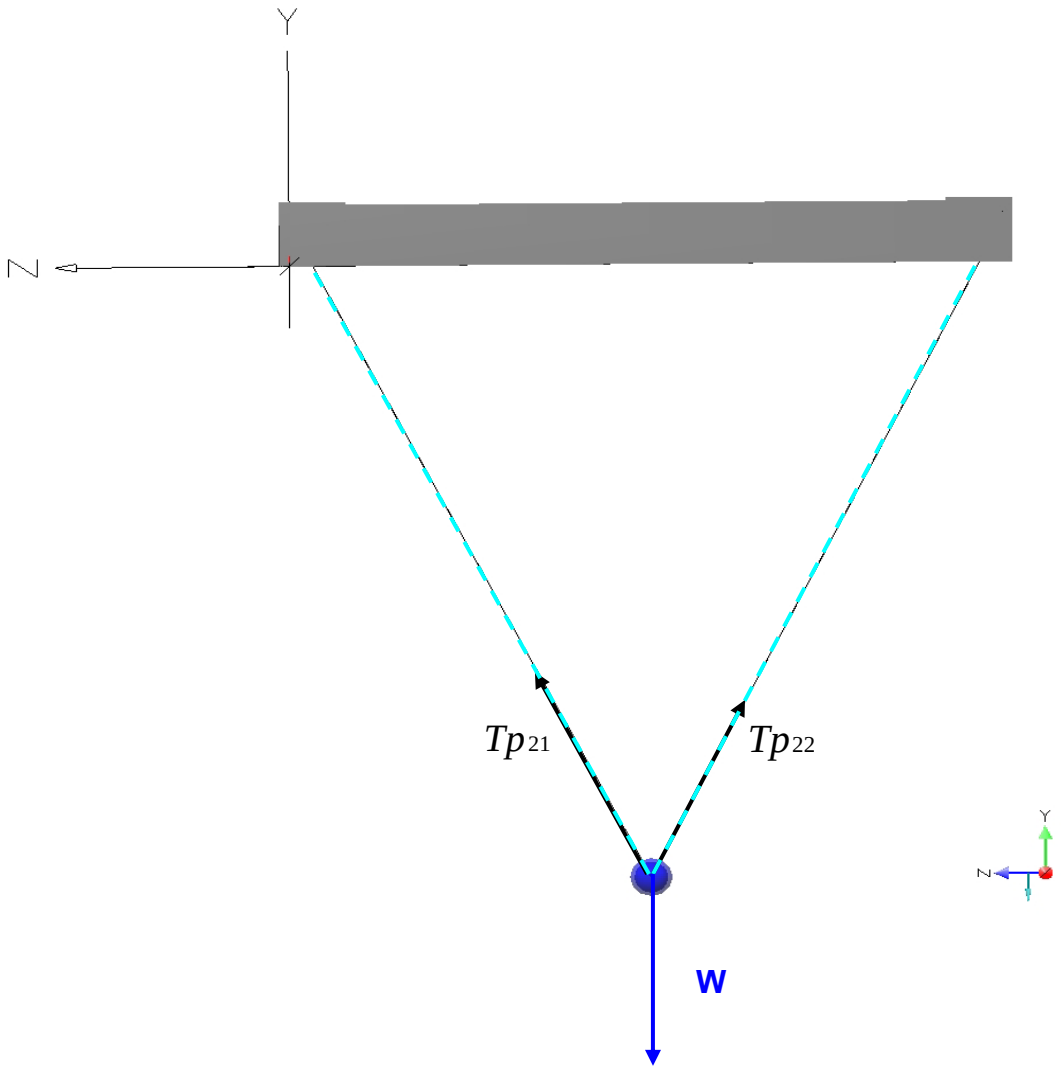

Figure 110. 4-pendulum front view tension breakdown

Initially, it will be assumed that $\ddot{X} = 0$. Thus, the analysis will be similar to the one completed for the 2-pendulum. In the figure above, the side view of the 4-pendulum shows that the strings, represented as dashed turquoise lines, lay on the same plane with the turquoise non vertical lines of Figure 109. If one of these dashed turquoise lines substituted each side pair of strings, the principal tension Tp in each of those will be in accordance with equations(2.62).

$$Tp21 = \frac{m}{2}\left(\frac{(\ddot{Y}+g)}{\cos\phi_2}+\frac{\ddot{Z}}{\sin\phi_2}\right)$$
$$Tp22 = \frac{m}{2}\left(\frac{(\ddot{Y}+g)}{\cos\phi_2}-\frac{\ddot{Z}}{\sin\phi_2}\right) \quad (3.1)$$

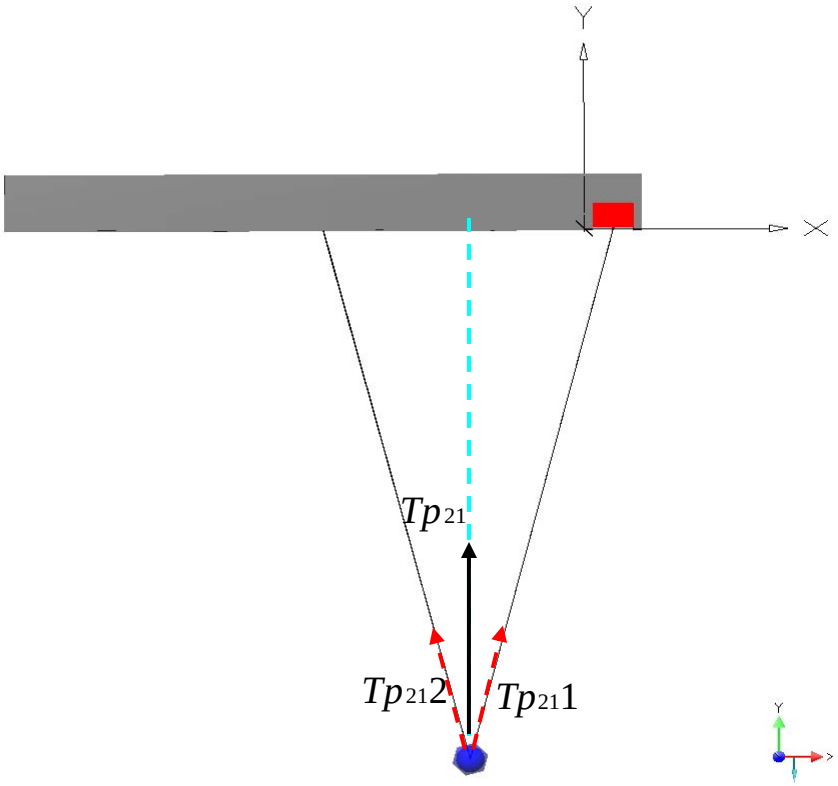

Figure 111. 4-pendulum side view tension breakdown

Looking the same model from the left-side view, $Tp21$ can be analyzed into two components, $Tp211$ and $Tp212$, since they correspond to string **1** and **2**, respectively. Let us name the angle that each of those tension components forms with the resultant tension, $\varphi_{partial2}$. These two components are equal and their magnitude is

$$Tp211 = Tp212 = \frac{Tp21}{2\cos\phi_{partial2}} \quad (3.2)$$

Then, combining equations (3.1) and (3.2),

$$Tp_{21}1 = Tp_{21}2 = \frac{m}{4\cos\phi_{partial2}}\left(\frac{(\ddot{Y}+g)}{\cos\phi_2}+\frac{\ddot{Z}}{\sin\phi_2}\right) \tag{3.3}$$

Performing the same analysis for strings **3** and **4** we yield to

$$Tp_{22}3 = Tp_{22}4 = \frac{m}{4\cos\phi_{partial2}}\left(\frac{(\ddot{Y}+g)}{\cos\phi_2}-\frac{\ddot{Z}}{\sin\phi_2}\right) \tag{3.4}$$

If we rename the tensions using simpler symbology to *T1, T2, T3,* and *T4,* respectively, and perform the same methodology for the case that $\ddot{Z}$ =0, the yielding results are

$$\begin{aligned} T1 = T4 &= \frac{m}{4\cos\phi_{partial1}}\left(\frac{(\ddot{Y}+g)}{\cos\phi_1}+\frac{\ddot{X}}{\sin\phi_1}\right) \\ T2 = T3 &= \frac{m}{4\cos\phi_{partial1}}\left(\frac{(\ddot{Y}+g)}{\cos\phi_1}-\frac{\ddot{X}}{\sin\phi_1}\right) \end{aligned} \tag{3.5}$$

Introducing three new and more generalized variables *H*, as the vertical position of the mass measured along the negative Y-axis, *Lfront*, as the frontal distance between the support points, and *Lside*, as the side view distance between the support points, the principal characteristic angles can be expressed as follows:

$$\begin{aligned} \phi_1 &= \arctan\left(\frac{Lside}{2H}\right) \\ \phi_2 &= \arctan\left(\frac{Lfront}{2H}\right) \end{aligned} \tag{3.6}$$

Additionally, let us define Lp_1 and Lp_2, the lengths of the pseudo-strings of the principal tensions (green and turquoise non-vertical lines in Figure 101), and l, the length of each string. So,

$$
\begin{aligned}
Lp1 &= \frac{H}{\cos\phi_1} \\
Lp2 &= \frac{H}{\cos\phi_2} \\
l &= \sqrt{H^2 + (\frac{Lfront}{2})^2 + (\frac{Lside}{2})^2} \\
\phi_{partial1} &= \arccos(\frac{Lp1}{l}) \\
\phi_{partial2} &= \arccos(\frac{Lp2}{l})
\end{aligned}
\tag{3.7}
$$

It can easily be proved, using the two previous equations, that

$$
\frac{1}{\cos\phi_{partial1}\cos\phi_1} = \frac{\sqrt{H^2 + (\frac{Lfront}{2})^2 + (\frac{Lside}{2})^2}}{H} = \frac{1}{\cos\phi_{partial2}\cos\phi_2} \tag{3.8}
$$

Therefore, combining (3.3), (3.4), (3.5) and (3.8), the tensions exerted on the four strings for every combination of forward, lateral and vertical accelerations are

$$
\begin{aligned}
T1 &= \frac{m}{4}(\frac{(\ddot{Y}+g)}{H} + \frac{2\ddot{X}}{Lside} + \frac{2\ddot{Z}}{Lfront})\sqrt{H^2 + (\frac{Lfront}{2})^2 + (\frac{Lside}{2})^2} \\
T2 &= \frac{m}{4}(\frac{(\ddot{Y}+g)}{H} - \frac{2\ddot{X}}{Lside} + \frac{2\ddot{Z}}{Lfront})\sqrt{H^2 + (\frac{Lfront}{2})^2 + (\frac{Lside}{2})^2} \\
T3 &= \frac{m}{4}(\frac{(\ddot{Y}+g)}{H} - \frac{2\ddot{X}}{Lside} - \frac{2\ddot{Z}}{Lfront})\sqrt{H^2 + (\frac{Lfront}{2})^2 + (\frac{Lside}{2})^2} \\
T1 &= \frac{m}{4}(\frac{(\ddot{Y}+g)}{H} + \frac{2\ddot{X}}{Lside} - \frac{2\ddot{Z}}{Lfront})\sqrt{H^2 + (\frac{Lfront}{2})^2 + (\frac{Lside}{2})^2}
\end{aligned}
\tag{3.9}
$$

This set of equations can be used, as already done for the corresponding one of the 2-pendulum, to predict the stability of the 4-pendulum, i.e., at which point that at least one of the string tensions will be equal to zero.

2. Tension Analysis Validation

Aiming to validate the above set of equations, the VN 4-D model was used. The setup of the model was complicated due to the required level of dimensional precision. Finally, the method that provided the most reasonable results (absence of nonlinearities in tension) was to combine two separate runs of the software -- one with no forward acceleration and one with no lateral acceleration -- and then superimpose the results. In this specific model *m*=1kgr, the frontal distance between the support points is *Lfront*=2m; the side distance is *Lside*=1m; and the vertical position of the mass is *H*= 2 m. Finally, the applied accelerations are $\ddot{X} = 2t(m/\sec^2)$, $\ddot{Z} = 4t(m/\sec^2)$, and $\ddot{Y} = 0$ (t in seconds).

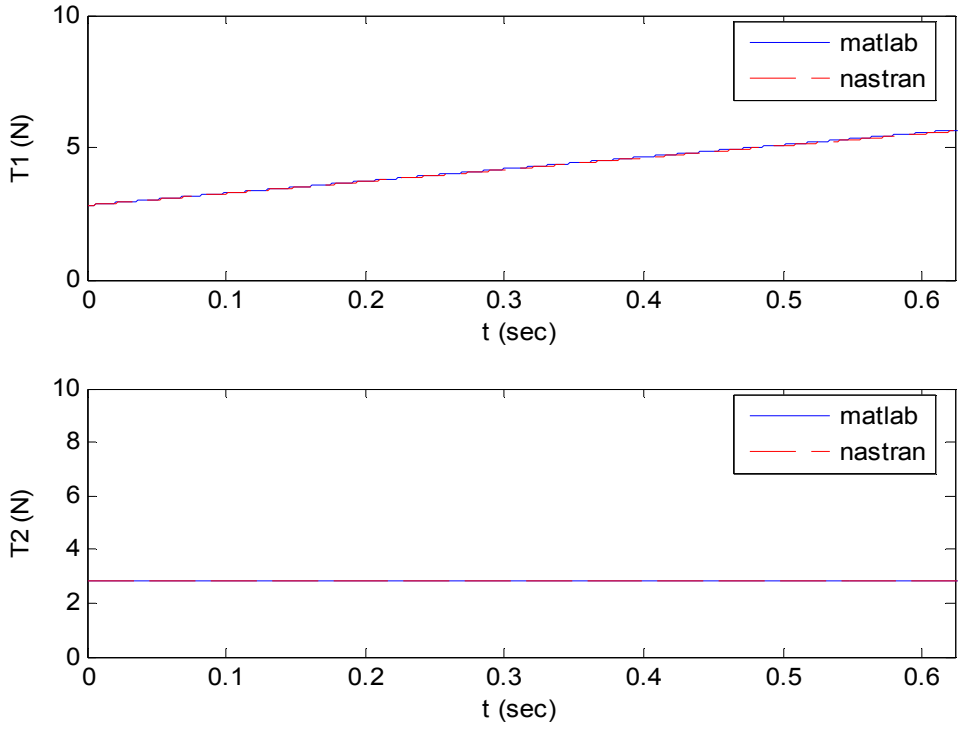

Figure 112. Strings **1** and **2** tension validation

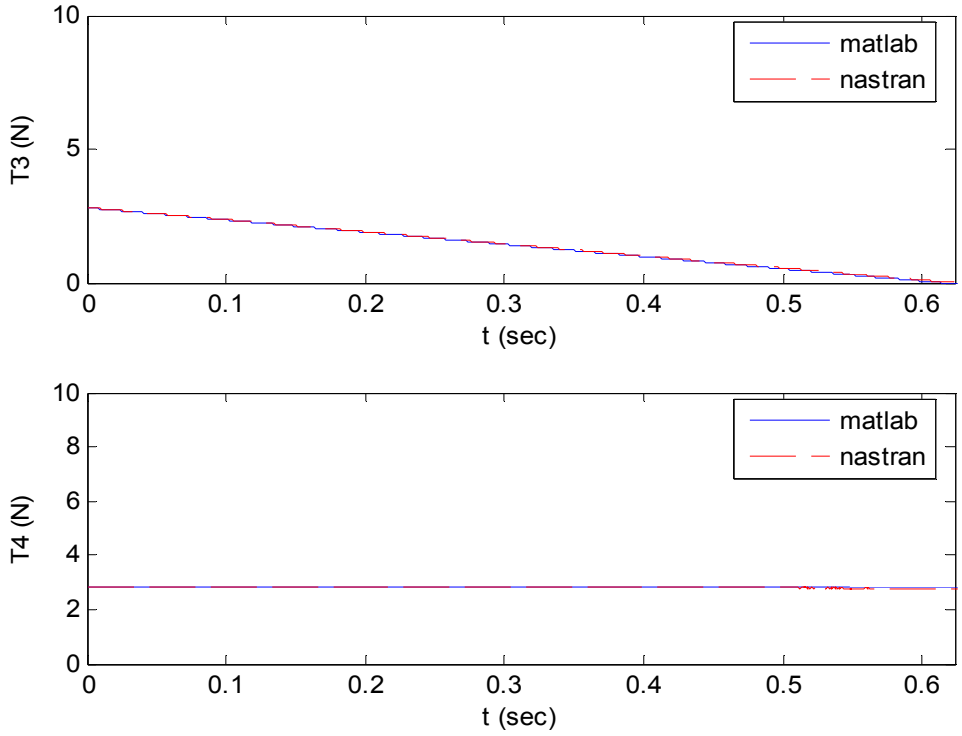

Figure 113. Strings **3** and **4** tension validation

B. 4-PENDULUM DESIGN OPTIMIZATION

The procedure of design optimization for the 4-pendulum requires that one defines the objective function, the design variables, and the constraints -- just like it was done for the 2-pendulum. Once again, the objective function is to minimize the tension that will be exerted on a string for a given set of accelerations. The design variables are the distances *H, Lfront* and *Lside*.

According to (3.9) set of equations, the $Lfront$, $Lside$, and *H* substitute ϕ_1 and ϕ_2 as the design variables. Nevertheless, we can constrain the value of *H* with an equality constraint, instead of an inequality one, to be able to obtain a 2-D visualization of the objective function.

In the following example, the known values are *H*=1m, $Lfront_{\min} = Lside_{\min} = 0.2m$, and

$$\ddot{X}_{\max} = \ddot{Z}_{\max} = \ddot{Y}_{\max} = \frac{g}{3}$$

$$\ddot{Y}_{\min} = -\ddot{Y}_{\max}$$

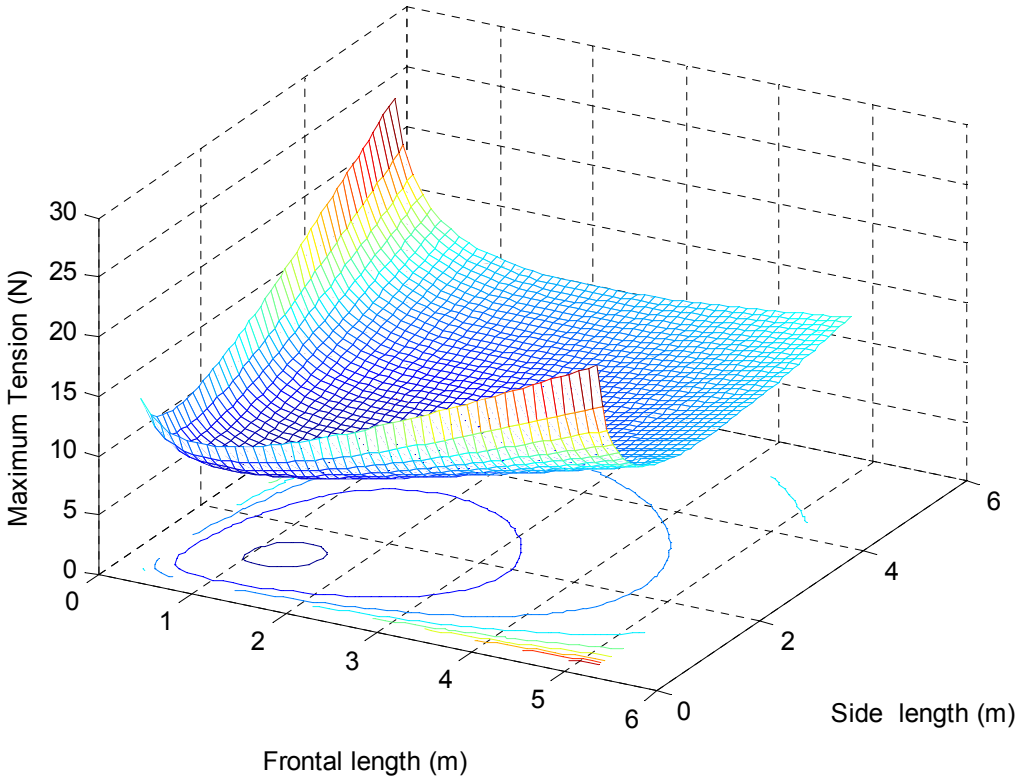

Figure 114. Maximum exerted tension for arbitrary accelerations

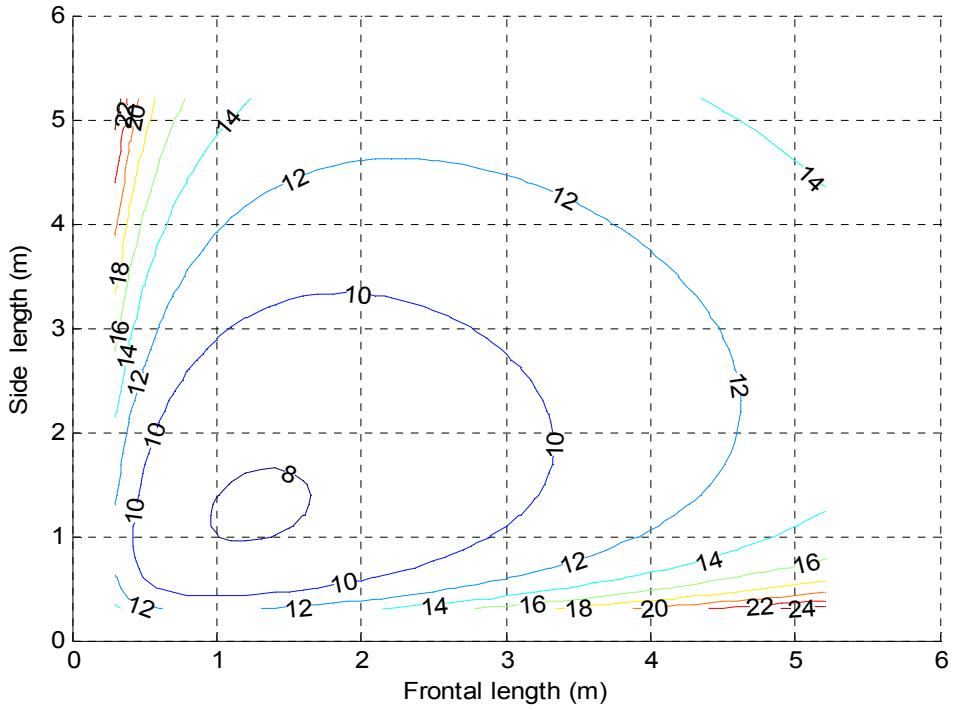

Figure 115. Maximum tensions exerted for arbitrary accelerations

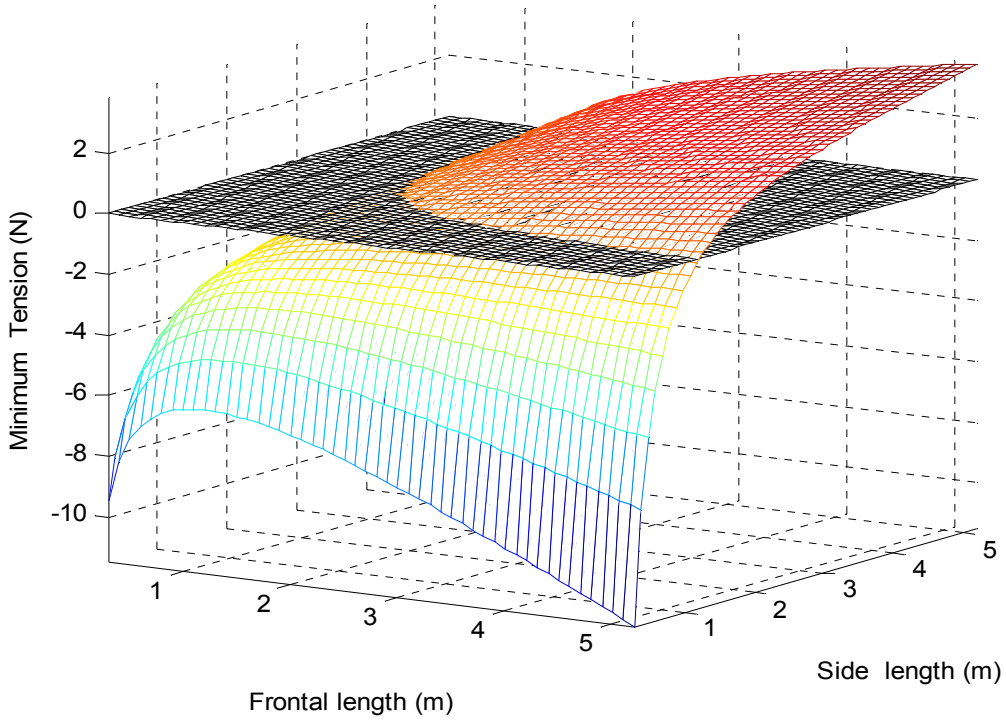

Figure 116. Visualization of designs that fulfill the stability constraint

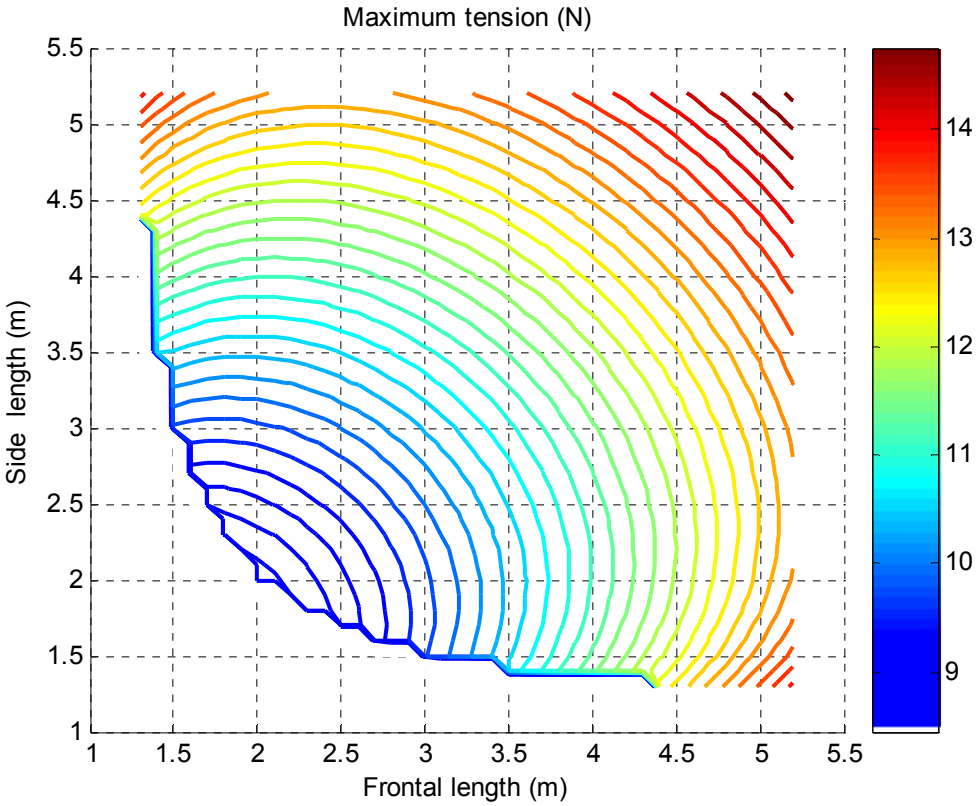

Figure 117. Final visualization of maximum tensions for arbitrary accelerations

In Figure 117, we can visualize the acceptable *Lfront* and *Lside* combinations and at the same time find the optimum solution to our problem. Clearly the optimum solution is *Lfront*= *Lside*=2m. This solution can also be verified using the `fmincon` optimization Matlab function, which also yields the same result.

IV. CONCLUSIONS AND RECOMMENDATIONS

A. SUMMARY AND CONCLUSIONS

The following table summarizes the basic equations developed throughout this thesis.

A/A	Description	Equation	Equation No
1	Free oscillation of 2-pendulum	$\ddot{\theta}+\frac{g}{l}\sin\theta\cos\alpha+\frac{g}{l}\cos\theta\sin\alpha\,\mathrm{sign}\,\theta=0$ subject to $\dot{\theta}_{+i}=\dot{\theta}_{-i}\sqrt{(\sin(90-2\alpha))^2+(r\cos(90-2\alpha))^2}$	(2.18) and (2.55)
2	SCPA method prediction	$\theta=\mathrm{A}\cos\left(\omega_0+\frac{2P}{\pi A\omega_0}\right)t$ $\omega_0^2=\frac{g}{l}\cos\alpha$ $P=\frac{g}{l}\sin\alpha$	(2.32) and (2.24)
3	Energy method prediction	$\ddot{\theta}+F\frac{g}{l}\sin\theta=0$ $F=\int_0^{\theta_0} mg\sin(\alpha+\theta)d\theta/\int_0^{\theta_0} mg\sin\theta d\theta$	(2.39) and (2.38)
4	Driven 2-pendulum	$\ddot{\theta}+(\frac{(g+\ddot{Y})}{l}\cos\alpha+\frac{\ddot{X}}{l}\sin\alpha)\sin\theta+$ $(\frac{(g+\ddot{Y})}{l}\sin\alpha-\frac{\ddot{X}}{l}\cos\alpha)sign\theta\cos\theta=0$	(2.60)

5	Stability criterion for driven 2-pendulum	$\frac{\left\|\ddot{X}\right\|}{\tan\alpha}-\ddot{Y}>g$	(2.63)
6	String tensions for driven 2-pendulum while in equilibrium position	$T1=\frac{m}{2}(\frac{(\ddot{Y}+g)}{\cos\alpha}+\frac{\ddot{X}}{\sin\alpha})$ $T2=\frac{m}{2}(\frac{(\ddot{Y}+g)}{\cos\alpha}-\frac{\ddot{X}}{\sin\alpha})$	(2.62)
7	String tensions for driven 4-pendulum while in equilibrium position	$T1=\frac{m}{4}(\frac{(\ddot{Y}+g)}{H}+\frac{2\ddot{X}}{Lside}+\frac{2\ddot{Z}}{Lfront})\sqrt{H^2+(\frac{Lfront}{2})^2+(\frac{Lside}{2})^2}$ $T2=\frac{m}{4}(\frac{(\ddot{Y}+g)}{H}-\frac{2\ddot{X}}{Lside}+\frac{2\ddot{Z}}{Lfront})\sqrt{H^2+(\frac{Lfront}{2})^2+(\frac{Lside}{2})^2}$ $T3=\frac{m}{4}(\frac{(\ddot{Y}+g)}{H}-\frac{2\ddot{X}}{Lside}-\frac{2\ddot{Z}}{Lfront})\sqrt{H^2+(\frac{Lfront}{2})^2+(\frac{Lside}{2})^2}$ $T4=\frac{m}{4}(\frac{(\ddot{Y}+g)}{H}+\frac{2\ddot{X}}{Lside}-\frac{2\ddot{Z}}{Lfront})\sqrt{H^2+(\frac{Lfront}{2})^2+(\frac{Lside}{2})^2}$	(3.9)

Table 2. Equations summary

Based on the analysis performed throughout this thesis, including both the analytical formulation of the mathematical equations and their validation performed with the aid of VN 4-D, we can draw the following conclusions:

- The 2-pendulum's configuration of two strings per mass introduces two distinct nonlinear oscillation characteristics. The first one results from the discontinuity in its stiffness around the equilibrium position, i.e. an instantaneous jump in the value of the restoring moment around zero. Four different methods, were used to incorporate this discontinuity in analytical equation formulation: Numerical solution with `ode45`, exact solution for a time increment, SCPA method and Energy method.

- The second nonlinear oscillation characteristic is related to the energy dissipation that takes place at the switch point. The dynamics that govern this behavior are correlated to the dynamics of a standard collision of a mass on a rigid wall, with specific velocity direction constraints before and after the collision. The idealized model is based on an instantaneous impact and total energy loss related to the mass' velocity component parallel to the taught string's direction. This assumption is validated by the VN 4-D simulation.

- Another characteristic that was analyzed was the stability of the 2-string pendulum in forced oscillation. This string configuration results in the absence of oscillatory behavior if the mass is initially at the equilibrium position and the driving horizontal and vertical accelerations do not exceed values determined exclusively by the characteristic angle α. This observation allows the rational design of support systems under given support motion characteristics.

- The general behavior of the driven 2-pendulum was investigated including the case of induced jumps. Specific examples demonstrated the highly non-nonlinear behavior of the 2-pendulum when extreme acceleration values of the support cause the strings to go slack.

- Finally, the analysis of the 2-pendulum was extended on the 4-pendulum configuration, which is a more common support design in practice. A typical optimization study was presented in order to visualize the practical design

advantages that such an analysis offers. It was shown that it is possible to reduce both motions and cable tensions by appropriate selections of string angles.

B. RECOMMENDATIONS

Further development of the analysis presented in this work could be in the application of angular support motion, both for the case of forced oscillations of the 2-pendulum and the trade off analysis. This work would provide a more realistic representation of the support motion analogous to the motion of the ship. Further extensions to this work by considering the effects of string elasticity are also recommended.

APPENDIX: COMPUTER PROGRAMS

```
%Program_1.m
%------------------------------------------------------------------------
%------------------------------------------------------------------------
%Computing the response of free 2-pendulum using three distinct
methods: Numerical solution, SCPA method and Energy method
%------------------------------------------------------------------------
%------------------------------------------------------------------------


clear all
clc
close all
global a omega2 A omega P maxy1 Thetao t increased_restoring
THETAo=pi/10            %initial angular displacement
THETAo_dot=0            %initial angular velocity


a=input('Give the characteristic angle a ');%2-pendulum's
characteristic
                                            %angle
g=9.81;                 %acceleration of gravity
ll=1;                   %equivalent string length which equals to the
                        %simple pendulum string length or the
                        %perpendicular distance of the mass from
                        %the plane of suspension
l=ll/cos(a)             %string length of complex pendulum
omega2=g/l;             %square of the natural frequency of the
                        % standard pendulum
omega2o=omega2*cos(a);  %square of the pseudo natural frequency of the
                        %2-pendulum
tf=3;                   %final time

%------------------------------------------------------------------------
%------------------------------------------------------------------------
%Numerical solution of the differential equation of motion
%------------------------------------------------------------------------
%------------------------------------------------------------------------

options = odeset('RelTol',1e-6,'AbsTol',[1e-6 1e-6]);
[t,x]=ode45('Ffull',[0:0.01:tf],[THETAo,THETAo_dot],options);
[t,x(:,1)];
X1=x;


                            figure (1)

          hold on
          title('\alpha=\pi/6')
                            plot(t,x(:,1),'g')
```

```
maxy1=max(x(:,1));
maxy2=max(x(:,2));

%-------------------------------------------------------------------------
%-------------------------------------------------------------------------
%SCPA method
%-------------------------------------------------------------------------
%-------------------------------------------------------------------------

 A=THETAo;
 B=sqrt(2*g*(ll-cos(THETAo+a))/l);
                                  t=0:0.01:tf;
[xap,yap,Tapprox,Uo,Texact,t1,Ain]=SCPA(t,a,omega2,A,omega,P,maxy1);


                                  plot(t,xap,'--r')

X1ap=[];
Y1ap=[];
for i=1:Tapprox*100;
   t=(i-1)*0.01;
   [xap,yap,Tapprox,Uo,Texact,t1,Ain]=SCPA(t,a,omega2,A,omega,P,maxy1);

X1ap(i)=xap;
Y1ap(i)=yap;
end

%-------------------------------------------------------------------------
%-------------------------------------------------------------------------
%Energy method
%-------------------------------------------------------------------------
%-------------------------------------------------------------------------

syms x Theta phi increasing_factor square_nat_freq phi t Initial_theta
Initial_theta_dot
y=int('sin(x)',x,0,Theta);
z=int('sin(phi+x)',x,0,Theta);
z=subs(z,phi,a);
z=subs(z,Theta,maxy1);
y=subs(y,Theta,maxy1);
increased_restoring=z/y;


[t,y]=ode45('E',[0:0.01:tf],[THETAo,THETAo_dot],options);
[t,y(:,1)];
plot(t,y(:,1),'-.b')
Y1=y;
%-------------------------------------------------------------------------
%-------------------------------------------------------------------------
```

```
                                t=0:0.01:tf;

                                xlabel('t (sec)')
                                ylabel('\theta (rad)')
                                grid on
                                box on
                                legend('ODE45 ','SCPA method','Energy
method')
                                axis([0 tf -1.25*maxy1 0.6])
             hold off

Tapprox1=Tapprox;   % Approximate Period of the Slowly Changing method
Texact1=Texact;     %Period from the analytical solution calculating
                    % for the time period when the sign of theta is
                    %constant



figure (2)
title('\alpha=\pi/6')
hold on
plot(X1(1:Texact1*100,1)./THETAo,X1(1:Texact1*100,2)./sqrt(omega2o),'g'
,X1ap./THETAo,Y1ap./sqrt(omega2o),'--r',
Y1(1:Tapprox1*100,1)./THETAo,Y1(1:Tapprox1*100,2)./sqrt(omega2o),'-.b')
grid on
box on
xlabel('\theta/\thetao');ylabel('\theta''/\omega\o')
legend('ODE45 ','SCPA method','Energy method')
axis([-1.5 1.5 -1  1])
hold off
```

```
%Subroutine Ffull.m of Program_1.m and Program_2.m
%------------------------------------------------------------------------
%------------------------------------------------------------------------
%Numerical solution of the differential equation of motion for
%the 2-pendulum
%------------------------------------------------------------------------
function xp=Ffull(t,x)
global a omega2

xp=zeros(2,1);
xp(1)=x(2);

xp(2)=-sin(x(1))*omega2*cos(a)-omega2*cos(x(1))*(sin(a))*sign(x(1));



%Subroutine E.m of Program_1a.m and Program_1b.m
%------------------------------------------------------------------------
%------------------------------------------------------------------------
%Numerical solution of the differential equation of motion for
%the 2-pendulum
%------------------------------------------------------------------------
%------------------------------------------------------------------------

function yp=E(t,y)
global a omega2 increased_restoring

yp=zeros(2,1);
yp(1)=y(2);

yp(2)=-sin(y(1))*omega2*increased_restoring;



%Subroutine SCPA.m of Program_1.m
%------------------------------------------------------------------------
%------------------------------------------------------------------------
%SCPA method
%------------------------------------------------------------------------
%------------------------------------------------------------------------

function
[xap,yap,Tapprox,Uo,Texact,t1,Ain]=SCPA(t,a,omega2,A,omega,P,maxy1);
global a omega2 A  omega P maxy1 Ain
P=omega2*sin(a);
omega =sqrt(omega2*cos(a));
t1=(1/sqrt(omega2))*acos(1/(1+(A*omega2*cos(a))/(omega2*sin(a))));
xap=A*cos((omega+2*P/(pi*omega*A))*t);
yap=A*(omega+2*P/(pi*omega*A))*sin((omega+2*P/(pi*omega*A))*t);
Tapprox=2*pi/(omega+2*P/(pi*omega*A));
Uo=-omega*(A+P/(omega.^2))*sin(omega*t1);
Ain=-Uo/omega -(P/(omega.^2))*sin(omega*t1);
Texact=(4/omega)*acos(1/(1+A*omega*omega/P));
```

```
%Program_2.m
%------------------------------------------------------------------------
%------------------------------------------------------------------------
%Computing the response of free 2-pendulum using three distinct
methods: Numerical solution, SCPA method and Energy method
%------------------------------------------------------------------------
%------------------------------------------------------------------------


clear all
clc
close all
global a omega2 A omega P maxy1 Thetao t increased_restoring
THETAo=0                %initial angular displacement
THETAo_dot=1.22         %initial angular velocity


a=input('Give the characteristic angle a ');%2-pendulum's
characteristic angle

g=9.81;                 %acceleration of gravity
ll=1;                   %equivalent string length which equals to the
%simple pendulum string length or the %perpendicular distance of the
mass from
%the plane of suspension
l=ll/cos(a)             %string length of complex pendulum
omega2=g/l;             %square of the natural frequency of the
                        % standard pendulum
omega2o=omega2*cos(a);  %square of the pseudo natural frequency of the
                        %2-pendulum
tf=3;                   %final time

%------------------------------------------------------------------------
%------------------------------------------------------------------------
%Numerical solution of the differential equation of motion
%------------------------------------------------------------------------
%------------------------------------------------------------------------

options = odeset('RelTol',1e-6,'AbsTol',[1e-6 1e-6]);
[t,x]=ode45('Ffull',[0:0.01:tf],[THETAo,THETAo_dot],options);
[t,x(:,1)];

%------------------------------------------------------------------------
%------------------------------------------------------------------------
%Predicting the maximum displacement based on the initial velocity
% using energy conservation and geometry
%------------------------------------------------------------------------
%------------------------------------------------------------------------

so=l*cos(a);
```

```
h=THETAo_dot*THETAo_dot*l*l/(2*g);
h1=ll-h;
THETAo2=acos(h1/l)-a;



                                figure (1)

           hold on
           title('\alpha=\pi/6')
                                plot(t,x(:,1),'g')



maxy1=max(x(:,1));

%-------------------------------------------------------------------------
%-------------------------------------------------------------------------
%SCPA method
%-------------------------------------------------------------------------
%-------------------------------------------------------------------------
A=THETAo2;
                                t=0:0.01:3;
[xap,Tapprox,Uo,Texact,t1,Ain]=SCPA_u(t,a,omega2,A,omega,P,maxy1);

                                plot(t,xap,'--r')


%-------------------------------------------------------------------------
%-------------------------------------------------------------------------
%Energy method
%-------------------------------------------------------------------------
%-------------------------------------------------------------------------

syms x Theta phi increasing_factor square_nat_freq phi t Initial_theta
Initial_theta_dot
y=int('sin(x)',x,0,Theta);
z=int('sin(phi+x)',x,0,Theta);
z=subs(z,phi,a);
z=subs(z,Theta,maxy1);
y=subs(y,Theta,maxy1);
increased_restoring=z/y;


[t,y]=ode45('E',[0:0.01:tf],[THETAo,THETAo_dot],options);
[t,y(:,1)];
plot(t,y(:,1),'-.b')

%-------------------------------------------------------------------------
%-------------------------------------------------------------------------
```

```
                                xlabel('t (sec)')
                                ylabel('\theta (rad)')
                                grid on
                                box on
                                legend('ODE45 ','SCPA method','Energy
method')
                                axis([0 tf -1.25*maxy1 3*maxy1])
            hold off
```

.

```
%Subroutine SCPA_U.m of Program_2.m
%-------------------------------------------------------------------------
%-------------------------------------------------------------------------
%SCPA method for initial velocity
%-------------------------------------------------------------------------
%-------------------------------------------------------------------------

function
[xap,Tapprox,Uo,Texact,t1,Ain]=SCPA(t,a,omega2,A,omega,P,maxy1);
global a omega2 A  omega P maxy1 Ain
P=omega2*sin(a);
omega =sqrt(omega2*cos(a));
t1=(1/sqrt(omega2))*acos(1/(1+(A*omega2*cos(a))/(omega2*sin(a))));
xap=A*sin((omega+2*P/(pi*omega*A))*t);
Tapprox=2*pi/(omega+2*P/(pi*omega*A));
Uo=-omega*(A+P/(omega.^2))*sin(omega*t1);
Ain=-Uo/omega -(P/(omega.^2))*sin(omega*t1);
Texact=(4/omega)*acos(1/(1+A*omega*omega/P));
```

```
%Program_3.m
%-------------------------------------------------------------------------
%-------------------------------------------------------------------------
%Computing the response of the driven 2-pendulum for a given and
% specific set of support motion
%-------------------------------------------------------------------------
%-------------------------------------------------------------------------


%-------------------------------------------------------------------------
%%%%%%%%%%%%%%%%%%%%%%%%%%%%%%ATTENTION%%%%%%%%%%%%%%%%%%%%%%%%%%%%%%%%
%this m-file is valid only when the appropriate and specific data_1.m
%and data_2.m data files exist in the same folder since those files
% contain both the support motion info and the corresponding results
% from Nastran for comparison and validation purposes
%-------------------------------------------------------------------------







clc
clear all
format long
fprintf('make sure that you have copied the data provided by Nastran')
datainput=input('if you already have press 1     ')
if datainput==1
    fprintf('good to go')
else
    break
end


%call the data file
dat=input('choose the data file, 1 for latteral and vertical motion, 2
for latteral  motion')
if dat==1
data_1
else
data_2
end
%-------------------------------------------------------------------------
%-------------------------------------------------------------------------
%response before the stability is broken
%-------------------------------------------------------------------------
%-------------------------------------------------------------------------


ti=0;                    %initial time condition
tf=length(data(:,2))/1000-0.001;%final time condition
dt=0.001;                %time step
```

```
nt=fix((tf-ti)/dt)      %number of time steps
a=pi/18;                %pendulation characteristic angle
g=9.81;                 %acceleration of gravity
ll=1;                   %equivalent string length which equals to the
                        %simple pendulum string length or the
                        %perpendicular distance of the mass from the
                        % plane of suspension
l=ll/cos(a);            %string length of complex pendulum
omega2=g/l;             %square of the natural frequency of the simple
                        %pendulum
omega2o=omega2*cos(a);  %square of the pseudo natural frequency of the
                        %2-pendulum
r=0;                    %restitution coefficient
m=1;                    %mass

%-----------------------------------------------------------------------
%initializing the  acceleration, velocity  and displacement vectors
%-----------------------------------------------------------------------
acc=zeros(1,nt+1);      %mass angular acceleration
vel=zeros(1,nt+1);      %mass angular velocity
disp=zeros(1,nt+1);     %mass angular displacement
force=zeros(1,nt+1);    %pseudo-restoring force on mass
Zabs=zeros(1,nt+1);     %absolute horizontal position of mass
Yabs=zeros(1,nt+1);     %absolute vertical position of mass
Z=zeros(1,nt+1);        %global horizontal position of mass
Y=zeros(1,nt+1);        %global vertical position of mass
Zs=zeros(1,nt+1);       %global horizontal position of support midpoint
Ys=zeros(1,nt+1);       %global vertical position of support midpoint
acc_rest=zeros(1,nt+1); %pseudo-acceleration corresponding to the case
%that the mass doesn't break stability
Zsddot=zeros(1,nt+1);   %global horizontal acceleration of support
%midpoint
Ysddot=zeros(1,nt+1);   %global vertical acceleration of support
%midpoint
Zsdot=zeros(1,nt+1);    %global horizontal velocity of support midpoint
Ysdot=zeros(1,nt+1);    %global vertical velocity of support midpoint
Zsdot(1,1)=0;
Ysdot(1,1)=0;
Zsddot(1,1)=0;
Ysddot(1,1)=0;
Vzj=zeros(1,nt+1);      %linear horizontal velocity of mass during jump
Vyj=zeros(1,nt+1);      %linear vertical velocity of mass during jump

%-----------------------------------------------------------------------
%applying the data input in the support midpoint motion
%-----------------------------------------------------------------------

if dat==1
Zs=data(:,2)'./1000;
Ys=data(:,3)'./1000;
else
Zs=data(:,2)'./1000;
Ys=zeros(1,nt+1);
end
```

```
%-------------------------------------------------------------------------
%initializing the  tension, support points position  and string length
%vectors
%-------------------------------------------------------------------------
Tright=zeros(1,nt+1);   %right string tension
Tleft=zeros(1,nt+1);    %left string tension
Zright=zeros(1,nt+1);   %horizontal position of right support point
Zleft=zeros(1,nt+1);    %horizontal position of left support point
Yright=zeros(1,nt+1);   %vertical position of right support point
Yleft=zeros(1,nt+1);    %vertical position of left support point
Lright=zeros(1,nt+1);   %distance of mass from right support point
Lleft=zeros(1,nt+1);    %distance of mass from left support point

for it=1:nt-1;          %calculating the support displacements and
%accelerations based on the support motion
    Zsdot(1,it+1)=(Zs(1,it+1)-Zs(1,it))/dt;
    Ysdot(1,it+1)=(Ys(1,it+1)-Ys(1,it))/dt;
    Zsddot(1,it+1)=(Zsdot(1,it+1)-Zsdot(1,it))/dt;
    Ysddot(1,it+1)=(Ysdot(1,it+1)-Ysdot(1,it))/dt;
end
vel(1,1)=0;             %initial angulat velocity condition
disp(1,1)=0;            %initial angular displacement condition
Zabs(1,1)=-l*(sin(abs(disp(1,1))+a)-sin(a));
Yabs(1,1)=ll-l*(cos(abs(disp(1,1))+a));
if abs(max(Ysddot))==0 && abs(max(Zsddot))==0&& abs(disp(1,1)==0)
%if there is no acceleration applied to the support points
%there is no delay for breaking the stability
    T=1;
else

for it=1:nt;
    acc_rest(1,it)=(abs(Zsddot(1,it)))/tan(a) -Ysddot(1,it);
    Tright(1,it)=(m/2)*((Ysddot(1,it)+g)/cos(a) +Zsddot(1,it)/sin(a));
    Tleft(1,it)=(m/2)*((Ysddot(1,it)+g)/cos(a) -Zsddot(1,it)/sin(a));
    Zright(1,it)=Zs(1,it)+l*tan(a);
    Zleft(1,it)=Zs(1,it)-l*tan(a);
    Yright(1,it)=Ys(1,it);
    Yleft(1,it)=Ys(1,it);

    if acc_rest(1,it)<g                    %if the combined applied
%acceleration is less than the required to break the stability
        disp(1,it)=0;                      %there is no oscillation
        vel(1,it)=0;
        acc(1,it)=0;
        Zabs(1,it)=-l*(sin(disp(1,1)+a)-sin(a));
        Yabs(1,it)=ll-l*(cos(abs(disp(1,1))+a));
        Z(1,it)=Zabs(1,it)+Zs(1,it);
        Y(1,it)=Yabs(1,it)+Ys(1,it)-ll;
        Lright(1,it)=sqrt((Z(1,it)-Zright(1,it)).^2+(Y(1,it)-
Yright(1,it)).^2);
```

```
        Lleft(1,it)=sqrt((Z(1,it)-Zleft(1,it)).^2+(Y(1,it)-
Yleft(1,it)).^2);

    else
        T=it;
        Zabs(1,it)=-l*(sin(disp(1,1)+a)-sin(a));
        Yabs(1,it)=ll-l*(cos(abs(disp(1,1))+a));
        Z(1,it)=Zabs(1,it)+Zs(1,it);
        Y(1,it)=Yabs(1,it)+Ys(1,it)-ll;
        Lright(1,it)=sqrt((Z(1,it)-Zright(1,it)).^2+(Y(1,it)-
Yright(1,it)).^2);
        Lleft(1,it)=sqrt((Z(1,it)-Zleft(1,it)).^2+(Y(1,it)-
Yleft(1,it)).^2);
        Vz1=Zsdot(1,T);
        Vy1=Ysdot(1,T);
        ACC=Zsddot(1,T);

    break
    end

end


end

%-------------------------------------------------------------------------
%-------------------------------------------------------------------------
%Step after the stability is broken
%-------------------------------------------------------------------------
%-------------------------------------------------------------------------

for it=T:nt;            %loop1 - initiating calculations after
%stability is brocken
  if (Tright(1,it)>0 || Tleft(1,it)>0)%condition1 - oscillations take
%place only if at least one of the tensions has a non-zero value
  force(1,it)=-
(omega2+Ysddot(1,it)/l)*(sin(a))*cos(disp(1,it))*sign(disp(1,it));
  acc(1,it)=force(1,it)-
(omega2+Ysddot(1,it)/l)*sin(disp(1,it))*cos(a)+(Zsddot(1,it))*((cos(abs
(disp(1,it))+a)))/l;
  vel(1,it+1)=vel(1,it)+acc(1,it)*dt;
    disp(1,it+1)=disp(1,it)+vel(1,it+1)*dt;
    if disp(1,it+1)*disp(1,it)>=0       %condition2 - calculations
%while the mass oscillates without changing strings
       disp(1,it+1)=disp(1,it)+vel(1,it+1)*dt;
       Zabs(1,it+1)=-sign((disp(1,it+1)))*l*(sin(abs(disp(1,it+1))+a)-
sin(a));
       Yabs(1,it+1)=ll-l*(cos(abs(disp(1,it+1))+a));
       Z(1,it+1)=Zabs(1,it+1)+Zs(1,it+1);
       Y(1,it+1)=Yabs(1,it+1)+Ys(1,it+1)-ll;
    Zright(1,it)=Zs(1,it)+l*tan(a);
    Zleft(1,it)=Zs(1,it)-l*tan(a);
    Yright(1,it)=Ys(1,it);
    Yleft(1,it)=Ys(1,it);
```

```
    Lright(1,it)=sqrt((Z(1,it)-Zright(1,it)).^2+(Y(1,it)-
Yright(1,it)).^2);
    Lleft(1,it)=sqrt((Z(1,it)-Zleft(1,it)).^2+(Y(1,it)-
Yleft(1,it)).^2);



    else                                %condition2 - the mass reached
%a string switch point
    T1=it;
    V=vel(1,T1);
    Vaft=sign(V)*sqrt((V*sin(pi/2 -2*a)).^2+(r*V*cos(pi/2 -2*a)).^2);
    vel(1,T1+1)=Vaft;
    disp(1,T1+1)=disp(1,it)+vel(1,T1+1)*dt;
       Zabs(1,it+1)=-sign((disp(1,it+1)))*l*(sin(abs(disp(1,it+1))+a)-
sin(a));
       Yabs(1,it+1)=ll-l*(cos(abs(disp(1,it+1))+a));
       Z(1,it+1)=Zabs(1,it+1)+Zs(1,it+1);
       Y(1,it+1)=Yabs(1,it+1)+Ys(1,it+1)-ll;
    Zright(1,it)=Zs(1,it)+l*tan(a);
    Zleft(1,it)=Zs(1,it)-l*tan(a);
    Yright(1,it)=Ys(1,it);
    Yleft(1,it)=Ys(1,it);
    Lright(1,it)=sqrt((Z(1,it)-Zright(1,it)).^2+(Y(1,it)-
Yright(1,it)).^2);
    Lleft(1,it)=sqrt((Z(1,it)-Zleft(1,it)).^2+(Y(1,it)-
Yleft(1,it)).^2);

    end                                 %condition2
    if disp(1,it+1)>0                   %condition3 - calculating
%the strings tension depending on which one of the strings is taught

Tright(1,it+1)=m*(vel(1,it+1)*vel(1,it+1)*l+Zsddot(1,it+1)*sin(abs(disp
(1,it+1))+a)+(g+Ysddot(1,it+1))*cos(abs(disp(1,it+1))+a));
       Tleft(1,it+1)=0;
       if Tright(1,it+1)>0
          Tright(1,it+1)=Tright(1,it+1);
       else
           Tright(1,it+1)=0;
       end
    else                                %condition3
       Tleft(1,it+1)=m*(vel(1,it+1)*vel(1,it+1)*l-
Zsddot(1,it+1)*sin(abs(disp(1,it+1))+a)+(g+Ysddot(1,it+1))*cos(abs(disp
(1,it+1))+a));
       Tright(1,it+1)=0;
       if Tleft(1,it+1)>0
          Tleft(1,it+1)=Tleft(1,it+1);
       else
          Tleft(1,it+1)=0;
       end
    end                                 %condition3
  else                                  %condition1 - the first
%jump starts
```

```
    T2=it

    V=vel(1,T2);
    disp(1,T2+1)=disp(1,T2)+vel(1,T2)*dt;
    Zabs(1,it)=-sign((disp(1,it)))*l*(sin(abs(disp(1,it))+a)-sin(a));
    Yabs(1,it+1)=ll-l*(cos(abs(disp(1,it))+a));
    Z(1,it)=Zabs(1,it)+Zs(1,it);
    Y(1,it)=Yabs(1,it)+Ys(1,it)-ll;
    Zright(1,it)=Zs(1,it)+l*tan(a);
    Zleft(1,it)=Zs(1,it)-l*tan(a);
    Yright(1,it)=Ys(1,it);
    Yleft(1,it)=Ys(1,it);
    Lright(1,it)=sqrt((Z(1,it)-Zright(1,it)).^2+(Y(1,it)-
Yright(1,it)).^2);
    Lleft(1,it)=sqrt((Z(1,it)-Zleft(1,it)).^2+(Y(1,it)-
Yleft(1,it)).^2);
    if disp(1,T2)>0                          %condition4 - calculating
%the linear velocity of the mass at the moment where the jump initiates
        Vmagn=abs(l*vel(1,T2));
        Vz2=-sign(V)*Vmagn*cos((disp(1,T2)+a))+Zsdot(1,T2-1);
        Vy2=sign(V)*Vmagn*sin((disp(1,T2)+a))+Ysdot(1,T2-1);
        break
    else                                     %condition4
        Vmagn=l*abs(vel(1,T2));
        Vz2=-sign(V)*Vmagn*cos((abs(disp(1,T2))+a))+Zsdot(1,T2-1);
        Vy2=-sign(V)*Vmagn*sin((abs(disp(1,T2))+a))+Ysdot(1,T2-1);
        break
    end                                      %condition4
  end                                        %condition1


  end                                        %loop1

  %correcting the computation rounding errors
  LLright=Lright(1,T2)-0.004;
  LLleft=Lleft(1,T2)-0.004;
  Lright(1,T2)=Lright(1,T2)-0.004;
  Lleft(1,T2)=Lleft(1,T2)-0.004;


  while it<nt
  jump
  afterjump
  end







time =data(:,1);
if dat==1
```

```
figure (4)
plot(time,disp,time,data(:,4),'--r')
xlabel('t (sec)');ylabel('\theta(rad)');
axis([0 tf -pi/2 pi/2])
grid on
figure (5)
subplot(2,1,1);plot(time,Zabs,time,data(:,10)./1000,'--r'  )
xlabel('t (sec)');ylabel('absolute horizontal position (m)');
grid on
axis([0 tf -1 1])
subplot(2,1,2);plot(time,Yabs,time,data(:,9)./1000+ll ,'--r' )
xlabel('t (sec)');ylabel('absolute vertical position (m)');
grid on
axis([0 tf -1 1])

figure (6)
subplot(2,1,1);plot(time,Z,time,data(:,8)./1000 ,'--r' )
xlabel('t (sec)');ylabel('total horizontal position (m)');
grid on
axis([0 tf -1 3])
subplot(2,1,2);plot(time,Y,time,data(:,7)./1000 ,'--r' )
xlabel('t (sec)');ylabel('total vertical position (m)');
grid on
axis([0 tf -1 1])
else
 figure (4)
plot(time,disp,time,data(:,3),'--r')
xlabel('t (sec)');ylabel('\theta(rad)');
axis([0 tf -pi/2 pi/2])
grid on
figure (5)
subplot(2,1,1);plot(time,Zabs,time,data(:,4)./1000-Zs','--r'  )
xlabel('t (sec)');ylabel('absolute horizontal position (m)');
grid on
axis([0 tf -1 1])
subplot(2,1,2);plot(time,Yabs,time,data(:,5)./1000+ll-Ys' ,'--r' )
xlabel('t (sec)');ylabel('absolute vertical position (m)');
grid on
axis([0 tf -1 1])

figure (6)
subplot(2,1,1);plot(time,Z,time,data(:,4)./1000 ,'--r' )
xlabel('t (sec)');ylabel('total horizontal position (m)');
grid on
axis([0 tf -1 5])
subplot(2,1,2);plot(time,Y,time,data(:,5)./1000 ,'--r' )
xlabel('t (sec)');ylabel('total vertical position (m)');
grid on
axis([0 tf -1 0])
end

figure (7)
subplot(2,1,1);plot(time,Lright )
xlabel('t (sec)');ylabel('absolute horizontal position (m)');
grid on
```

```
axis([0 tf 0 2])
subplot(2,1,2);plot(time,Lleft )
xlabel('t (sec)');ylabel('absolute vertical position (m)');
grid on
axis([0 tf 0 2])



figure (8)
subplot(2,1,1);plot(time,Zs )
xlabel('t (sec)');ylabel(' horizontal support position (m)');
grid on
axis([0 tf 0 5])

subplot(2,1,2);plot(time,Ys )
xlabel('t (sec)');ylabel('vertical support position (m)');
grid on
axis([0 tf -1 2])


figure (10)
plot(time,Tright, time, Tleft)
xlabel('t (sec)');
ylabel('tension (N)')
legend('right string','left string')
axis tight







%jump.m subroutine - part of the Program_3.m code
%-----------------------------------------------------------------------
%-----------------------------------------------------------------------
%Computing the response of the driven 2-pendulum when a jump is
initiated
%-----------------------------------------------------------------------
%-----------------------------------------------------------------------



%-----------------------------------------------------------------------
%-----------------------------------------------------------------------
%collecting data from the main file
%-----------------------------------------------------------------------
%-----------------------------------------------------------------------

Lright(1,T2)=LLright;
Lleft(1,T2)=LLleft;
Vyj(1,T2)=Vy2;
Vzj(1,T2)=Vz2;
```

```
for it=T2+1:nt;                                    %loop1 - initiating
%calculations
  if (Lleft(1,it-1)>l || Lright(1,it-1)>l)      %condition1 - if the
%length of at least one of the strings is equal to l, the the jump is
%terminated
    T3=it;
    Zright(1,it)=Zs(1,it)+l*tan(a);
    Zleft(1,it)=Zs(1,it)-l*tan(a);
    Yright(1,it)=Ys(1,it);
    Yleft(1,it)=Ys(1,it);
    Vzj(1,it)=Vz2;
    Vyj(1,it)=Vyj(1,it-1)-(g)*dt;
    Z(1,it)=Z(1,it-1)+Vz2*dt;
    Y(1,it)=Y(1,it-1)+Vyj(1,it)*dt;
    Zabs(1,it)=Z(1,it)-Zs(1,it);
    Yabs(1,it)=ll+Y(1,it)-Ys(1,it);
    vel(1,it)=0;
    disp(1,it)=0;
    Vzj1=Vzj(1,it);
    Vyj1=Vyj(1,it);
    Lright(1,it)=sqrt((Z(1,it)-Zright(1,it)).^2+(Y(1,it)-
Yright(1,it)).^2)-0.004;
    Lleft(1,it)=sqrt((Z(1,it)-Zleft(1,it)).^2+(Y(1,it)-
Yleft(1,it)).^2)-0.004;
    Vmagnj=sqrt(Vzj1*Vzj1+Vyj1+Vyj1);

break
  else
    Vzj(1,it)=Vz2;                                 %condition1 - the mass
%follows a projectile path
    Vyj(1,it)=Vyj(1,it-1)-(g)*dt;                  %during the jump
    Z(1,it)=Z(1,it-1)+Vz2*dt;
    Y(1,it)=Y(1,it-1)+Vyj(1,it)*dt;
    Zabs(1,it)=Z(1,it)-Zs(1,it);
    Yabs(1,it)=ll+Y(1,it)-Ys(1,it);
    Zright(1,it)=Zs(1,it)+l*tan(a);
    Zleft(1,it)=Zs(1,it)-l*tan(a);
    Yright(1,it)=Ys(1,it);
    Yleft(1,it)=Ys(1,it);
    Lright(1,it)=sqrt((Z(1,it)-Zright(1,it)).^2+(Y(1,it)-
Yright(1,it)).^2)-0.004;
    Lleft(1,it)=sqrt((Z(1,it)-Zleft(1,it)).^2+(Y(1,it)-
Yleft(1,it)).^2)-0.004;
    vel(1,it)=0;
    disp(1,it)=0;
  end                                              %condition1
end                                                %loop1


if Lright(1,T3)>Lleft(1,T3)
%condition2 - calculating the angular displacement
```

```
     phi=atan((Zright(1,T3)-Z(1,T3))/(Yright(1,T3)-Y(1,T3)));   %and
%the velocity of the mass after the
     alpha=atan(Vyj1/Vzj1);                                     %jump
%is terminated depending on which string is taught
     vel(1,T3)=(1/l)*(-Vzj1*cos(phi)+Vyj1*sin(phi));
     disp(1,T3)=phi-a;

Tright(1,T3)=m*(vel(1,T3)*vel(1,T3)*l+Zsddot(1,T3)*sin(abs(disp(1,T3))+
a)+(g+Ysddot(1,T3))*cos(abs(disp(1,T3))+a));
     Tleft(1,T3)=0;
        if  Tright(1,it+1)>0                    %condition3 - ensuring
%that the string doesn't support compressive loads
            Tright(1,it+1)=Tright(1,it+1);
        else
            Tright(1,it+1)=0;
        end
else   %condition2
     phi=atan((Z(1,T3)-Zleft(1,T3))/(Yleft(1,T3)-Y(1,T3)));
     phit=-phi;
     alpha=atan(Vzj1/Vyj1);
     alpha*180/pi;
     vel(1,T3)=(1/l)*(-Vzj1*cos(phi)-Vyj1*sin(phi));
     disp(1,T3)=-(phi-a);

Tleft(1,T3)=m*(vel(1,T3)*vel(1,T3)*l+Zsddot(1,T3)*sin(abs(disp(1,T3))+a
)+(g+Ysddot(1,T3))*cos(abs(disp(1,T3))+a));
     Tright(1,T3)=0;
        if  Tleft(1,it+1)>0                      %condition3
            Tleft(1,it+1)=Tleft(1,it+1);
        else
            Tleft(1,it+1)=0;
        end
end     %condition2
```

```
%afterjump.m subroutine - part of the Program_3.m code
%------------------------------------------------------------------------
%------------------------------------------------------------------------
%Computing the response of the driven 2-pendulum after a jump is
%terminated
%------------------------------------------------------------------------
%------------------------------------------------------------------------



for it=T3:nt; %loop1 - initiating calculations after stability is
%broken
  if (Tright(1,it)>0 || Tleft(1,it)>0) %condition1 - oscillations take
%place only if at least one of the tensions has a non-zero value

  force(1,it)=-
(omega2+Ysddot(1,it)/l)*(sin(a))*cos(disp(1,it))*sign(disp(1,it));
  acc(1,it)=force(1,it)-
(omega2+Ysddot(1,it)/l)*sin(disp(1,it))*cos(a)+(Zsddot(1,it))*((cos(abs
(disp(1,it))+a)))/l;
  vel(1,it+1)=vel(1,it)+acc(1,it)*dt;
    disp(1,it+1)=disp(1,it)+vel(1,it+1)*dt;
    if disp(1,it+1)*disp(1,it)>=0       %condition2 - calculations
%while the mass oscillates without changing strings

       disp(1,it+1)=disp(1,it)+vel(1,it+1)*dt;
       Zabs(1,it+1)=-sign((disp(1,it+1)))*l*(sin(abs(disp(1,it+1))+a)-
sin(a));
       Yabs(1,it+1)=ll-l*(cos(abs(disp(1,it+1))+a));
       Z(1,it+1)=Zabs(1,it+1)+Zs(1,it+1);
       Y(1,it+1)=Yabs(1,it+1)+Ys(1,it+1)-ll;
    Zright(1,it)=Zs(1,it)+l*tan(a);
    Zleft(1,it)=Zs(1,it)-l*tan(a);
    Yright(1,it)=Ys(1,it);
    Yleft(1,it)=Ys(1,it);
    Lright(1,it)=sqrt((Z(1,it)-Zright(1,it)).^2+(Y(1,it)-
Yright(1,it)).^2);
    Lleft(1,it)=sqrt((Z(1,it)-Zleft(1,it)).^2+(Y(1,it)-
Yleft(1,it)).^2);




    else                                %condition2 - the mass reached
%a string switch point

    T2=it;
    V=vel(1,T2);
    Vaft=sign(V)*sqrt((V*sin(pi/2 -2*a)).^2+(r*V*cos(pi/2 -2*a)).^2);
    vel(1,T2+1)=Vaft;
    disp(1,T2+1)=disp(1,T2)+vel(1,T2+1)*dt;
       Zabs(1,it+1)=-sign((disp(1,it+1)))*l*(sin(abs(disp(1,it+1))+a)-
sin(a));
```

```
       Yabs(1,it+1)=ll-l*(cos(abs(disp(1,it+1))+a));
       Z(1,it+1)=Zabs(1,it+1)+Zs(1,it+1);
       Y(1,it+1)=Yabs(1,it+1)+Ys(1,it+1)-ll;
    Zright(1,it)=Zs(1,it)+l*tan(a);
    Zleft(1,it)=Zs(1,it)-l*tan(a);
    Yright(1,it)=Ys(1,it);
    Yleft(1,it)=Ys(1,it);
    Lright(1,it)=sqrt((Z(1,it)-Zright(1,it)).^2+(Y(1,it)-
Yright(1,it)).^2);
    Lleft(1,it)=sqrt((Z(1,it)-Zleft(1,it)).^2+(Y(1,it)-
Yleft(1,it)).^2);




    end                                         %condition2

    if disp(1,it+1)>0                           %condition3 - calculating
the strings tension depending on which one of the strings is taught

Tright(1,it+1)=m*(vel(1,it+1)*vel(1,it+1)*l+Zsddot(1,it+1)*sin(abs(disp
(1,it+1))+a)+(g+Ysddot(1,it+1))*cos(abs(disp(1,it+1))+a));
       Tleft(1,it+1)=0;
       if Tright(1,it+1)>0                %condition4 - ensuring that
%the string doesn't support compressive loads

          Tright(1,it+1)=Tright(1,it+1);
       else
           Tright(1,it+1)=0;
       end
    else                                        %condition3
       Tleft(1,it+1)=m*(vel(1,it+1)*vel(1,it+1)*l-
Zsddot(1,it+1)*sin(abs(disp(1,it+1))+a)+(g+Ysddot(1,it+1))*cos(abs(disp
(1,it+1))+a));
       Tright(1,it+1)=0;
       if Tleft(1,it+1)>0                   %condition4 - ensuring that
%the string doesn't support compressive loads

          Tleft(1,it+1)=Tleft(1,it+1);
       else
          Tleft(1,it+1)=0;
       end
    end                                         %condition3

  else                                          %condition1
    T2=it

    V=vel(1,T2);
    disp(1,T2+1)=disp(1,it)+vel(1,T2)*dt;
    Zabs(1,it)=-sign((disp(1,it)))*l*(sin(abs(disp(1,it))+a)-sin(a));
    Yabs(1,it+1)=ll-l*(cos(abs(disp(1,it))+a));
    Z(1,it)=Zabs(1,it)+Zs(1,it);
```

```
    Y(1,it)=Yabs(1,it)+Ys(1,it)-ll;
    Zright(1,it)=Zs(1,it)+l*tan(a);
    Zleft(1,it)=Zs(1,it)-l*tan(a);
    Yright(1,it)=Ys(1,it);
    Yleft(1,it)=Ys(1,it);
    Lright(1,it)=sqrt((Z(1,it)-Zright(1,it)).^2+(Y(1,it)-
Yright(1,it)).^2);
    Lleft(1,it)=sqrt((Z(1,it)-Zleft(1,it)).^2+(Y(1,it)-
Yleft(1,it)).^2);
    if disp(1,T2+1)>0                       %condition5 – calculating
%the velocity when ont of the strings becomes taught
        Vmagn=abs(l*vel(1,T2));
        Vz2=-sign(V)*Vmagn*cos((disp(1,T2)+a))+Zsdot(1,T2-1);
        Vy2=sign(V)*Vmagn*sin((disp(1,T2)+a))+Ysdot(1,T2-1);
        break
    else                                    %condition5
        Vmagn=abs(l*vel(1,T2));
        Vz2=-sign(V)*Vmagn*cos((abs(disp(1,T2))+a))+Zsdot(1,T2-1);
        Vy2=-sign(V)*Vmagn*sin((abs(disp(1,T2))+a))+Ysdot(1,T2-1);
        break
    end                                     %condition5
  end                                       %condition1


  end                                       %loop1

vel(1,T2);
Vz2;
Vy2;
LLright=Lright(1,T2)-0.004;
LLleft=Lleft(1,T2)-0.004;
```

LIST OF REFERENCES

[1] Baker, Gregory L, and James A. Blackburn, The Pendulum. New York, Oxford: Oxford UP, 2006.

[2] Hagedorn, Peter. Nonlinear Oscillations, Trans. Wolfram Stadler. New York: Oxford UP, 1981.

[3] Moore, Douglas B., and Steven W. Shaw, "The Experimental Response of an Impacting Pendulum System." International Journal of NonLinear Mechanics 25 (1990): 1-16.

[4] Stronge, W. J., Impact Mechanics. Cambridge: Cambridge UP, 2000.

[5] Goriely, Alain, Philippe Boulanger and Jules Leroy, "Toy models: The jumping pendulum." American Journal of Physics 74 (2006): 784-788The driven pendulum

[6] McMillen, Tyler, and Alain Goriely, "Whip Waves." Physica D 184 (2003): 192-225

THIS PAGE INTENTIONALLY LEFT BLANK

INITIAL DISTRIBUTION LIST

1. Defense Technical Information Center
   Ft. Belvoir, Virginia

2. Dudley Knox Library
   Naval Postgraduate School
   Monterey, California

3. Mechanical and Astronautical Engineering Department Chairman
   Naval Postgraduate School
   Monterey, California

4. Professor Fotis Papoulias, Code MAE
   Department of Mechanical and Astronautical Engineering
   Naval Postgraduate School
   Monterey, California

5. Professor Joshua Gordis, Code MAE
   Department of Mechanical and Astronautical Engineering
   Naval Postgraduate School
   Monterey, California

6. Alexandros Dendis
   Hellenic Navy
   Athens, Greece

7. Embassy of Greece
   Office of Naval Attaché
   Washington, DC